Tempered Particle Filtering

Edward Herbst
Federal Reserve Board

Frank Schorfheide*
University of Pennsylvania
PIER, CEPR, NBER

July 21, 2017

Abstract

The accuracy of particle filters for nonlinear state-space models crucially depends on the proposal distribution that mutates time $t-1$ particle values into time t values. In the widely-used bootstrap particle filter, this distribution is generated by the state-transition equation. While straightforward to implement, the practical performance is often poor. We develop a self-tuning particle filter in which the proposal distribution is constructed adaptively through a sequence of Monte Carlo steps. Intuitively, we start from a measurement error distribution with an inflated variance, and then gradually reduce the variance to its nominal level in a sequence of tempering steps. We show that the filter generates an unbiased and consistent approximation of the likelihood function. Holding the run time fixed, our filter is substantially more accurate in two DSGE model applications than the bootstrap particle filter.

JEL CLASSIFICATION: C11, C15, E10

KEY WORDS: Bayesian analysis, DSGE models, nonlinear filtering, Monte Carlo methods

*Correspondence: E. Herbst: Board of Governors of the Federal Reserve System, 20th Street and Constitution Avenue N.W., Washington, D.C. 20551. Email: edward.p.herbst@frb.gov. F. Schorfheide: Department of Economics, 3718 Locust Walk, University of Pennsylvania, Philadelphia, PA 19104-6297. We thank Sylvia Kaufmann (guest editor), three anonymous referees, Drew Creal, Andras Fulop, Juan Rubio-Ramirez, and participants at various seminars and conferences for helpful comments. Email: schorf@ssc.upenn.edu. Schorfheide gratefully acknowledges financial support from the National Science Foundation under the grant SES 1424843. The views expressed in this paper are those of the authors and do not necessarily reflect the views of the Board of Governors or the Federal Reserve System.

1 Introduction

Estimated dynamic stochastic general equilibrium (DSGE) models are now widely used by academics to conduct empirical research in macroeconomics as well as by central banks to interpret the current state of the economy, to analyze the impact of changes in monetary or fiscal policies, and to generate predictions for macroeconomic aggregates. In most applications, the estimation uses Bayesian techniques, which require the evaluation of the likelihood function of the DSGE model. If the model is solved with a (log)linear approximation and driven by Gaussian shocks, then the likelihood evaluation can be efficiently implemented with the Kalman filter. If, however, the DSGE model is solved nonlinearly, the resulting state-space representation is nonlinear and the Kalman filter can no longer be used.

Fernández-Villaverde and Rubio-Ramírez (2007) proposed using a particle filter to evaluate the likelihood function of a nonlinear DSGE model, and many other papers have since followed this approach. However, configuring the particle filter so that it generates an accurate approximation of the likelihood function remains a key challenge. The contribution of this paper is to develop a self-tuning tempered particle filter that in our applications is substantially more accurate than the widely-used bootstrap particle filter.

Our starting point is the state-space representation of a potentially nonlinear DSGE model given by a measurement equation and a state-transition equation:

$$\begin{aligned} y_t &= \Psi(s_t;\theta) + u_t, \quad u_t \sim N\big(0, \Sigma_u(\theta)\big) \\ s_t &= \Phi(s_{t-1}, \epsilon_t;\theta), \quad \epsilon_t \sim F_\epsilon(\cdot;\theta). \end{aligned} \tag{1}$$

The functions $\Psi(s_t;\theta)$ and $\Phi(s_{t-1}, \epsilon_t;\theta)$ are generated numerically when solving the DSGE model. Here y_t is a $n_y \times 1$ vector of observables, u_t is a $n_y \times 1$ vector of normally distributed measurement errors, and s_t is an $n_s \times 1$ vector of hidden states.[1] To obtain the likelihood increments $p(y_{t+1}|Y_{1:t},\theta)$, where $Y_{1:t} = \{y_1, \ldots, y_t\}$, it is necessary to integrate out the latent states:

$$p(y_{t+1}|Y_{1:t},\theta) = \int\int p(y_{t+1}|s_{t+1},\theta)p(s_{t+1}|s_t,\theta)p(s_t|Y_{1:t},\theta)ds_{t+1}ds_t, \tag{2}$$

which can be done recursively with a filter.

[1] In principle both $\Psi(\cdot)$ and $\Phi(\cdot)$ could depend on the time period t in a deterministic manner. We omit this dependency in our notation. The u_t's do not literally have to be measurement errors. They could also be innovations to fundamentals. All we require is a non-degenerate distribution of $y_t|s_t$ with a scalable covariance matrix.

Particle filters represent the distribution of the hidden state vector s_t conditional on time t information $Y_{1:t} = \{y_1, \ldots, y_t\}$ through a swarm of particles $\{s_t^j, W_t^j\}_{j=1}^M$ such that, for a function of interest $h(s_t)$,

$$\frac{1}{M}\sum_{j=1}^{M} h(s_t^j)W_t^j \approx \int h(s_t)p(s_t|Y_{1:t},\theta)ds_t. \tag{3}$$

The approximation here is in the sense of a strong law of large numbers (SLLN) or a central limit theorem (CLT). The approximation error vanishes as the number of particles M tends to infinity. The filter recursively generates approximations of $p(s_t|Y_{1:t},\theta)$ for $t = 1, \ldots, T$ and produces approximations of the likelihood increments $p(y_t|Y_{1:t},\theta)$ as a by-product. There exists a large literature on particle filters. Surveys and tutorials are provided, for instance, by Arulampalam, Maskell, Gordon, and Clapp (2002), Cappé, Godsill, and Moulines (2007), Doucet and Johansen (2011), Creal (2012), and Herbst and Schorfheide (2015). Textbook treatments of the statistical theory underlying particle filters can be found in Liu (2001), Cappé, Moulines, and Ryden (2005), and Del Moral (2013).

The conceptually most straightforward version of the particle filter is the bootstrap particle filter proposed by Gordon, Salmond, and Smith (1993). This filter uses the state-transition equation to turn s_{t-1}^j particles into s_t^j particles, which are then reweighted based on their success in predicting the time t observation, measured by $p(y_t|s_t^j,\theta)$. While the bootstrap particle filter is easy to implement, it relies on the state-space model's ability to accurately predict y_t by forward simulation of the state-transition equation. In general, the lower the average density $p(y_t|s_t^j,\theta)$, the more uneven the distribution of the updated particle weights, and the less accurate the approximation in (3).

Ideally, the proposal distribution for s_t^j should not just be based on the state-transition equation $p(s_t|s_{t-1},\theta)$ but also account for the observation y_t. In fact, conditional on s_{t-1}^j the optimal proposal distribution is the posterior[2]

$$p(s_t|y_t, s_{t-1}^j, \theta) \propto p(y_t|s_t,\theta)p(s_t|s_{t-1}^j,\theta), \tag{4}$$

where $\propto$ denotes proportionality. Unfortunately, in a generic nonlinear state-space model, it is not possible to directly sample from this distribution. Constructing an approximation

[2]It is optimal in the sense that it minimizes the variance of the particle weights conditional on $\{s_{t-1}^j, W_{t-1}^j\}_{j=1}^M$. In importance sampling it is approximately true that the smaller the variance of the importance weights, the smaller is the asymptotic variance of the Monte Carlo approximation.

for $p(s_t|y_t, s_{t-1}^j, \theta)$ in a generic state-space model typically involves tedious model-specific calculations that have to be executed by the user of the algorithm prior to its implementation.[3] The innovation in this paper is to generate this approximation in a sequence of Monte Carlo steps. The basic idea goes back to Godsill and Clapp (2001). Our starting point is the observation that the larger the measurement error variance, the more accurate the filter becomes, because holding everything else constant, the variance of the particle weights decreases. Building on this insight, in each period t, we generate s_t^j by forward simulation but then update the particle weights based on a density $p_1(y_t|s_t, \theta)$ with an inflated measurement error variance. In a sequence of tempering iterations we reduce this inflated measurement error variance to its nominal level. These iterations mimic a sequential Monte Carlo (SMC) algorithm designed for a static parameter. Such algorithms have been successfully used to approximate posterior distributions for parameters of econometric models.[4]

We show that our proposed tempered particle filter produces a valid approximation of the likelihood function and substantially reduces the Monte Carlo error relative to the bootstrap particle filter, even after controlling for computational time. Our algorithm can be embedded into particle Markov chain Monte Carlo (MCMC) algorithms that replace the true likelihood by a particle-filter approximation; see, for instance, Fernández-Villaverde and Rubio-Ramírez (2007) for DSGE model applications and Andrieu, Doucet, and Holenstein (2010) for the underlying statistical theory.

The idea of adding tempering steps to the particle filter dates back to Godsill and Clapp (2001), but it has not been used in the DSGE model literature. Contemporaneously with our paper, Johansen (2016) developed a particle filter that involves tempering iterations to track $p(s_t, s_{t-1}, \ldots, s_{t-L}|Y_{1:t})$. While his algorithm allows for the mutation of particles representing blocks of lagged states, no clear guidance is provided on how the algorithm should be tailored in a specific application and whether the additional computational cost of mutating lagged states is compensated by improvements in the accuracy of the likelihood approximation. Moreover, the paper does not contain any theoretical results and the numerical illustration is restricted to a univariate model rather than DSGE models with multidimensional state spaces. In addition, in each time period t we are choosing the tempering schedule adaptively,

[3] Attempts include approximations based on the one-step Kalman filter updating formula applied to a linearized version of the DSGE model. Alternatively, one could use the updating step of an approximate filter, e.g., the ones developed by Andreasen (2013) or Kollmann (2015).

[4] Chopin (2002) first showed how to use sequential Monte Carlo methods to conduct inference on a parameter that does not evolve over time. Applications to the estimation of DSGE model parameters have been considered in Creal (2007) and Herbst and Schorfheide (2014). Durham and Geweke (2014) and Bognanni and Herbst (2015) provide applications to the estimation of other econometric time-series models.

building on work by Jasra, Stephens, Doucet, and Tsagaris (2011), Del Moral, Doucet, and Jasra (2012), Schäfer and Chopin (2013), Geweke and Frischknecht (2014), and Zhou, Johansen, and Aston (2015).

There are essentially two methods of establishing theoretical properties of SMC approximations. On the one hand, Del Moral (2004) and Del Moral (2013) use high-level random field theory to establish theoretical properties of SMC methods through the lens of the Feynman-Kac formula and its role in stochastic differential equations. While mathematically elegant, the approach relies on theory that is unfamiliar to most econometricians. On the other hand, Chopin (2004) proves a CLT for SMC approximations recursively, using familiar (to econometricians) CLTs for non-identically and independently distributed random variables. In a similar fashion, Pitt, Silva, Giordani, and Kohn (2012) show how one can prove the unbiasedness of particle filter approximation without making use of the Feynman-Kac formula. We follow this second route and show how the arguments in Chopin (2004) and Pitt, Silva, Giordani, and Kohn (2012) can be extended to account for the tempering iterations used in our algorithm. While the theoretical results in our paper are restricted to a non-adaptive version of the filter, theoretical results for adaptive SMC algorithms have recently been obtained by Beskos, Jasra, Kantas, and Thiery (2014).

The remainder of the paper is organized as follows. The proposed tempered particle filter is presented in Section 2. We provide a SLLN for the particle filter approximation of the likelihood function in Section 3 and show that the approximation is unbiased. Here we are focusing on a version of the filter that is non-adaptive. The filter is applied to a small-scale New Keynesian DSGE model and the Smets-Wouters model in Section 4 and Section 5 concludes. Theoretical derivations, computational details, DSGE model descriptions, and data sources are relegated to the Online Appendix. To simplify the notation, we often drop θ from the conditioning set of densities $p(\cdot|\cdot)$.

2 The Tempered Particle Filter

A key determinant of the accuracy of a particle filter is the distribution of the normalized weights

$$\tilde{W}_t^j = \frac{\tilde{w}_t^j W_{t-1}^j}{\frac{1}{M}\sum_{j=1}^M \tilde{w}_t^j W_{t-1}^j},$$

where W_{t-1}^j is the (normalized) weight associated with the jth particle at time $t-1$, $\tilde{w}_t^j$ is the incremental weight after observing y_t, and $\tilde{W}_t^j$ is the normalized weight accounting for this new observation.[5] For the bootstrap particle filter, the incremental weight is simply the likelihood of observing y_t given the jth particle, $p(y_t|s_t^j)$. It is approximately true that, all else equal, the larger the variance of $\tilde{W}_t^j$'s, the less accurate the Monte Carlo approximations generated by the particle filter.

One can show that, as the measurement error variance increases, the variance of the particle weights $\{\tilde{W}_t\}_{j=1}^M$ decreases. Let Σ_u/ϕ_n, $0 < \phi_n \leq 1$ be an inflated measurement error covariance matrix. Then,

$$p_n(y_t|s_t) \propto \exp\left\{-\frac{1}{2}\phi_n(y_t - \Psi(s_t))'\Sigma_u^{-1}(y_t - \Psi(s_t))\right\}. \tag{5}$$

Assuming that a resampling step equalized the particle weights $W_{t-1}^j = 1$, it is straightforward to verify that

$$\lim_{\phi_n \longrightarrow 0} \tilde{W}_t^j = \frac{p_n(y_t|s_t^j)}{\frac{1}{M}\sum_{j=1}^M p_n(y_t|s_t^j)} = 1. \tag{6}$$

Thus, in the limit, the variance of the particle weights is equal to zero. With a bit more algebra, it can be verified that the variance of the particle weights monotonically decreases as $\phi_n \longrightarrow 0$ (see the Online Appendix for details). We use this insight to construct a tempered particle filter in which we generate proposed particle values $\tilde{s}_t^j$ sequentially, by reducing the measurement error variance from an inflated initial level Σ_u/ϕ_1 to the nominal level Σ_u using a sequence of scale factors $0 < \phi_1 < \phi_2 < \ldots < \phi_{N^\phi} = 1$. The reduction of the measurement error variance is achieved by a sequence of Monte Carlo steps that we borrow from the literature of SMC approximations for posterior moments of static parameters.

By construction, $p_{N^\phi}(y_t|s_t) = p(y_t|s_t)$. Based on $p_n(y_t|s_t)$, we can define the bridge distributions

$$p_n(s_t|y_t, s_{t-1}) \quad \propto \quad p_n(y_t|s_t)p(s_t|s_{t-1}). \tag{7}$$

Integrating out s_{t-1} under the distribution $p(s_{t-1}|Y_{1:t-1})$ yields the bridge posterior density

[5] In the notation developed subsequently, the tilde on $\tilde{W}_t^j$ indicates that this is the weight associated with particle j before any resampling of the particles.

for s_t conditional on the observables:

$$p_n(s_t|Y_{1:t}) = \int p_n(s_t|y_t, s_{t-1})p(s_{t-1}|Y_{1:t-1})ds_{t-1}. \tag{8}$$

In the remainder of this section, we describe the proposed tempered particle filter. Section 2.1 presents the main algorithm that iterates over periods $t = 1, \ldots, T$ to approximate the likelihood increments $p(y_t|Y_{1:t-1})$ and the filtered states $p(s_t|Y_{1:t})$. In Section 2.2, we focus on the novel component of our algorithm, which in every period t uses N^ϕ steps to reduce the measurement error variance from Σ_u/ϕ_1 to Σ_u. We provide specific guidance for practitioners on tuning the tempered particle filter in Section 2.3. Finally, in Section 2.4 we briefly discuss the relationship between the tempered and the conditionally-optimal particle filter.

2.1 The Main Iterations

The tempered particle filter has the same structure as the bootstrap particle filter. In every period t, we draw innovations ϵ_t and use the state-transition equation to simulate the state vector forward; we update the particle weights; and we resample the particles. The key difference is to start out with a fairly large measurement error variance, which is then iteratively reduced to the nominal level Σ_u. During this tempering, we adjust the innovations to the state-transition equation as well as the particle weights.

The tempering sequence and the number of tempering stages may differ for every time period t. Thus, a concise notation takes the form

$$\phi_{1,t} < \phi_{2,t} < \ldots < \phi_{N_t^\phi} = 1 \quad \text{instead of} \quad \phi_1 < \phi_2 < \ldots < \phi_{N^\phi} = 1.$$

Starting from the distribution $p(s_{t-1}|Y_{1:t-1})$ and using a sequence of tempering iterations, our filter tracks the bridge distributions $p_n(s_t|Y_{1:t})$ defined in (8) for $n = 1, \ldots, N_t^\phi$. As our filter cycles through the tempering iterations and mutates the particle values $s_t^{j,n}$, it keeps the particle values s_{t-1}^{j,N_{t-1}^ϕ} unchanged. The pairs $(s_t^{j,n}, s_{t-1}^{j,N_{t-1}^\phi})$ with their associated particle weights approximate the distributions

$$p_n(s_t, s_{t-1}|Y_{1:t}) = p_n(s_t|s_{t-1}, Y_{1:t})p(s_{t-1}|Y_{1:t}) \quad \text{for } n = 1, \ldots, N_t^\phi.$$

Because it is convenient for the implementation of the mutation steps, we will include ϵ_t in the vector of particle values and track the triplet $(s_t, \epsilon_t, s_{t-1})$ with the understanding

that this triplet always satisfies the state-transition equation $s_t = \Phi(s_{t-1}, \epsilon_t)$. Algorithm 1 summarizes the iterations over periods $t = 1, \ldots, T$. For now, it is assumed that the initial scalings of the measurement error variances $\phi_{1,t}$, $t = 1, \ldots, T$, are given. We use $h(s_t, s_{t-1})$ to denote a generic integrable function of interest.

Algorithm 1 (Tempered Particle Filter)

1. **Period $t = 0$ Initialization.** *Let $N_0^\phi = 1$. Draw the initial particles from the distribution $s_0^j \overset{iid}{\sim} p(s_0)$, $j = 1, \ldots, M$. Let $s_0^{j,N_0^\phi} = s_0^j$ and $W_0^{j,N_0^\phi} = 1$.*

2. **Period t Iterations.** *For $t = 1, \ldots, T$:*

   (a) **Particle Initialization.**

   i. *Starting from $\{s_{t-1}^{j,N_{t-1}^\phi}, W_{t-1}^{j,N_{t-1}^\phi}\}$, generate $\tilde{\epsilon}_t^{j,1} \sim F_\epsilon(\cdot)$ and define*

$$\tilde{s}_t^{j,1} = \Phi(s_{t-1}^{j,N_{t-1}^\phi}, \tilde{\epsilon}_t^{j,1}).$$

   ii. *Compute the incremental weights:*

$$\tilde{w}_t^{j,1} = p_1(y_t|\tilde{s}_t^{j,1}) \propto \exp\left\{ -\frac{1}{2}\phi_{1,t}\big(y_t - \Psi(\tilde{s}_t^{j,1})\big)'\Sigma_u^{-1}\big(y_t - \Psi(\tilde{s}_t^{j,1})\big)\right\}. \tag{9}$$

   iii. *Normalize the incremental weights:*

$$\tilde{W}_t^{j,1} = \frac{\tilde{w}_t^{j,1} W_{t-1}^{j,N_{t-1}^\phi}}{\frac{1}{M}\sum_{j=1}^M \tilde{w}_t^{j,1} W_{t-1}^{j,N_{t-1}^\phi}} \tag{10}$$

   to obtain the particle swarm $\{\tilde{s}_t^{j,1}, \tilde{\epsilon}_t^{j,1}, s_{t-1}^{j,N_{t-1}^\phi}, \tilde{W}_t^{j,1}\}$, which leads to

$$\tilde{h}_t^1 = \frac{1}{M}\sum_{j=1}^M h(\tilde{s}_t^{j,1}, s_{t-1}^{j,N_{t-1}^\phi})\tilde{W}_t^{j,1} \approx \int h(s_t, s_{t-1}) p_1(s_t, s_{t-1}|Y_{1:t}) ds_t ds_{t-1}. \tag{11}$$

   Moreover,

$$\frac{1}{M}\sum_{j=1}^M \tilde{w}_t^{j,1} W_{t-1}^{j,N_{t-1}^\phi} \approx p_1(y_t|Y_{1:t-1}). \tag{12}$$

   iv. *Resample the particles:*

$$\{\tilde{s}_t^{j,1}, \tilde{\epsilon}_t^{j,1}, s_{t-1}^{j,N_{t-1}^\phi}, \tilde{W}_t^{j,1}\} \mapsto \{s_t^{j,1}, \epsilon_t^{j,1}, s_{t-1}^{j,N_{t-1}^\phi}, W_t^{j,1}\},$$

to obtain the approximation

$$\bar{h}_t^1 = \frac{1}{M}\sum_{j=1}^{M} h(s_t^{j,1}, s_{t-1}^{j,N_{t-1}^{\phi}})W_t^{j,1} \approx \int h(s_t, s_{t-1})p_1(s_t, s_{t-1}|Y_{1:t})ds_t ds_{t-1}. \quad (13)$$

(b) **Tempering Iterations:** *Execute Algorithm 2 (see next section) to*

i. convert the particle swarm

$$\{s_t^{j,1}, \epsilon_t^{j,1}, s_{t-1}^{j,N_{t-1}^{\phi}}, W_t^{j,1}\} \mapsto \{s_t^{j,N_t^{\phi}}, \epsilon_t^{j,N_t^{\phi}}, s_{t-1}^{j,N_{t-1}^{\phi}}, W_t^{j,N_t^{\phi}}\}$$

to approximate

$$\begin{aligned} \bar{h}_t^{N_t^{\phi}} &= \frac{1}{M}\sum_{j=1}^{M} h(s_t^{j,N_t^{\phi}}, s_{t-1}^{j,N_{t-1}^{\phi}})W_t^{j,N_t^{\phi}} \\ &\approx \int h(s_t, s_{t-1})p(s_t, s_{t-1}|Y_{1:t})ds_t ds_{t-1}; \end{aligned} \quad (14)$$

ii. compute the approximation $\hat{p}(y_t|Y_{1:t-1})$ of the likelihood increment.

3. **Likelihood Approximation**

$$\hat{p}(Y_{1:T}) = \prod_{t=1}^{T} \hat{p}(y_t|Y_{1:t-1}). \quad \blacksquare \quad (15)$$

If one sets $\phi_{1,t} = 1$, $N_t^{\phi} = 1$, and omits Step 2.(b) for all t, then Algorithm 1 is exactly identical to the bootstrap particle filter: the s_{t-1}^j particle values are simulated forward using the state-transition equation; the weights are then updated based on how well the new state $\tilde{s}_t^j$ predicts the time t observations, measured by the predictive density $p(y_t|\tilde{s}_t^j)$; and finally the particles are resampled using a standard resampling algorithm, such as multinominal resampling, or systematic resampling.[6] Once the resampling step has been executed, the particle weights are equalized: $W_t^{j,1} = 1$ for $j = 1, \ldots, M$.

The drawback of the bootstrap particle filter is that the proposal distribution for the innovation $\tilde{\epsilon}_t^j \sim F_\epsilon(\cdot)$ is not adapted to the period t observation y_t. This typically leads to a large variance of $\tilde{w}_t^j$, which translates into inaccurate Monte Carlo approximations. Taking the states $\{s_{t-1}^j\}_{j=1}^M$ as given and assuming that a $t-1$ resampling step has equalized

[6]Detailed textbook treatments of resampling algorithms can be found in Liu (2001) and Cappé, Moulines, and Ryden (2005).

the particle weights, that is, $W_{t-1}^j = 1$, the conditionally optimal choice for the proposal distribution is $p(\tilde{\epsilon}_t^j | s_{t-1}^j, y_t)$. However, because of the nonlinearity in state-transition and measurement equation, it is not possible to directly generate draws from this distribution. Our algorithm sequentially adapts the proposal distribution for the innovations to the current observation y_t by raising ϕ_n from a small initial value to $\phi_{N^\phi} = 1$. This is done in Step 2(b), which is described in detail in Algorithm 2 in the next section.

2.2 Tempering the Measurement Error Variance

The idea of including tempering iterations into a particle filter dates back to Godsill and Clapp (2001). These iterations build on Neal's (1998) annealed importance sampling and mimic the steps of SMC algorithms that have been developed for static parameters (e.g., Chopin (2002), Del Moral, Doucet, and Jasra (2006), Durham and Geweke (2014), and Herbst and Schorfheide (2014, 2015)). SMC algorithms for static parameters generate draws from a sequence of bridge posteriors $p_n(\theta|Y)$. These bridge posteriors can be generated by tempering the likelihood function, i.e., $p_n(\theta|Y) \propto \big[p(Y|\theta)\big]^{\phi_n} p(\theta)$, $n = 1, \ldots, N^\phi$ with $\phi_{N^\phi} = 1$. At each iteration, the algorithm cycles through three stages: the particle weights are updated in the *correction* step; the particles are being resampled and the particle weights are equalized in the *selection* step; and the particle values are changed in the *mutation* step. The analogue of $\big[p(Y|\theta)\big]^{\phi_n}$ in our algorithm is $p_n(y_t|s_t)$ given in (5), which reduces to $p(y_t|s_t)$ for $\phi_n = 1$. Algorithm 2 comprises of the correction, selection, and mutation steps. Note that the sequence $\phi_{n,t}$, $n = 1, \ldots, N_t^\phi$, and the number of stages, N_t^ϕ, is an output of the algorithm that is determined in Step 1(a)iii. in conjunction with the termination condition $\phi_{n,t} = 1$ of the *do*-loop. Thus, the filter is adaptive with respect to the tempering schedule.

Algorithm 2 (Tempering Iterations) *This algorithm receives as input the particle swarm* $\{s_t^{j,1}, \epsilon_t^{j,1}, s_{t-1}^{j,N_{t-1}^\phi}, W_t^{j,1}\}$ *and returns as output the particle swarm* $\{s_t^{j,N_t^\phi}, \epsilon_t^{j,N_t^\phi}, s_{t-1}^{j,N_{t-1}^\phi}, W_t^{j,N_t^\phi}\}$ *and the likelihood increment* $\hat{p}_{N_t^\phi}(y_t|Y_{1:t-1})$. *Set* $n = 1$ *and* $N_t^\phi = 1$.

1. *Do until* $\phi_{n,t} = 1$*:*

   (a) **Correction:** *Let* $n = n + 1$. *Then,*

i. for $j = 1, \ldots, M$ and given $\phi_{n-1,t}$ define the incremental weight function

$$\begin{aligned} \tilde{w}_t^{j,n}(\phi_n) &= \frac{p_n(y_t|s_t^{j,n-1})}{p_{n-1}(y_t|s_t^{j,n-1})} \\ &= \left(\frac{\phi_n}{\phi_{n-1,t}}\right)^{n_y/2} \exp\Big\{ -\frac{1}{2}\big[y_t - \Psi(s_t^{j,n-1})\big]' \\ &\quad \times(\phi_n - \phi_{n-1,t})\Sigma_u^{-1}\big[y_t - \Psi(s_t^{j,n-1})\big]\Big\}. \end{aligned} \tag{16}$$

ii. Define the normalized weights

$$\tilde{W}_t^{j,n}(\phi_n) = \frac{\tilde{w}_t^{j,n}(\phi_n) W_t^{j,n-1}}{\frac{1}{M}\sum_{j=1}^M \tilde{w}_t^{j,n}(\phi_n) W_t^{j,n-1}}, \tag{17}$$

($W_t^{j,n-1} = 1$ because the resampling step was executed in iteration $n-1$), and the inefficiency ratio

$$\mathit{InEff}(\phi_n) = \frac{1}{M}\sum_{j=1}^M \big(\tilde{W}_t^{j,n}(\phi_n)\big)^2. \tag{18}$$

iii. If $\mathit{InEff}(1) \leq r^*$

let $\phi_{n,t} = 1$, $N_t^\phi = n$, and $\tilde{W}_t^{j,n} = \tilde{W}_t^{j,n}(1)$ (terminate do*-loop after iteration n);*

else

let $\phi_{n,t}$ be the solution to $\mathit{InEff}(\phi_{n,t}) = r^*$, $\tilde{W}_t^{j,n} = \tilde{W}_t^{j,n}(\phi_{n,t})$.

iv. The particle swarm $\{s_t^{j,n-1}, \epsilon_t^{j,n-1}, s_{t-1}^{j,N_{t-1}^\phi}, \tilde{W}_t^{j,n}\}$ approximates

$$\begin{aligned} \tilde{h}_t^n &= \frac{1}{M}\sum_{j=1}^M h(s_t^{j,n-1}, s_{t-1}^{j,N_{t-1}^\phi})\tilde{W}_t^{j,n} \\ &\approx \int h(s_t, s_{t-1}) p_n(s_t, s_{t-1}|Y_{1:t}) ds_t ds_{t-1}. \end{aligned} \tag{19}$$

(b) **Selection:** *Resample the particles:*

$$\{s_t^{j,n-1}, \epsilon_t^{j,n-1}, s_{t-1}^{j,N_{t-1}^\phi}, \tilde{W}_t^{j,n}\} \mapsto \{\hat{s}_t^{j,n}, \hat{\epsilon}_t^{j,n}, s_{t-1}^{j,N_{t-1}^\phi}, W_t^{j,n}\},$$

which leads to $W_t^{j,n} = 1$ for $j = 1, \ldots, M$. Keep track of the correct ancestry information such that $\hat{s}_t^{j,n} = \Phi(s_{t-1}^{j,N_{t-1}^\phi}, \hat{\epsilon}_t^{j,n})$ for each j. This leads to the approximation

$$\hat{h}_t^n = \frac{1}{M}\sum_{j=1}^{M} h(\hat{s}_t^{j,n}, s_{t-1}^{j,N_{t-1}^{\phi}}) W_t^{j,n} \approx \int h(s_t, s_{t-1}) p_n(s_t, s_{t-1}|Y_{1:t}) ds_t ds_{t-1}. \quad (20)$$

(c) **Mutation:** *Use a Markov transition kernel* $K_n(s_t|\hat{s}_t; s_{t-1})$ *with the invariance property*

$$p_n(s_t|y_t, s_{t-1}) = \int K_n(s_t|\hat{s}_t; s_{t-1}) p_n(\hat{s}_t|y_t, s_{t-1}) d\hat{s}_t \quad (21)$$

to mutate the particle values (see Algorithm 3 for an implementation). This leads to the particle swarm $\{s_t^{j,n}, \epsilon_t^{j,n}, s_{t-1}^{j,N_{t-1}^{\phi}}, W_t^{j,n}\}$*, which approximates*

$$\bar{h}_t^n = \frac{1}{M}\sum_{j=1}^{M} h(s_t^{j,n}, s_{t-1}^{j,N_{t-1}^{\phi}}) W_t^{j,n} \approx \int h(s_t, s_{t-1}) p_n(s_t, s_{t-1}|Y_{1:t}) ds_t ds_{t-1}. \quad (22)$$

2. Approximate the likelihood increment:

$$\hat{p}(y_t|Y_{1:t-1}) = \hat{p}_{N_t^{\phi}}(y_t|Y_{1:t-1}) = \prod_{n=1}^{N_t^{\phi}} \left(\frac{1}{M}\sum_{j=1}^{M} \tilde{w}_t^{j,n} W_t^{j,n-1} \right) \quad (23)$$

with the understanding that $W_t^{j,0} = W_{t-1}^{j,N_{t-1}^{\phi}}$. ■

Correction. The correction step adapts the stage $n-1$ particle swarm to the reduced measurement error variance in stage n by reweighting the particles. The incremental weights in (16) capture the change in the measurement error variance from $\Sigma_u/\phi_{n-1,t}$ to Σ_u/ϕ_n and yield an importance sampling approximation of $p_n(s_t|Y_{1:t})$ based on the stage $n-1$ particle values. We choose $\phi_{n,t}$ to achieve a targeted inefficiency ratio $r^* > 1$. This approach of adaptively choosing the tempering schedule has been used in the SMC literature by Jasra, Stephens, Doucet, and Tsagaris (2011), Del Moral, Doucet, and Jasra (2012), Schäfer and Chopin (2013), and Zhou, Johansen, and Aston (2015). It also has proven useful in the context of global optimization of nonlinear functions; see Geweke and Frischknecht (2014).

To relate the inefficiency ratio to ϕ_n, we begin by defining

$$e_{j,t} = \frac{1}{2}(y_t - \Psi(s_t^{j,n-1}))'\Sigma_u^{-1}(y_t - \Psi(s_t^{j,n-1})).$$

Assuming that the particles were resampled in iteration $n-1$ and $W_t^{j,n-1} = 1$, we can then express the inefficiency ratio as

$$\text{InEff}(\phi_n) = \frac{1}{M}\sum_{j=1}^{M}\left(\tilde{W}_t^{j,n}(\phi_n)\right)^2 = \frac{\frac{1}{M}\sum_{j=1}^{M}\exp[-2(\phi_n - \phi_{n-1,t})e_{j,t}]}{\left(\frac{1}{M}\sum_{j=1}^{M}\exp[-(\phi_n - \phi_{n-1,t})e_{j,t}]\right)^2}. \tag{24}$$

For $\phi_n = \phi_{n-1,t}$ the inefficiency ratio is $\text{InEff}(\phi_n) = 1 < r^*$. We show in the Online Appendix that the function is monotonically increasing on the interval $[\phi_{n-1,t}, 1]$, which is the justification for Step 1(a)iii of Algorithm 3. Thus, we are raising ϕ_n as closely to one as we can without exceeding a user-defined bound on the variance of the particle weights. We use the same approach to set the initial scaling factor ϕ_1 in Algorithm 1.

Selection. The selection step is executed in every iteration n to ensure that we can find a unique $\phi_{n,t}$ based on the function $\text{InEff}(\phi_n)$ in (24) in the correction step. Thus, $W_t^{j,n} = 1$ and in principle we could drop the weights from the formulas.

Mutation. In the mutation step, we are using a Markov transition kernel to change the particle values from $(\hat{s}_t^{j,n}, \hat{\epsilon}_t^{j,n})$ to $(s_t^{j,n}, \epsilon_t^{j,n})$, maintaining an approximation of $p_n(s_t, s_{t-1}|Y_{1:t})$. It can be implemented with a random walk Metropolis-Hastings (RWMH) algorithm; see Algorithm 3 below. In the absence of the mutation step, the initial particle values $(s_t^{j,1}, \epsilon_t^{j,1})$ would never change and we would essentially reproduce the bootstrap particle filter by computing $p(y_t|\tilde{s}_t^j)$ as the limit of a sequence of measurement error covariance matrices that converges to Σ_u. Unlike in the algorithm proposed by Johansen (2016), we do not mutate the particle values $s_{t-l}^{j,N_{t-l}^{\phi}}$, $l = 1, \ldots, L$. The advantage is that the state vector that we are mutating has a smaller dimension, which tends to increase the probability that a particle value changes during the mutation step. Thus, our algorithm should be able to attain a desired probability of mutating the particle values with fewer steps of the RWMH algorithm and therefore be faster. A potential disadvantage is that we are not adapting as well to the joint distribution $p_n(s_t, s_{t-1}, \ldots, s_{t-L}|Y_{1:t})$.

Algorithm 3 (RWMH Mutation Step) *This algorithm receives as input the particle swarm* $\{\hat{s}_t^{j,n}, \hat{\epsilon}_t^{j,n}, s_{t-1}^{j,N_{t-1}^{\phi}}, W_t^{j,n}\}$ *and returns as output the particle swarm* $\{s_t^{j,n}, \epsilon_t^{j,n}, s_{t-1}^{j,N_{t-1}^{\phi}}, W_t^{j,n}\}$.

1. **Execute N^{MH} Metropolis-Hastings Steps for Each Particle:** *For $j = 1, \ldots M$:*

   (a) *Set $\hat{\epsilon}_t^{j,n,0} = \hat{\epsilon}_t^{j,n}$. Then, for $l = 1, \ldots, N^{MH}$:*

      i. *Generate a proposed innovation:* $e_t^j \sim N\left(\hat{\epsilon}_t^{j,n,l-1}, c_n^2 I_{n_\epsilon}\right)$.

ii. Compute the acceptance rate:

$$\alpha(e_t^j|\hat{\epsilon}_t^{j,n,l-1}) = \min\left\{1, \frac{p_n(y_t|e_t^j, s_{t-1}^{j,N_{t-1}^{\phi}})p_\epsilon(e_t^j)}{p_n(y_t|\hat{\epsilon}_t^{j,n,l-1}, s_{t-1}^{j,N_{t-1}^{\phi}})p_\epsilon(\hat{\epsilon}_t^{j,n,l-1})}\right\}.$$

iii. Update particle values:

$$\hat{\epsilon}_t^{j,n,l} = \begin{cases} e_t^j & \textit{with prob. } \alpha(e_t^j|\hat{\epsilon}_t^{j,n,l-1}) \\ \hat{\epsilon}_t^{j,n,l-1} & \textit{with prob. } 1-\alpha(e_t^j|\hat{\epsilon}_t^{j,n,l-1}) \end{cases}$$

(b) Define $\epsilon_t^{j,n} = \hat{\epsilon}_t^{j,n,N^{MH}}$ *and* $s_t^{j,n} = \Phi(s_{t-1}^{j,N_{t-1}^{\phi}}, \epsilon_t^{j,n})$. ■

As the covariance matrix for the proposal distribution in the RWMH algorithm we use the identity matrix I_{n_ϵ} scaled by c_n.[7] We set c_n adaptively to achieve a desired acceptance rate. We compute the average empirical rejection rate $\hat{R}_{n-1}(c_{n-1})$ across the N^{MH} RWMH steps of the mutation phase in iteration $n-1$. We set $c_1 = c^*$ and let

$$c_n = c_{n-1} f\big(1 - \hat{R}_{n-1}(c_{n-1})\big), \quad f(x) = 0.95 + 0.10\frac{e^{20(x-0.40)}}{1+e^{20(x-0.40)}}, \quad n \geq 2. \tag{25}$$

Thus, we increase (decrease)the scaling factor by 5 percent if the acceptance rate is well above (below) 0.40. For acceptance rates near 0.40, the increase (or decrease) of c_n is attenuated by the logistic component of $f(x)$. In our empirical applications, the performance of the filter was robust to variations of the rule.

2.3 Tuning of the Algorithm

In order to run Algorithm 3, the user has to specify the number of particles M, the initial measurement error precision scalings $\phi_{1,t}$ in Algorithm 1, the targeted inefficiency ratio r^*, the initial scaling of the proposal covariance matrix c_*, and the number of Metropolis-Hastings steps N^{MH}. In principle, the user can also adjust the target acceptance rate (and potentially the speed of adjustment) in (25). Each of these tuning parameters affects the statistical properties of the filter, and can potentially affect the computational cost associated with the filter. We now discuss some issues in selecting each of these parameters.

[7] Herbst and Schorfheide (2014) use the particle approximation of the posterior covariance matrix from the selection step to specify the stage-n proposal covariance matrix. In the tempered particle filter, the cost of computing this object tends to outweigh the gains from adapation, so we instead use the identity matrix.

The selection of M is an issue for *any* particle filter. A higher M is associated with a more precise approximation at the cost of a longer run time of the filter. In practice, this is usually done through experimentation. If the particle filter is embedded in a MCMC algorithm, a heuristic suggested by Pitt, Silva, Giordani, and Kohn (2012), is to increase M until the standard deviation of the filter's log likelihood estimate at some parameter value is less than one. Particle filter approximations typically satisfy a CLT according to which the variance is proportional to $1/M$.

The initial measurement error precisions $\phi_{1,t}$ can either be user-specified or determined adaptively by targeting a desired variance of particle weights as in Step 1(a)iii of Algorithm 2. The targeted inefficiency ratio, $r^* \in (1, \infty)$ controls the targeted degree of "unevenness" of the distribution of particle weights that pins down the particular $\phi_{n,t}$ sequences. If r^* is close to 1, loosely speaking, $\phi_{n,t}$ will be "close" to $\phi_{n-1,t}$ and generally there will be many stages (N_t^ϕ will be large.) In contrast, if r^* is very large, bridge distributions can be very different, and in general N_t^ϕ will be small. In the limit, as $r^* \longrightarrow \infty$, the algorithm converges to the resample-move variant of the bootstrap particle filter, where $N_t^\phi = 1$ for all t. The particles are mutated at each time t, but there are no intermediate bridge distributions.

A low r^* delivers weighted particles with low variance, which all else equal are associated with more precise Monte Carlo estimates. Of course, a low r^* is also associated with many bridge distributions, which increases the run time of the filter. At some point increasing the number of tempering iterations further could in principle result in less precise estimates because of the variability induced by the additional resampling and mutation steps. In practice, we don't find this to be an issue, and so r^* works as a complement to M, with both having a trade-off between statistical precision and computational cost. In Section 4 we examine the effects of different choices of M and r^* in two DSGE models.

The other two tuning parameters, namely, the initial scaling of the proposal covariance matrix c_* and the number of RWMH steps N^{MH}, are less important. If there are many bridge distributions, the influence of the initial scaling factor c_* is diminished because it is adjusted in each subsequent iteration. While many intermediate RWMH steps help to ensure that the particles are both diverse and well-adapted to any given bridge distribution, often this effect can be achieved by choosing a lower r^*. Of course, this is not to say that c_* and N^{MH} do not affect the variance of the Monte Carlo estimates. In any particular application, experimentation with these parameters may enhance the performance of the algorithm.

Finally, we could replace the draws of $\tilde{\epsilon}_t^{j,1}$ from the innovation distribution $F_\epsilon(\cdot)$ in

Step 2(a)i of Algorithm 1 with draws from a tailored distribution with density $g_t^1(\tilde{\epsilon}_t^{j,1}|s_{t-1}^{j,N_{t-1}^\phi})$ and then adjust the incremental weight $\tilde{\omega}_t^{j,1}$ by the ratio $p_\epsilon(\tilde{\epsilon}_t^{j,1})/g_t^1(\tilde{\epsilon}_t^{j,1}|s_{t-1}^{j,N_{t-1}^\phi})$, as it is done in the generalized version of the particle filter. Here the $g_t(\cdot)$ density might be constructed based on a linearized version of the DSGE model or be obtained through the updating steps of a conventional nonlinear filter, such as an extended Kalman filter, unscented Kalman filter, or a Gaussian quadrature filter; see Herbst and Schorfheide (2015). Thus, the proposed tempering steps can be used either to relieve the user from the burden of having to construct a $g_t^1(\tilde{\epsilon}_t^{j,1}|s_{t-1}^{j,N_{t-1}^\phi})$ in the first place, or it could be used to improve upon the accuracy obtained with a readily available $g_t^1(\tilde{\epsilon}_t^{j,1}|s_{t-1}^{j,N_{t-1}^\phi})$.

2.4 Relationship to Conditionally-Optimal Particle Filter

We mentioned in the introduction that conditional on the s_{t-1}^j particles it is optimal to generate draws from the proposal distribution $p(s_t|y_t, s_{t-1})$ given in (4). The tempered particle filter generates a sequence of approximations $p_n(s_t, s_{t-1}|y_t, Y_{1:t-1})$ that converge to $p(s_t, s_{t-1}|y_t, Y_{1:t-1})$ as $n \longrightarrow N^\phi$. This raises the question to what extent this filter can achieve conditional optimality. Because $p(s_t|y_t, s_{t-1})$ and $p_n(s_t, s_{t-1}|y_t, Y_{1:t-1})$ are not the same objects, we provide a comparison of the two approaches by embedding the conditionally-optimal proposal distribution into Algorithm 1.

Suppose in Step 2(a)i we draw $\tilde{s}_{t,*}^{j,1}$ (we are using the $*$ subscript to indicate draws and weights associated with the conditionally-optimal proposal) from

$$p_1(s_t|y_t, s_{t-1}^{j,N_{t-1}^\phi}) \propto p_1(y_t|s_t)p(s_t|s_{t-1}^{j,N_{t-1}^\phi}), \tag{26}$$

where $p_1(y_t|s_t)$ is based on scaling the precision of the measurement errors by $\phi_{1,t}$.[8] The incremental weights for $\tilde{s}_{t,*}^{j,1}$ are given by

$$\tilde{w}_{t,*}^{j,1} = p_1(y_t|\tilde{s}_{t,*}^{j,1})\frac{p(\tilde{s}_{t,*}^{j,1}|s_{t-1}^{j,N_{t-1}^\phi})}{p_1(\tilde{s}_{t,*}^{j,1}|y_t, s_{t-1}^{j,N_{t-1}^\phi})} = p_1(y_t|s_{t-1}^{j,N_{t-1}^\phi}). \tag{27}$$

For every choice $\tilde{\phi}_1$ of the measurement error precision, the variance of the $\tilde{w}_{t,*}^{j,1}$ weights is smaller than the variance of the weights $\tilde{w}_t^{j,1}$ obtained under the bootstrap proposal, because

[8] If one can sample from the conditionally-optimal proposal for $\phi_{n,t} = 1$, then it is reasonable to assume that one can sample from this density for $0 < \phi_{n,t} \leq 1$. This is certainly true for normally distributed measurement errors.

the conditionally-optimal proposal is designed to minimize the variance of the particle weights conditional on the swarm $\{s_{t-1}^{j,N_{t-1}^{\phi}}, W_{t-1}^{j,N_{t-1}^{\phi}}\}$. Moreover, we know from (24) that the variance of the particle weights is an increasing function of $\phi_{1,t}$. Thus, if we choose $\phi_{1,t}$ adaptively according to Step 1(a)iii of Algorithm 2 by targeting a specific variance of the particle weights (or a particular inefficiency ratio), then it has to be the case that the precision chosen under the conditionally-optimal proposal, say $\phi_{1,t}^*$, is larger (and closer to one) than the precision $\phi_{1,t}$ chosen under the bootstrap proposal.

This leads to the following conclusions: (i) if the variance of the $\tilde{w}_{t,*}^{j,1}$ is sufficiently small, then $\phi_{1,t}^* = 1$ and the tempering iterations become obsolete. (ii) If the variance of the $\tilde{w}_{t,*}^{j,1}$ is large enough such that $\phi_{1,t}^* < 1$, then, because $\phi_{1,t}^* \geq \phi_{1,t}$, the tempered particle filter with the conditionally-optimal proposal distribution will be more accurate than the tempered particle filter based on the bootstrap proposal. The former will either use fewer iterations to bridge the discrepancy between $p_1(s_t, s_{t-1}|Y_{1:t})$ and $p(s_t, s_{t-1}|Y_{1:t})$ or it will use the same number of iterations with smaller gaps between $p_{n-1}(s_t, s_{t-1}|Y_{1:t})$ and $p_n(s_t, s_{t-1}|Y_{1:t})$.

The implementation of the conditionally-optimal particle filter is typically infeasible in practice. Thus, the tempered particle filter is meant to be a feasible alternative that dominates the widely-used bootstrap particle filter. However, the discussion emphasizes an important point made at the end of Section 2.3: if a better proposal than $p(s_t|s_{t-1}^{j,N_{t-1}^{\phi}})$ is available, then it should be used along with the tempering iterations.

3 Theoretical Properties of the Filter

We will now examine the asymptotic (with respect to the number of particles M) and finite sample properties of the particle filter approximation of the likelihood function. Section 3.1 provides a SLLN, and Section 3.2 shows that the likelihood approximation is unbiased. Detailed proofs are provided in the Online Appendix. Throughout this section, we will focus on a version of the filter that is non-adaptive[9], replacing Algorithm 2 by Algorithm 4 and Algorithm 3 by Algorithm 5:

Algorithm 4 (Tempering Iterations – Non-Adaptive) *This algorithm is identical to Algorithm 2, with the exception that the tempering schedule* $\{\phi_n\}_{n=1}^{N^{\phi}}$ *is pre-determined. The*

[9]To simplify notation, we also assume that the tempering schedule is the same for all t. This assumption can be easily relaxed as long as the tempering schedule remains predetermined. Asymptotic results for adaptive SMC algorithms are available in the literature, e.g., Herbst and Schorfheide (2014) and Beskos, Jasra, Kantas, and Thiery (2014).

Do until $\phi_{n,t} = 1$-*loop is replaced by a* For $n = 1$ to N^{ϕ}-*loop and Step 1(a)iii is eliminated.* ■

Algorithm 5 (RWMH Mutation Step – Non-Adaptive) *This algorithm is identical to Algorithm 3 with the exception that the sequence* $\{c_n\}_{n=1}^{N^{\phi}}$ *is pre-determined.* ■

3.1 Asymptotic Properties

Under suitable regularity conditions, the Monte Carlo approximations generated by a particle filter satisfy a SLLN and a CLT. Proofs for a generic particle filter are provided in Chopin (2004). We will subsequently establish a SLLN for the tempered particle filter by modifying the recursive proof developed by Chopin (2004) to account for the tempering iterations of Algorithm 4. In this paper, we are primarily interested in establishing an almost-sure limit for the Monte Carlo approximation of the likelihood function:

$$\hat{p}(Y_{1:T}) = \prod_{t=1}^{T} \hat{p}(y_t|Y_{1:t-1}) \xrightarrow{a.s.} \prod_{t=1}^{T} \left(p_1(y_t|Y_{1:t-1}) \prod_{n=2}^{N^{\phi}} \frac{p_n(y_t|Y_{1:t-1})}{p_{n-1}(y_t|Y_{1:t-1})} \right) = p(Y_{1:T}). \tag{28}$$

Here we used $p_{N^{\phi}}(y_t|Y_{1:t-1}) = p(y_t|Y_{1:t-1})$. The limit is obtained by letting the number of particles $M \longrightarrow \infty$. We assume that the length of the sample T is fixed. We use $C < \infty$ to denote a generic finite constant.

As a by-product, we also derive an almost-sure limit for Monte Carlo approximations of moments of the filtered states:

$$\bar{h}_t^n = \frac{1}{M} \sum_{j=1}^{M} h(s_t^{j,n}, s_{t-1}^{j,N^{\phi}}) W_t^{j,n} \xrightarrow{a.s.} \int \int h(s_t, s_{t-1}) p_n(s_t, s_{t-1}|Y_{1:t}) ds_t ds_{t-1}, \tag{29}$$

where

$$p_n(s_t, s_{t-1}|Y_{1:t}) = \frac{p_n(y_t|s_t)p(s_t|s_{t-1})p(s_{t-1}|Y_{1:t-1})}{\int \int p_n(y_t|s_t)p(s_t|s_{t-1})p(s_{t-1}|Y_{1:t-1}) ds_{t-1} ds_t ds_{t-1}}.$$

By integrating over s_{t-1} we recover

$$\int p_n(s_t, s_{t-1}|Y_{1:t}) ds_{t-1} = p_n(s_t|Y_{1:t}),$$

where $p_n(s_t|Y_{1:t})$ was previously introduced in (8). For technical reasons that will be explained below, we consider expectations of generic functions $h(s_t, s_{t-1})$ that may vary with

both s_t and s_{t-1}.[10] A special case is a function that is constant with respect to s_{t-1}. We simply denote such a function by $h(s_t)$.

To guarantee the almost-sure convergence, we need to impose some regularity conditions on the functions $h(s_t, s_{t-1})$. We define the following classes of functions:

$$\begin{aligned}\mathcal{H}_t^1 \;=\; \Bigg\{ h(s_t, s_{t-1}) \Bigg| & \int \mathbb{E}_{p(s_t|s_{t-1})}[|h(s_t, s_{t-1})|]p(s_{t-1}|Y_{1:t-1})ds_{t-1} < \infty, \\ & \exists \delta > 0 \text{ s.t. } f_\delta(s_{t-1}) = \mathbb{E}_{p(s_t|s_{t-1})}\left[\left|h(s_t, s_{t-1}) - \mathbb{E}_{p(s_t|s_{t-1})}[h(s_t, s_{t-1})]\right|^{1+\delta}\right] < C, \\ & g(s_{t-1}) = \mathbb{E}_{p(s_t|s_{t-1})}[h(s_t, s_{t-1})] \in \mathcal{H}_{t-1}^{N^\phi} \Bigg\}\end{aligned} \tag{30}$$

and for $n = 2, \ldots, N^\phi$:

$$\begin{aligned}\mathcal{H}_t^n \;=\; \Bigg\{ h(s_t, s_{t-1}) \Bigg| & \; h(s_t, s_{t-1}) \in \mathcal{H}_t^{n-1}, \; \exists \delta > 0 \text{ s.t.} \\ & f_\delta(\hat{s}_t, s_{t-1}) = \mathbb{E}_{K_n(s_t|\hat{s}_t; s_{t-1})}\left[\left|h(s_t, s_{t-1}) - \mathbb{E}_{K_n(s_t|\hat{s}_t, s_{t-1})}[h(s_t, s_{t-1})]\right|^{1+\delta}\right] < C, \\ & g(\hat{s}_t, s_{t-1}) = \mathbb{E}_{K_n(s_t|\hat{s}_t; s_{t-1})}[h(s_t, s_{t-1})] \in \mathcal{H}_t^{n-1} \Bigg\}.\end{aligned} \tag{31}$$

Here $\mathbb{E}_{p(s_t|s_{t-1})}[\cdot]$ and $\mathbb{E}_{K_n(s_t|\hat{s}_t, s_{t-1})}[\cdot]$ are conditional expectations under the density $p(s_t|s_{t-1})$ and the Markov transition kernel $K_n(s_t|\hat{s}_t; s_{t-1})$. By definition, $\mathcal{H}_t^{\tilde{n}} \subseteq \mathcal{H}_t^n$ for $\tilde{n} > n$. The classes $\mathcal{H}_t^n$ are chosen such that the moment bounds that guarantee the almost sure convergence of Monte Carlo averages of $h(s_t^{j,n}, s_{t-1}^{j,N^\phi})$ are satisfied. The key assumption here is that there exists a uniform bound for the centered $1+\delta$ conditional moment of the function $h(s_t, s_{t-1})$ under the state-transition density $p(s_t|s_{t-1})$ and the transition kernel of the mutation step of Algorithm 5, $K_n(s_t|\hat{s}_t; s_{t-1})$. This will allow us to apply a SLLN to the particles generated by the forward simulation of the model and the mutation step in the tempering iterations.

For the class $\mathcal{H}_1^1$ to be properly defined according to (30), we need to define $\mathcal{H}_0^{N^\phi}$. Let $\mathcal{H}_0 = \mathcal{H}_0^{N^\phi}$ and note that $\mathbb{E}_{p(s_1|s_0)}[h(s_1, s_0)]$ is a function of s_0 only. Thus, we define

$$\mathcal{H}_0 = \left\{ h(s_0) \;\middle|\; \int |h(s_0)|p(s_0)ds_0 < \infty \right\}. \tag{32}$$

[10] Spoiler alert: we need the s_{t-1} because the Markov transition kernel generated by Algorithm 4 (or Algorithm 2) is invariant under the distribution $p_n(s_t|y_t, s_{t-1})$, which is conditioned on s_{t-1}, instead of the distribution $p_n(s_t|Y_{1:t})$.

Under the assumption that the initial particles are generated by *i.i.d.* sampling from $p(s_0)$, the integrability conditions ensure that we can apply Kolmogorov's SLLN. Notice that any bounded function $|h(\cdot)| < C$ is an element of $\mathcal{H}_t^n$ for all t and n. Under the assumption that the measurement errors have a multivariate normal distribution, the densities $p_n(y_t|s_t)$ and the density ratios $p_n(y_t|s_t)/p_{n-1}(y_t|s_t)$ are bounded uniformly in s_t, which means that these functions are elements of all $\mathcal{H}_t^n$.

By changing the definition of the classes $\mathcal{H}_t^n$ and requiring moments of order $2+\delta$ to exist, the subsequent theoretical results can be extended to a CLT following arguments in Chopin (2004) and Herbst and Schorfheide (2014). The CLT provides a justification for computing numerical standard errors from the variation of Monte Carlo approximations across multiple independent runs of the filter.

3.1.1 Algorithm 1

To prove the convergence of the Monte Carlo approximations generated in Step 2(a) of Algorithm 1, we can use well established arguments for the bootstrap particle filter, which we adapt from the presentation in Herbst and Schorfheide (2015). We use $\xrightarrow{a.s.}$ to denote almost-sure convergence as $M \longrightarrow \infty$. The starting point is the following recursive assumption:

Assumption 1 *The particle swarm* $\{s_{t-1}^{j,N^\phi}, W_{t-1}^{j,N^\phi}\}$ *generated by the period* $t-1$ *iteration of Algorithm 1 approximates:*

$$\bar{h}_{t-1}^{N^\phi} = \frac{1}{M}\sum_{j=1}^{M} h(s_{t-1}^{j,N^\phi}) W_{t-1}^{j,N^\phi} \xrightarrow{a.s.} \int h(s_{t-1}) p(s_{t-1}|Y_{1:t-1}) ds_{t-1} \tag{33}$$

for functions $h(s_{t-1}) \in \mathcal{H}_{t-1}^{N^\phi}$.

In our statement of the recursive assumption, we only consider functions that vary with s_{t-1}, which is why we write $h(s_{t-1})$ (instead of $h(s_{t-1}, s_{t-2})$). As discussed previously, if the filter is initialized by direct sampling from $p(s_0)$, then the recursive assumption is satisfied for $t = 1$. We obtain the following convergence results:

Lemma 1 *Suppose that Assumption 1 is satisfied. Then for $h \in \mathcal{H}_t^1$:*

$$\tilde{h}_{t|t-1}^1 = \frac{1}{M}\sum_{j=1}^{M} h(\tilde{s}_t^{j,1}, s_{t-1}^{j,N^\phi}) W_{t-1}^{j,N^\phi} \xrightarrow{a.s.} \int\int h(s_t, s_{t-1}) p_1(s_t, s_{t-1}|Y_{1:t-1}) ds_t ds_{t-1} \quad (34)$$

$$\tilde{h}_t^1 = \frac{\frac{1}{M}\sum_{j=1}^{M} h(\tilde{s}_t^{j,1}, s_{t-1}^{j,N^\phi}) \tilde{w}_t^{j,1} W_{t-1}^{j,N^\phi}}{\frac{1}{M}\sum_{j=1}^{M} \tilde{w}_t^{j,1} W_{t-1}^{j,N^\phi}} \xrightarrow{a.s.} \int\int h(s_t, s_{t-1}) p_1(s_t, s_{t-1}|Y_{1:t}) ds_t ds_{t-1} \quad (35)$$

$$\bar{h}_t^1 = \frac{1}{M}\sum_{j=1}^{M} h(s_t^{j,1}, s_{t-1}^{j,N^\phi}) W_t^{j,1} \xrightarrow{a.s.} \int\int h(s_t, s_{t-1}) p_1(s_t, s_{t-1}|Y_{1:t}) ds_t ds_{t-1}. \quad (36)$$

Moreover,

$$\hat{p}_1(y_t|Y_{1:t-1}) = \frac{1}{M}\sum_{j=1}^{M} \tilde{w}_t^{j,1} W_{t-1}^{j,N^\phi} \xrightarrow{a.s.} \int p_1(y_t|s_t) p_1(s_t|Y_{1:t-1}) ds_t. \quad (37)$$

3.1.2 Algorithm 4

The convergence results for the tempering iterations rely on the following recursive assumption, which according to Lemma 1 is satisfied for $n = 2$.

Assumption 2 *For $n \geq 2$, the particle swarm $\{s_t^{j,n-1}, s_{t-1}^{j,N^\phi}, W_t^{j,n-1}\}$ generated by iteration $n-1$ of Algorithm 4 approximates:*

$$\bar{h}_t^{n-1} = \frac{1}{M}\sum_{j=1}^{M} h(s_t^{j,n-1}, s_{t-1}^{j,N^\phi}) W_t^{j,n-1} \xrightarrow{a.s.} \int\int h(s_t, s_{t-1}) p_{n-1}(s_t, s_{t-1}|Y_{1:t}) ds_t ds_{t-1} \quad (38)$$

for functions $h \in \mathcal{H}_t^{n-1}$.

The convergence results are stated in the following lemma:

Lemma 2 *Suppose that Assumption 2 is satisfied. Then for $n \geq 2$ and $h \in \mathcal{H}_t^{n-1}$:*

$$\begin{aligned} \tilde{h}_t^n &= \frac{\frac{1}{M}\sum_{j=1}^{M} h(s_t^{j,n-1}, s_{t-1}^{j,N^\phi}) \tilde{w}_t^{j,n} W_t^{j,n-1}}{\frac{1}{M}\sum_{j=1}^{M} \tilde{w}_t^{j,n} W_t^{j,n-1}} \quad (39) \\ &\xrightarrow{a.s.} \int\int h(s_t, s_{t-1}) p_n(s_t, s_{t-1}|Y_{1:t}) ds_t ds_{t-1} \\ \hat{h}_t^n &= \frac{1}{M}\sum_{j=1}^{M} h(\hat{s}_t^{j,n}, s_{t-1}^{j,N^\phi}) W_t^{j,n} \xrightarrow{a.s.} \int\int h(s_t, s_{t-1}) p_n(s_t, s_{t-1}|Y_{1:t}) ds_t ds_{t-1}. \quad (40) \end{aligned}$$

Moreover,

$$\frac{1}{M}\sum_{j=1}^{M}\tilde{w}_t^{j,n}W_t^{j,n-1} \xrightarrow{a.s.} \frac{p_n(y_t|Y_{1:t-1})}{p_{n-1}(y_t|Y_{1:t-1})} \tag{41}$$

and for $h \in \mathcal{H}_t^n$,

$$\bar{h}_t^n = \frac{1}{M}\sum_{j=1}^{M} h(s_t^{j,n}, s_{t-1}^{j,N^\phi})W_t^{j,n} \xrightarrow{a.s.} \int\int h(s_t, s_{t-1})p_n(s_t, s_{t-1}|Y_{1:t})ds_t ds_{t-1}. \tag{42}$$

The convergence in (42) implies that the recursive Assumption 2 is satisfied for iteration $n+1$ of Algorithm 4. Thus, we deduce that the convergence in (42) holds for $n = N^\phi$. This, in turn, implies that if the recursive Assumption 2 for Algorithm 1 is satisfied at the beginning of period t, it will also be satisfied at the beginning of period $t+1$. Thus, Lemmas 1 and 2 yield almost-sure approximations of the likelihood increment for every period $t = 1, \ldots, T$. Because T is fixed and $p_{N^\phi}(y_t|Y_{1:t-1}) = p(y_t|Y_{1:t-1})$, we obtain the following theorem:

Theorem 1 *Consider the nonlinear state-space model (1) with Gaussian measurement errors. Suppose that the initial particles are generated by i.i.d. sampling from* $p(s_0)$*. Then the Monte Carlo approximation of the likelihood function generated by Algorithms 1, 4, 5 is consistent in the sense of (28).*

3.2 Unbiasedness

Particle filter approximations of the likelihood function are often embedded into posterior samplers for the parameter vector θ, e.g., a Metropolis-Hastings algorithm or a SMC algorithm; see Herbst and Schorfheide (2015) for a discussion and further references in the context of DSGE models. A necessary condition for the convergence of the posterior sampler is that the likelihood approximation of the particle filter is unbiased.

Theorem 2 *Suppose that the tempering schedule is deterministic and that the number of stages* N^ϕ *is the same for each time period* $t \geq 1$*. Then, the particle filter approximation of the likelihood generated by Algorithm 1 is unbiased:*

$$\mathbb{E}\big[\hat{p}(Y_{1:T})\big] = \mathbb{E}\left[\prod_{t=1}^{T}\left(\prod_{n=1}^{N^\phi}\left(\frac{1}{M}\sum_{j=1}^{M}\tilde{w}_t^{j,n}W_t^{j,n-1}\right)\right)\right] = p(Y_{1:T}). \tag{43}$$

Our proof of Theorem 2 (see Online Appendix) exploits the recursive structure of the algorithm and extends the proof by Pitt, Silva, Giordani, and Kohn (2012) to account for the tempering iterations.

4 DSGE Model Applications

We now assess the performance of the tempered particle filter (TPF) and the bootstrap particle filter (BSPF) based on the accuracy of the likelihood approximation.[11] We consider two models in the subsequent analysis. The first is a small-scale New Keynesian DSGE model that comprises a consumption Euler equation, a New Keynesian Phillips curve, a monetary policy rule, and three exogenous shock processes. The second model is the medium-scale DSGE model by Smets and Wouters (2007), which is the core of many of the models that are used in academia and at central banks. Detailed model descriptions are provided in the Online Appendix. While the presentation of the algorithms has focused on the nonlinear state-space model (1), the numerical illustrations are based on linearized versions of the DSGE models. Linearized DSGE models (with normally distributed innovations) lead to a linear Gaussian state-space representation. This allows us to use the Kalman filter to compute the exact values of the likelihood function $p(Y_{1:T}|\theta)$ and the filtered states $\mathbb{E}[s_t|Y_{1:t}, \theta]$.

We assess the accuracy of the particle filter approximations by studying the sampling distribution of their output across N_{run} independent runs. We focus on the distribution of the log likelihood approximation error

$$\hat{\Delta} = \ln \hat{p}(Y_{1:T}|\theta) - \ln p(Y_{1:T}|\theta). \tag{44}$$

Because the particle filter approximation of the likelihood function is unbiased (see Theorem 2), Jensen's inequality applied to the concave logarithmic transformation implies that the expected value of $\hat{\Delta}$ is negative. Because there is always a trade-off between accuracy and speed, we also assess the run-time of the filters.[12] The run-time of any particle filter is sensitive to the exact computing environment used. Thus, we provide some information about the implementation in the Online Appendix. In this regard, it is important to note

[11] Some results on each filter's ability to track the filtered states are reported in the Online Appendix.

[12] The run-times reported below do not account for the fact that the user of the TPF might experiment with the choice of tuning constants. Moreover, the computing times for both filters will increase if the linear solution is replaced by a nonlinear solution. The larger the time it takes to solve the model, the smaller the percentage reduction in combined run-time for solution and filter attainable by the TPF.

that the tempered particle filter is designed to work with a small number of particles (i.e., on a desktop computer). Therefore, we restrict the computing environment to a single machine, and we do not try to leverage large-scale parallelism via a computing cluster, as in Gust, Herbst, Lopez-Salido, and Smith (2017).

As described in Section 2.3, implementing the bootstrap particle filter requires choosing the number of particles M, while the tempered particle filter requires additionally choosing the tuning parameters r^*, c_*, and N^{MH}. We discuss these choices and their effect on the accuracy of the filters below. Results for the small-scale New Keynesian DSGE model are presented in Section 4.1 and results for the Smets-Wouters model appear in Section 4.2.

4.1 A Small-Scale DSGE Model

We first use the BSPF and the TPF to evaluate the likelihood function associated with the small-scale New Keynesian DSGE model used in Herbst and Schorfheide (2015). From the perspective of the particle filter, the key feature of the model is that it has three observables (output growth, inflation, and the federal funds rate). To facilitate the use of particle filters, we augment the measurement equations by independent measurement errors, whose standard deviations we set to be 20% of the standard deviation of the observables.[13]

Great Moderation Sample. The data span is 1983Q1 to 2002Q4, for a total of 80 observations for each series. We assess the performance of the particle filters for two parameter vectors, which are denoted by θ^m and θ^l and tabulated in Table 1. The value θ^m is chosen as a high likelihood point, close to the posterior mode of the model. The log likelihood at θ^m is $\ln p(Y|\theta^m) = -306.49$. The second parameter value, θ^l, is chosen to be associated with a lower log-likelihood value. Based on our choice, $\ln p(Y|\theta^l) = -313.36$. The sample and the parameter values are identical to those used in Chapter 8 of Herbst and Schorfheide (2015).

We compare the BSPF with two variants of the TPF, which differ with respect to the targeted inefficiency ratio: $r^* = 2$ and $r^* = 3$. For the BSPF, we use $M = 40,000$ particles, and for the TPF, we consider $M = 4,000$ and $M = 40,000$ particles, respectively. In Algorithm 3, we use $N^{MH} = 1$ Metropolis-Hastings steps and set the initial scale of the proposal covariance matrix to $c_* = 0.3$. We also report results for two related algorithms. The first algorithm is the resample-move variant of the bootstrap particle filter (RMPF) described in Section 2.3 which sets $r^* = \infty$. This algorithm does not utilize any bridge

[13]The measurement error standard deviations are 0.1160 for output growth, 0.2942 for inflation, and 0.4476 for the interest rates.

Table 1: Small-Scale Model: Parameter Values

Parameter	θ^m	θ^l	Parameter	θ^m	θ^l
τ	2.09	3.26	κ	0.98	0.89
ψ_1	2.25	1.88	ψ_2	0.65	0.53
ρ_r	0.81	0.76	ρ_g	0.98	0.98
ρ_z	0.93	0.89	$r^{(A)}$	0.34	0.19
$\pi^{(A)}$	3.16	3.29	$\gamma^{(Q)}$	0.51	0.73
σ_r	0.19	0.20	σ_g	0.65	0.58
σ_z	0.24	0.29	$\ln p(Y\|\theta)$	-306.5	-313.4

distributions, but unlike the BSPF it involves a mutation step that changes the particle values. The second algorithm is the conditionally-optimal particle filter (COPF). While the implementation of the COPF is generally infeasible for nonlinear DSGE models, in case of a linearized model we can directly sample from $p(s_t|y_t, s_{t-1}^j)$ using a Kalman filter updating step and compare the accuracy of the proposed TPF to this infeasible benchmark.

Figure 1 displays density estimates based on $N_{run} = 100$ for the sampling distribution of $\hat{\Delta}$ associated with the BSPF and the four variants of the TPF for $\theta = \theta^m$ (left panel) and $\theta = \theta^l$ (right panel). For $\theta = \theta^m$, the $TPF(r^* = 2)$ with $M = 40,000$ (the green line) is the most accurate of all the filters considered, with $\hat{\Delta}$ distributed tightly around zero. The distribution of $\hat{\Delta}$ associated with $TPF(r^* = 3)$ with $M = 40,000$ is slightly more disperse, with a larger left tail, as the higher tolerance for particle inefficiency translates into a higher variance for the likelihood estimate. Reducing the number of particles to $M = 4,000$ for both of these filters results in a higher variance estimate of the likelihood. The most poorly performing TPF (with $r^* = 3$ and $M = 4,000$) is associated with a distribution for $\hat{\Delta}$ that is similar to the one associated with the BSPF that uses $M = 40,000$. Overall, the TPF compares favorably with the BSPF when $\theta = \theta^m$. The performance differences become even more stark when we consider $\theta = \theta^l$; depicted in the right panel of Figure 1. While the sampling distributions indicate that the likelihood estimates are less accurate for all the particles filters, the BSPF deteriorates by the largest amount. The TPF, by targeting an inefficiency ratio, adaptively adjusts to account for the relatively worse fit of θ^l.

Table 2 displays summary statistics for the likelihood approximation errors as well as information about the average number of stages and run time of each filter. We compute the mean-squared error (MSE), the bias, and the variance of $\hat{\Delta}$ across $N_{run} = 200$ runs. For each r^*, we run two versions of the TPF: one with same number of particles as the BSPF

Figure 1: Small-Scale Model: Distribution of Log-Likelihood Approximation Errors

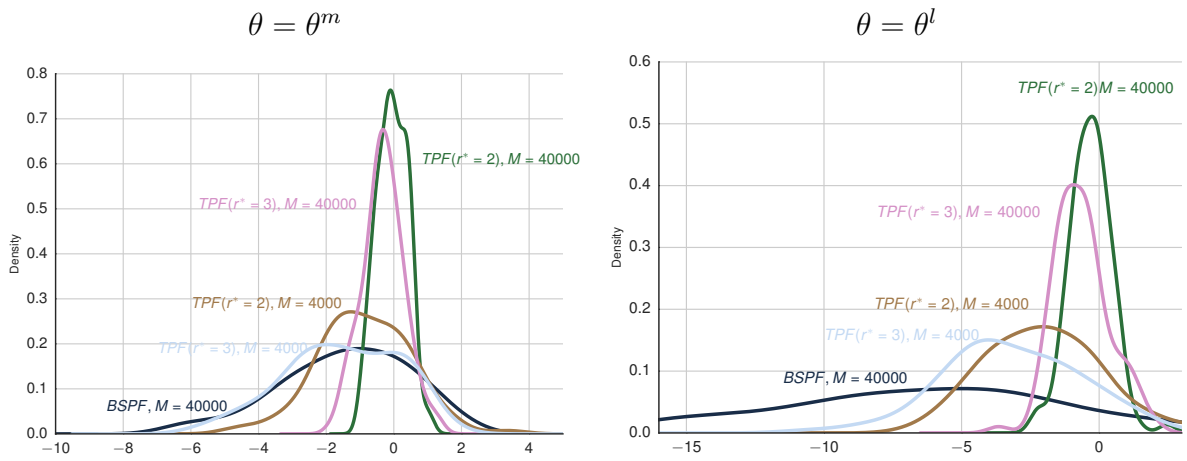

Notes: Density estimate of $\hat{\Delta} = \ln \hat{p}(Y_{1:T}|\theta) - \ln p(Y_{1:T}|\theta)$ based on $N_{run} = 100$ runs of the particle filter.

($M = 40,000$) and one with M calibrated so that the respective TPF has approximately the same run time as the BSPF. The results convey essentially the same story as Figure 1. Using a resample-move step without the bridge distribution (RMPF) leads to only a slightly more accurate likelihood estimate than the BSPF, despite having a sustantially longer run time (we are using $N^{MH} = 10$ for this algorithm). The generally infeasible COPF with $M = 400$ particles is an order of magnitude more accurate than all the other filters. Thus, while the use of the tempering iterations leads to a significant improvement in accuracy, it remains substantially worse than the COPF. The results in Table 2 are comparable to those reported in Table 8.2 of Herbst and Schorfheide (2015). For the COPF the numbers are very similar, while for the BSPF the differences are a bit larger. The discrepancies are due to the fact that we are computing the means and standard deviations of the approximation errors based on "only" $N_{run} = 200$ independent runs of the algorithms. In Table 8.2 of Herbst and Schorfheide (2015) we also showed results for an auxiliary PF (see Pitt and Shephard (1999) and Doucet and Johansen (2011)), but we found that the auxiliary PF did not improve much over the BSPF.

The row labeled $T^{-1}\sum_{t=1}^{T} N_t^{\phi}$ shows the average number of tempering iterations associated with each particle filter. The BSPF has, by construction, always an average of one. When $r^* = 2$, the TPFs uses on average 4.3 stages per time period. With a higher tolerance for inefficiency, when $r^* = 3$, the average number of stages falls to 3.2. Note that when considering θ^l, the TPF always uses a slightly larger number of stages, reflecting the relatively

Table 2: Small-Scale Model: PF Summary Statistics

	BSPF	TPF				RMPF	COPF
Number of Particles M	40,000	7,000	8,500	40,000	40,000	40,000	400
Target Ineff. Ratio r^*		2	3	2	3	∞	
High Posterior Density: $\theta = \theta^m$							
MSE($\hat{\Delta}$)	6.49	1.77	2.63	0.26	0.32	4.90	0.14
Bias($\hat{\Delta}$)	-1.52	-0.71	-0.90	-0.17	-0.16	-1.19	-0.11
Variance($\hat{\Delta}$)	4.18	1.27	1.82	0.23	0.29	3.48	0.12
$T^{-1}\sum_{t=1}^{T} N_{\phi,t}$	1.00	4.31	3.24	4.31	3.24	1.00	0.00
Average Run Time (sec)	0.48	0.52	0.48	2.92	2.26	2.05	0.02
Low Posterior Density: $\theta = \theta^l$							
MSE($\hat{\Delta}$)	75.33	6.86	11.52	1.25	2.29	52.06	0.23
Bias($\hat{\Delta}$)	-6.93	-1.94	-2.64	-0.49	-0.85	-5.86	-0.19
Variance($\hat{\Delta}$)	27.30	3.09	4.53	1.01	1.57	17.76	0.19
$T^{-1}\sum_{t=1}^{T} N_{\phi,t}$	1.00	4.36	3.29	4.35	3.28	1.00	0.00
Average Run Time (sec)	0.47	0.49	0.46	2.70	2.02	2.16	0.02

Notes: The results are based on $N_{run} = 200$ independent runs of the particle filters. The log likelihood discrepancy is defined as $\hat{\Delta} = \ln \hat{p}(Y_{1:T}|\theta) - \ln p(Y_{1:T}|\theta)$.

worse fit of the model under $\theta = \theta^l$ compared with $\theta = \theta^m$.

Table 2 also displays the average run time of each filter (in seconds). When using the same number of $M = 40,000$ particles, the BSPF runs much more quickly than the TPFs, reflecting the fact that the additional tempering iterations require many more likelihood evaluations, in addition to the computational costs associated with the mutation phase. However, holding computational time fixed, the TPFs deliver much more accurate approximations, as evident in the results in columns (3) and (4). For θ^m the two configurations of the TPF are able to achieve MSE reductions by 73% and 59%, respectively. For θ^l the MSE reductions increase to 90% and 85% respectively.[14]

Great Recession Sample. We previously pointed out that the BSPF is very sensitive to outliers. To examine the extent to which this is also true for the TPF, we re-run the previous experiments on the sample 2003Q1 to 2013Q4. This period includes the Great Recession, which was a large outlier from the perspective of the small-scale DSGE model (and most other econometric models). Figure 2 plots the density of the approximation errors of the

[14]Some results on the accuracy of the filtered states are provided in the Online Appendix.

Figure 2: Small-Scale Model: Distribution of Log-Likelihood Approximation Errors, Great Recession Sample

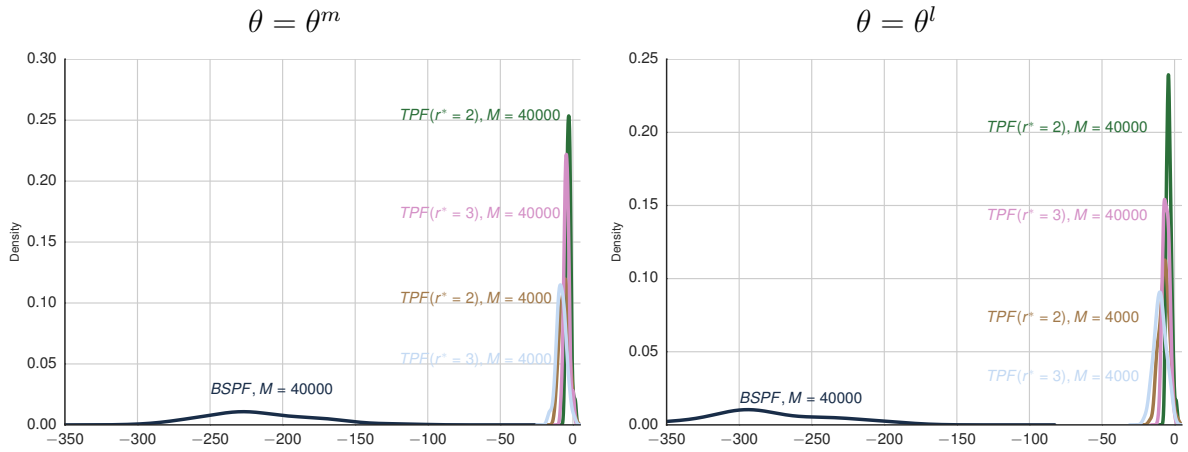

Notes: Density estimate of $\hat{\Delta} = \ln \hat{p}(Y_{1:T}|\theta) - \ln p(Y_{1:T}|\theta)$ based on $N_{run} = 100$ runs of the particle filters.

log likelihood estimates associated with each of the filters. The difference in the distribution of approximation errors between the BSPF and the TPFs is massive. For $\theta = \theta^m$ and $\theta = \theta^l$, the approximation errors associated with the BSPF are concentrated in the range of -200 to -300, almost two orders of magnitude larger than the errors associated with the TPFs. This happens because the large drop in output in 2008Q4 is not predicted by the forward simulation in the BSPF. In turn, the filter collapses, in the sense that the likelihood increment in that quarter is estimated using essentially only one particle.

Table 3 tabulates the results for each of the filters. Consistent with Figure 2, the MSEs associated with the log-likelihood estimate of the BSPF are $47,534$ and $79,473$ for $\theta = \theta^m$ and $\theta = \theta^l$, respectively, compared to 85 and 150 for the better of the two TPF configurations, holding computational time fixed. If we increase the number of particles to $M = 40,000$, then for $\theta = \theta^m$ the $TPF(r^* = 2)$ with has an MSE of 33, which is about 1,425 times smaller than the BSPF and only raises the computational time by a factor of 10. A key driver of this result is the adaptive nature of the TPF. While the average number of stages used is about 5 for $r^* = 2$ and 4 for $r^* = 3$, for $t = 2008Q4$ – the period with the largest outlier – the TPF uses about 15 stages, on average.

Figure 3 provides an illustration of why the TPF provides much more accurate approximations than the BSPF. We focus on one particular state, namely model-implied output growth, which is observed output growth minus its measurement error. We focus on $t = 2008Q4$. The

Table 3: Small-Scale Model: PF Summary Statistics – The Great Recession

	BSPF	TPF			
Number of Particles M	40,000	5,500	7,000	40,000	40,000
Target Ineff. Ratio r^*		2	3	2	3
High Posterior Density: $\theta = \theta^m$					
MSE($\hat{\Delta}$)	47,533.80	85.02	143.88	33.37	66.99
Bias($\hat{\Delta}$)	-215.22	-8.54	-11.49	-5.33	-7.74
Variance($\hat{\Delta}$)	1,215.88	12.08	11.78	4.94	7.08
$T^{-1}\sum_{t=1}^{T} N_{\phi,t}$	1.00	5.13	3.88	5.10	3.86
Average Run Time (sec)	0.26	0.27	0.27	2.02	1.42
Low Posterior Density: $\theta = \theta^l$					
MSE($\hat{\Delta}$)	79,473.19	150.63	244.44	64.03	116.84
Bias($\hat{\Delta}$)	-278.88	-11.72	-15.14	-7.62	-10.47
Variance($\hat{\Delta}$)	1,700.42	13.25	15.14	5.92	7.20
$T^{-1}\sum_{t=1}^{T} N_{\phi,t}$	1.00	5.36	4.06	5.32	4.04
Average Run Time (sec)	0.27	0.29	0.28	2.12	1.49

Notes: The results are based on $N_{run} = 200$ independent runs of the particle filters. The log likelihood discrepancy is defined as $\hat{\Delta} = \ln \hat{p}(Y_{1:T}|\theta) - \ln p(Y_{1:T}|\theta)$.

Figure 3: Small-Scale Model: BSPF versus TPF in 2008Q4

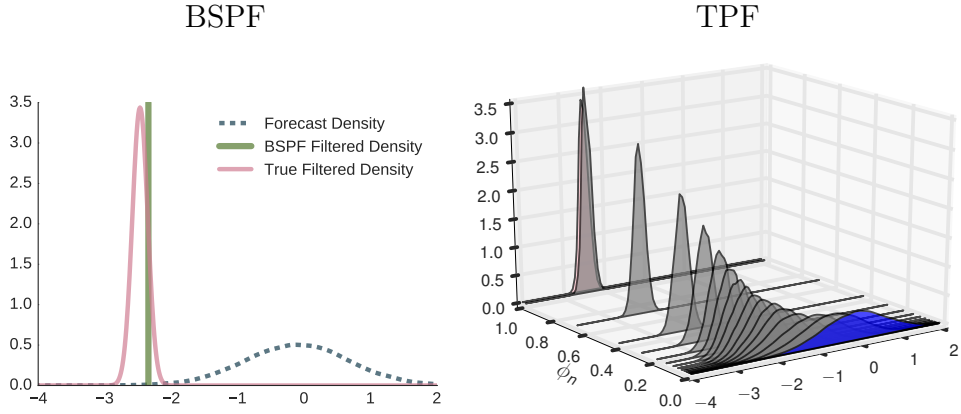

Notes: Here $t = 2008Q4$ and s_t equals model-implied output growth. Left panel: forecast density $\hat{p}(s_t|Y_{1:t-1})$, BSPF filtered density $\hat{p}(s_t|Y_{1:t})$, and true filtered density $p(s_t|Y_{t-1})$. Right panel: forecast density $\hat{p}(s_t|Y_{1:t-1})$ (blue), waterfall plot of density estimates $\hat{p}_n(s_t|Y_{1:t})$ for $n = 1, \ldots, N_t^{\phi}$, and true filtered density $p(s_t|Y_{1:t})$ (red).

left panel depicts the BSPF approximations $\hat{p}(s_t|Y_{1:t-1})$ and $\hat{p}(s_t|Y_{1:t})$ as well as the "true" density $p(s_t|Y_{1:t})$. The BSPF essentially generates draws from the forecast density $\hat{p}(s_t|Y_{1:t-1})$

and reweights them to approximate the density $p(s_t|Y_{1:t})$. In 2008Q4, these densities have very little overlap. This implies that essentially one draw from the forecast density receives all the weight and the BSPF filtered density is a point mass. This point mass provides a poor approximation of $p(s_t|Y_{1:t})$.

The right panel of Figure 3 displays a waterfall plot of density estimates $\hat{p}_n(s_t|Y_{1:t})$ for $n = 1, \ldots, N_t^\phi = 15$. The densities are placed on the y-axis at the corresponding value of $\phi_{n,t}$. The first iteration in the tempering phase has $\phi_{1,t} = 0.002951$, which corresponds to an inflation of the measurement error variance by a factor over 300. This density looks similar to the predictive distribution $p(s_t|Y_{1:t-1})$, with a 1-step-ahead prediction for output growth of about -1% (in quarterly terms). As we move through the iterations, $\phi_{n,t}$ increases slowly at first and $\hat{p}_n(s_t|Y_{1:t})$ gradually adds more density where $s_t \approx -2.5$. Each correction step of Algorithm 2 requires only modest reweighting of the particles and the mutation steps refresh the particle values. The filter begins to tolerate relatively large changes from $\phi_{n,t}$ to $\phi_{n+1,t}$, as more particles lie in this region, needing only three stages to move from $\phi_{n,t} \approx 0.29$ to 1. Alongside $\hat{p}_{N_t^\phi}(s_t|Y_{1:t})$ we also show the true filtered density in red, obtained from the Kalman filter recursions. The TPF approximation at $n = N_t^\phi$ matches the true density extremely well.

4.2 The Smets-Wouters Model

We next assess the performance of the tempered particle filter for the Smets and Wouters (2007), henceforth SW, model. This model forms the core of the latest vintage of DSGE models. We estimate the model over the period 1966Q1 to 2004Q4 using seven observables: real per capita growth rates of output, consumption, investment, wages; hours worked; inflation; and the federal funds rate. The SW model has a high-dimensional state space s_t with more than a dozen state variables. The performance of the BSPF deteriorates quickly due to the increased state space and the fact that it is much more difficult to predict seven observables than it is to predict three observables with a DSGE model. As a consequence, the estimation of nonlinear variants of the SW model has proven to be extremely difficult.

We compute the particle filter approximations conditional on two sets of parameter values: θ^m and θ^l. θ^m is the parameter vector associated with the highest likelihood value among the draws that we generated with a posterior sampler. θ^l is a parameter vector that attains a lower likelihood value. The log-likelihood difference between the two parameter vectors is approximately 13. The standard deviations of the measurement errors are chosen

Figure 4: Smets-Wouters Model: Distribution of Log-Likelihood Approximation Errors

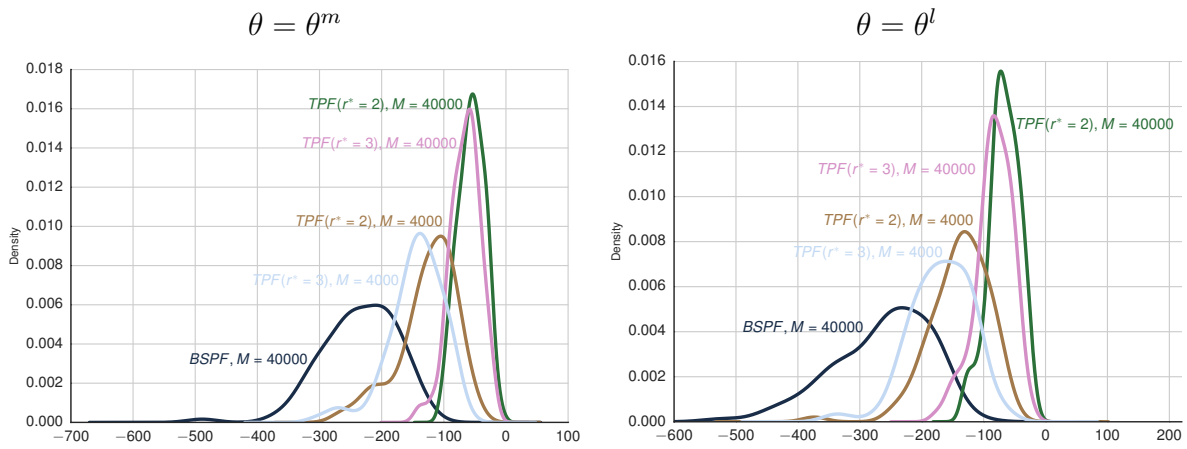

Notes: Density estimate of $\hat{\Delta} = \ln \hat{p}(Y_{1:T}|\theta^m) - \ln p(Y_{1:T}|\theta^m)$ based on $N_{run} = 100$ runs of the particle filters and $N^{MH} = 10$.

to be approximately 20% of the sample standard deviation of the time series.[15] For comparison purposes, the parameter values and the data are identical to the ones used in Chapter 8 of Herbst and Schorfheide (2015) and their values are tabulated in the Online Appendix.

For the small-scale New Keynesian model we only used one mutation step at each tempering stage, i.e., $N^{MH} = 1$, which worked well. After some experimentation with the SW model, we increased the number of mutation steps to $N^{MH} = 10$. This allows the particles to better adapt to the current density because it increases the probability that their values change. The subsequently-reported results are based on $N^{MH} = 10$, whereas results for $N^{MH} = 1$ are relegated to the Online Appendix.

Figure 4 displays density estimates of the approximation errors associated with the log-likelihood estimates under $\theta = \theta^m$ and $\theta = \theta^l$. We use $M = 40,000$ particles for the BSPF. For the TPF, we use $M = 4,000$ or $M = 40,000$, consider $r^* = 2$ and $r^* = 3$ and set $c_* = 0.3$ in the mutation step. Under both parameter values, the BSPF exhibits the most bias, with its likelihood estimates substantially below the true likelihood value. The distribution of the bias falls mainly between -400 and -100. Thus, drawing from the posterior distribution of the SW model using a particle MCMC algorithm based on the BSPF, would be nearly impossible. The TPFs perform better, although they also underestimate the likelihood by a

[15]The standard deviations for the measurement errors are 0.1731 (output growth), 0.1394 (consumption growth), 0.4515 (investment growth), 0.1128 (wage growth), 0.5838 (log hours), 0.1230 (inflation), and 0.1653 (interest rates).

Table 4: SW Model: PF Summary Statistics

	BSPF	TPF			
Number of Particles M	40,000	2,000	2,800	40,000	40,000
Target Ineff. Ratio r^*		2	3	2	3
High Posterior Density: $\theta = \theta^m$					
MSE($\hat{\Delta}$)	63,881.68	1,164.15	1,135.35	57.79	93.05
Bias($\hat{\Delta}$)	-245.64	-30.94	-30.41	-6.55	-8.51
Variance($\hat{\Delta}$)	3,543.79	206.58	210.51	14.92	20.56
$T^{-1}\sum_{t=1}^{T} N_{\phi,t}$	1.00	6.12	4.69	6.07	4.68
Average Run Time (sec)	3.33	3.00	3.49	62.57	48.85
Low Posterior Density: $\theta = \theta^l$					
MSE($\hat{\Delta}$)	69,612.88	1,489.59	1,993.62	108.39	191.56
Bias($\hat{\Delta}$)	-255.06	-36.20	-41.66	-9.36	-12.36
Variance($\hat{\Delta}$)	4,559.09	179.24	258.30	20.82	38.88
$T^{-1}\sum_{t=1}^{T} N_{\phi,t}$	1.00	6.18	4.76	6.14	4.71
Average Run Time (sec)	3.28	3.34	3.33	63.98	49.56

Notes: Results are based on $N_{run} = 200$ independent runs of the particle filters and $N_{MH} = 10$. The log likelihood discrepancy is defined as $\hat{\Delta} = \ln \hat{p}(Y_{1:T}|\theta) - \ln p(Y_{1:T}|\theta)$.

large amount.

Table 4 underscores the results in Figure 4. The best-performing TPF reduces the MSE in the log-likelihood approximation for θ^m from 63,881.68 to 58 for θ^m. This increased performance comes at a computational cost: the $TPF(r^* = 2), M = 40,000$ filter takes about 62 seconds, while the BSPF takes only about 3 seconds. However, even if we reduce the number of particles for the TPFs to achieve approximately the same run time as the BSPF (see columns 3 and 4), the TPFs come out ahead by a wide margin. Across the two parameter values and the two filter specifications, the TPF still is able to reduce the MSE by a factor of at least 35. We conclude that holding computational time fixed, tempering leads to a significant improvement in the accuracy of the likelihood approximation.

5 Conclusion

We developed a particle filter that automatically adapts the proposal distribution for the particles s_t^j to the current observation y_t. We start with a forward simulation of the state-transition equation under an inflated measurement error variance and then gradually reduce

the variance to its nominal level. In each step, the particle values and weights change so that the distribution slowly adapts to $p(s_t^j|y_t, s_{t-1}^j)$. We demonstrate in two DSGE model applications that controlling for run time the algorithm generates significantly more accurate approximations than the standard bootstrap particle filter, in particular in instances in which the model generates very inaccurate one-step-ahead predictions of y_t. The tempering iterations can also be used to improve a particle filter with a more general initial proposal distribution than the BSPF. Moreover, our filter can be easily embedded in particle MCMC algorithms.

References

Andreasen, M. M. (2013): "Non-Linear DSGE Models and the Central Difference Kalman Filter," *Journal of Applied Econometrics*, 28(6), 929–955.

Andrieu, C., A. Doucet, and R. Holenstein (2010): "Particle Markov Chain Monte Carlo Methods," *Journal of the Royal Statistical Society Series B*, 72(3), 269–342.

Arulampalam, S., S. Maskell, N. Gordon, and T. Clapp (2002): "A Tutorial on Particle Filters for Online Nonlinear/Non-Gaussian Bayesian Tracking," *IEEE Transactions on Signal Processing*, 50(2), 174–188.

Beskos, A., A. Jasra, N. Kantas, and A. H. Thiery (2014): "On the Convergence of Adaptive Sequential Monte Carlo Methods," *arXiv Working Paper*.

Bognanni, M., and E. P. Herbst (2015): "Estimating (Markov-Switching) VAR Models without Gibbs Sampling: A Sequential Monte Carlo Approach," *Finance and Economics Discussion Paper Series, Board of Governors*, 2015-116(116), 154.

Cappé, O., S. J. Godsill, and E. Moulines (2007): "An Overview of Existing Methods and Recent Advances in Sequential Monte Carlo," *Proceedings of the IEEE*, 95(5), 899–924.

Cappé, O., E. Moulines, and T. Ryden (2005): *Inference in Hidden Markov Models*. Springer Verlag, New York.

Chopin, N. (2002): "A Sequential Particle Filter for Static Models," *Biometrika*, 89(3), 539–551.

——— (2004): "Central Limit Theorem for Sequential Monte Carlo Methods and Its Application to Bayesian Inference," *Annals of Statistics*, 32(6), 2385–2411.

Creal, D. (2007): "Sequential Monte Carlo Samplers for Bayesian DSGE Models," *Manuscript, University Chicago Booth*.

——— (2012): "A Survey of Sequential Monte Carlo Methods for Economics and Finance," *Econometric Reviews*, 31(3), 245–296.

Del Moral, P. (2004): *Feynman-Kac Formulae*. Springer Verlag.

——— (2013): *Mean Field Simulation for Monte Carlo Integration*. Chapman & Hall/CRC, Boca Raton.

Del Moral, P., A. Doucet, and A. Jasra (2006): "Sequential Monte Carlo Samplers," *Journal of the Royal Statistical Society, Series B*, 68(Part 3), 411–436.

——— (2012): "An AdaptiveSequential Monte Carlo Method for Approximate Bayesian Computation," *Statistical Computing*, 22, 1009–1020.

Doucet, A., and A. M. Johansen (2011): "A Tutorial on Particle Filtering and Smoothing: Fifteen Years Later," in *Handook of Nonlinear Filtering*, ed. by D. Crisan, and B. Rozovsky. Oxford University Press, Oxford.

Durham, G., and J. Geweke (2014): "Adaptive Sequential Posterior Simulators for Massively Parallel Computing Environments," in *Advances in Econometrics*, ed. by I. Jeliazkov, and D. Poirier, vol. 34, chap. 6, pp. 1–44. Emerald Group Publishing Limited, West Yorkshire.

Fernández-Villaverde, J., and J. F. Rubio-Ramírez (2007): "Estimating Macroeconomic Models: A Likelihood Approach," *Review of Economic Studies*, 74(4), 1059–1087.

Geweke, J., and B. Frischknecht (2014): "Exact Optimization By Means of Sequentially Adaptive Bayesian Learning," *Mimeo*.

Godsill, S. J., and T. Clapp (2001): "Improvement Strategies for Monte Carlo Particle Filters," in *Sequential Monte Carlo Methods in Practice*, ed. by A. Doucet, N. De Freitas, and N. Gordon, pp. 139–158. Springer Verlag, New York.

Gordon, N., D. Salmond, and A. F. Smith (1993): "Novel Approach to Nonlinear/Non-Gaussian Bayesian State Estimation," *Radar and Signal Processing, IEE Proceedings F*, 140(2), 107–113.

Gust, C., E. Herbst, D. Lopez-Salido, and M. E. Smith (2017): "The Empirical Implications of the Interest-Rate Lower Bound," *American Economic Review*, forthcoming.

Herbst, E., and F. Schorfheide (2014): "Sequential Monte Carlo Sampling for DSGE Models," *Journal of Applied Econometrics*, 29(7), 1073–1098.

——— (2015): *Bayesian Estimation of DSGE Models*. Princeton University Press, Princeton.

Jasra, A., D. A. Stephens, A. Doucet, and T. Tsagaris (2011): "Inference for Levy-Driven Stochastic Volatility Models via Adaptive Sequential Monte Carlo," *Scandinavian Journal of Statistics*, 38, 1–22.

Johansen, A. M. (2016): "On Blocks, Tempering and Particle MCMC for Systems Identification," *Manuscript, University of Warwick*.

Kollmann, R. (2015): "Tractable Latent State Filtering for Non-Linear DSGE Models Using a Second-Order Approximation and Pruning," *Computational Economics*, 45(2), 239–260.

Liu, J. S. (2001): *Monte Carlo Strategies in Scientific Computing*. Springer Verlag, New York.

Neal, R. M. (1998): "Annealed Importance Sampling," *Technical Report, Department of Statistics, University of Toronto*, 9805.

Pitt, M. K., and N. Shephard (1999): "Filtering via Simulation: Auxiliary Particle Filters," *Journal of the American Statistical Association*, 94(446), 590–599.

Pitt, M. K., R. d. S. Silva, P. Giordani, and R. Kohn (2012): "On Some Properties of Markov Chain Monte Carlo Simulation Methods Based on the Particle Filter," *Journal of Econometrics*, 171(2), 134–151.

Schäfer, C., and N. Chopin (2013): "Sequential Monte Carlo on Large Binary Sampling Spaces," *Statistical Computing*, 23, 163–184.

Smets, F., and R. Wouters (2007): "Shocks and Frictions in U.S. Business Cycles: A Bayesian DSGE Approach," *American Economic Review*, 97(3), 586–608.

White, H. (2001): *Asymptotic Theory For Econometricians*. Academic Press, New York.

Zhou, Y., A. M. Johansen, and J. A. Aston (2015): "Towards Automatic Model Comparison: An Adaptive Sequential Monte Carlo Approach," *arXiv Working Paper*, 1303.3123v2.

Online Appendix for *Tempered Particle Filtering*

Edward Herbst and Frank Schorfheide

A Theoretical Derivations

A.1 Monotonicity of Inefficiency Ratio

Recall the definitions

$$e_{j,t} = \frac{1}{2}(y_t - \Psi(s_t^{j,n-1}))'\Sigma_u^{-1}(y_t - \Psi(s_t^{j,n-1}))$$

and

$$\tilde{w}_t^{j,n}(\phi_n) = \left(\frac{\phi_n}{\phi_{n-1}}\right)^{n_y/2} \exp[-(\phi_n - \phi_{n-1})e_{j,t}].$$

Provided that the particles had been resampled and $W_t^{j,n-1} = 1$, the inefficiency ratio can be manipulated as follows:

$$\begin{aligned}
\text{InEff}(\phi_n) &= \frac{\frac{1}{M}\sum_{j=1}^M \left(\tilde{w}_t^{j,n}(\phi_n)\right)^2}{\left(\frac{1}{M}\sum_{j=1}^M \tilde{w}_t^{j,n}(\phi_n)\right)^2} \\
&= \frac{\frac{1}{M}\sum_{j=1}^M \left(\frac{\phi_n}{\phi_{n-1}}\right)^{n_y} \exp[-2(\phi_n - \phi_{n-1})e_{j,t}]}{\left(\frac{1}{M}\sum_{j=1}^M \left(\frac{\phi_n}{\phi_{n-1}}\right)^{n_y/2} \exp[-(\phi_n - \phi_{n-1})e_{j,t}]\right)^2} \\
&= \frac{\frac{1}{M}\sum_{j=1}^M \exp[-2(\phi_n - \phi_{n-1})e_{j,t}]}{\left(\frac{1}{M}\sum_{j=1}^M \exp[-(\phi_n - \phi_{n-1})e_{j,t}]\right)^2} \\
&= \frac{A_1(\phi_n)}{A_2(\phi_n)}.
\end{aligned}$$

Note that for $\phi_n = \phi_{n-1}$, we obtain $ESS(\phi_n) = 1$. We now will show that the inefficiency ratio is monotonically increasing on the interval $\phi_n \in [\phi_{n-1}, 1]$. Differentiating with respect

to ϕ_n yields (we use the superscript (1) to denote first derivatives):

$$\text{InEff}^{(1)}(\phi_n) = \frac{A_1^{(1)}(\phi_n)A_2(\phi_n) - A_1(\phi_n)A_2^{(1)}(\phi_n)}{[A_2(\phi_n)]^2},$$

where

$$\begin{aligned} A_1^{(1)}(\phi_n) &= -\frac{2}{M}\sum_{j=1}^{M} e_{j,t}\exp[-2(\phi_n - \phi_{n-1})e_{j,t}] \\ A_2^{(1)}(\phi_n) &= \left(\frac{2}{M}\sum_{j=1}^{M}\exp[-(\phi_n - \phi_{n-1})e_{j,t}]\right)\left(-\frac{1}{M}\sum_{j=1}^{M} e_{j,t}\exp[-(\phi_n - \phi_{n-1})e_{j,t}]\right). \end{aligned}$$

The denominator in $\text{InEff}^{(1)}(\phi_n)$ is always non-negative and strictly different from zero. Thus, we can focus on the numerator:

$$\begin{aligned} &A_1^{(1)}(\phi_n)A_2(\phi_n) - A_1(\phi_n)A_2^{(1)}(\phi_n) \\ &= \left(-\frac{2}{M}\sum_{j=1}^{M} e_{j,t}\exp[-2(\phi_n - \phi_{n-1})e_{j,t}]\right)\left(\frac{1}{M}\sum_{j=1}^{M}\exp[-(\phi_n - \phi_{n-1})e_{j,t}]\right)^2 \\ &\quad - \left(\frac{1}{M}\sum_{j=1}^{M}\exp[-2(\phi_n - \phi_{n-1})e_{j,t}]\right)\left(\frac{2}{M}\sum_{j=1}^{M}\exp[-(\phi_n - \phi_{n-1})e_{j,t}]\right) \\ &\quad \times\left(-\frac{1}{M}\sum_{j=1}^{M} e_{j,t}\exp[-(\phi_n - \phi_{n-1})e_{j,t}]\right) \\ &= 2\left(\frac{1}{M}\sum_{j=1}^{M}\exp[-(\phi_n - \phi_{n-1})e_{j,t}]\right) \\ &\quad \times\Bigg[\left(\frac{1}{M}\sum_{j=1}^{M}\exp[-2(\phi_n - \phi_{n-1})e_{j,t}]\right)\left(\frac{1}{M}\sum_{j=1}^{M} e_{j,t}\exp[-(\phi_n - \phi_{n-1})e_{j,t}]\right) \\ &\quad - \left(\frac{1}{M}\sum_{j=1}^{M} e_{j,t}\exp[-2(\phi_n - \phi_{n-1})e_{j,t}]\right)\left(\frac{1}{M}\sum_{j=1}^{M}\exp[-(\phi_n - \phi_{n-1})e_{j,t}]\right)\Bigg]. \end{aligned}$$

To simplify the notation, we now write e_j instead of $e_{j,t}$, let $\lambda = \phi_n - \phi_{n-1} \geq 0$, and define

$$x_j = \exp[-(\phi_n - \phi_{n-1})e_j] = \frac{1}{\exp[\lambda e_j]}.$$

Note that $0 < x_j \leq 1$ and $e_j \geq 0$. We scale the numerator of $\text{InEff}^{(1)}(\phi_n)$ by $M^3/2$, which leads to

$$\begin{aligned}
&\frac{M^3}{2}\left[A^{(1)}(\phi_n)A_2(\phi_n) - A_1(\phi_n)A_2^{(1)}(\phi_n)\right] \\
&= \left(\sum_{j=1}^{M} x_j\right)\left[\left(\sum_{j=1}^{M} x_j^2\right)\left(\sum_{j=1}^{M} e_j x_j\right) - \left(\sum_{j=1}^{M} e_j x_j^2\right)\left(\sum_{j=1}^{M} x_j\right)\right].
\end{aligned}$$

Thus, the sign of $\text{InEff}^{(1)}(\phi_n)$ is determined by the sign of

$$\Delta_M = \left(\sum_{j=1}^{M} e_j x_j\right)\left(\sum_{j=1}^{M} x_j^2\right) - \left(\sum_{j=1}^{M} e_j x_j^2\right)\left(\sum_{j=1}^{M} x_j\right).$$

Consider the special case of $M = 2$:

$$\begin{aligned}
\Delta_M &= +e_1x_1x_1^2 + e_1x_1x_2^2 + e_2x_2x_1^2 + e_2x_2x_2^2 \\
&\quad -e_1x_1^2x_1 - e_1x_1^2x_2 - e_2x_2^2x_1 - e_2x_2^2x_2 \\
&= e_1x_1x_2(x_2 - x_1) + e_2x_1x_2(x_1 - x_2) \\
&= x_1x_2(x_2 - x_1)(e_1 - e_2) \\
&= x_1x_2\left(\frac{1}{\exp[\lambda e_2]} - \frac{1}{\exp[\lambda e_1]}\right)(e_1 - e_2) \\
&\geq 0,
\end{aligned}$$

because for any $\lambda \geq 0$

$$\text{sign}\left(\frac{1}{\exp[\lambda e_2]} - \frac{1}{\exp[\lambda e_1]}\right) = \text{sign}(e_1 - e_2).$$

Now consider the general case:

$$\begin{aligned}
\Delta_M &= \sum_{j=1}^{M}\sum_{l=1}^{M} e_j x_j x_l^2 - \sum_{j=1}^{M}\sum_{l=1}^{M} e_j x_j^2 x_l \\
&= \sum_{j=1}^{M}\sum_{l\neq j} e_j x_j x_l^2 - \sum_{j=1}^{M}\sum_{l\neq j} e_j x_j^2 x_l \\
&= \sum_{j=1}^{M}\sum_{l\neq j} e_j x_j x_l (x_l - x_j) \\
&= \sum_{j=1}^{M}\sum_{l<j} e_j x_j x_l (x_l - x_j) + \sum_{l=1}^{M}\sum_{j<l} e_j x_j x_l (x_l - x_j) \\
&= \sum_{j=1}^{M}\sum_{l<j} e_j x_j x_l (x_l - x_j) + \sum_{j=1}^{M}\sum_{l<j} e_l x_l x_j (x_j - x_l) \\
&= \sum_{j=1}^{M}\sum_{l<j} e_j x_j x_l (x_l - x_j)(e_j - e_l)
\end{aligned}$$

The manipulations are similar to the case of $M = 2$. The first equality is obtained from the definition of Δ_M. The second equality is obtained by noticing that the $j = l$ terms cancel. In the third equality we combine the terms that arise in the two double summations. Now imagine that the right-hand-side terms are arranged in a matrix where j is the row index and l the column index:

$$\begin{bmatrix}
0 & e_1 x_1 x_2 (x_2 - x_1) & e_1 x_1 x_3 (x_3 - x_1) \\
e_2 x_2 x_1 (x_1 - x_2) & 0 & e_2 x_2 x_3 (x_3 - x_2) \\
e_3 x_3 x_1 (x_1 - x_3) & e_3 x_3 x_2 (x_2 - x_3) & 0
\end{bmatrix}$$

The fourth equality is obtained by separately summing the terms below and above the diagonal. The fifth equality is obtained by switching the j and the l index in the second summation. Finally, the last equality is obtained by combining the two double sums. Because,

$$\text{sign}\left(\frac{1}{\exp[\lambda e_l]} - \frac{1}{\exp[\lambda e_j]}\right) = \text{sign}(e_j - e_l),$$

we can deduce that

$$\Delta_M \geq 0$$

and conclude that the inefficiency ratio InEff(ϕ_n) is increasing in ϕ_n. ■

A.2 Proofs for Section 3.1

The proofs in this section closely follow Chopin (2004) and Herbst and Schorfheide (2014). Throughout this section, we will assume that $h(\cdot)$ is scalar and we use absolute values $|h|$ instead of a general norm $\|h\|$. Extensions to vector-valued-h functions are straightforward. We use C to denote a generic constant. We will make repeated use of the following moment bound for $r > 1$

$$\begin{aligned} \mathbb{E}\big[\big|X - \mathbb{E}[X]\big|^r\big] &\leq C_r\big(\mathbb{E}\big[\big|X\big|^r\big] + \big|\mathbb{E}[X]\big|^r\big) \\ &\leq 2C_r\mathbb{E}\big[\big|X\big|^r\big], \end{aligned} \tag{A.1}$$

where $C_r = 1$ for $r = 1$ and $C_r = 2^{r-1}$ for $r > 1$. The first inequality follows from the C_r inequality and the second inequality follows from Jensen's inequality.

We will make use of the following SLLN (Markov, see White (2001) p. 33): Let $\{Z_j\}$ be a sequence of independent random variables with finite means $\mu_j = \mathbb{E}[Z_j]$. If for some $\delta > 0$, $\sum_{j=1}^{\infty} \mathbb{E}\big[|Z_j - \mu_j|^{1+\delta}\big]/j^{1+\delta} < \infty$, then $\frac{1}{M}\sum_{j=1}^{M} Z_j - \mu_j \xrightarrow{a.s.} 0$. Note that $\mathbb{E}\big[|Z_j - \mu_j|^{1+\delta}\big] < C < \infty$ implies that the summability condition is satisfied because $\sum_{j=1}^{\infty}(1/j)^{1+\delta} < \infty$.

Recall that under a multivariate Gaussian measurement error distribution, the density $p_n(y_t|s_t)$ can be bounded from above. Thus, $p_n(y_t|s_t) \in \mathcal{H}_{\tilde{t}}^{\tilde{n}}$ and $\tilde{\omega}_t^{j,n} \in \mathcal{H}_{\tilde{t}}^{\tilde{n}}$ for any $\tilde{t}$ and $\tilde{n}$. Moreover, for any $h(s_t, s_{t-1}) \in \mathcal{H}_t^n$, we can deduce that $\tilde{h}(\cdot) = h(\cdot)\tilde{\omega}_t^{j,n} \in \mathcal{H}_t^n$.

Proof of Lemma 1.

Part (i). The forward iteration of the state-transition equation amounts to drawing s_t^j from the density $p(s_t|s_{t-1}^{j,N^\phi})$. Use $\mathbb{E}_{p(s_t|s_{t-1}^{j,N^\phi})}[\cdot]$ to denote expectations under this density and

consider the decomposition:

$$\begin{aligned}
&\tilde{h}^1_{t|t-1} - \int\int h(s_t, s_{t-1}) p(s_t, s_{t-1}|Y_{1:t-1}) ds_t ds_{t-1} \qquad \text{(A.2)}\\
&= \frac{1}{M}\sum_{j=1}^{M}\left(h(\tilde{s}_t^{j,1}, s_{t-1}^{N^\phi}) - \mathbb{E}_{p(s_t|s_{t-1}^{j,N^\phi})}[h(s_t, s_{t-1}^{j,N^\phi})]\right) W_{t-1}^{j,N^\phi}\\
&\quad + \frac{1}{M}\sum_{j=1}^{M}\left(\mathbb{E}_{p(s_t|s_{t-1}^{j,N^\phi})}[h(s_t, s_{t-1}^{j,N^\phi})] W_{t-1}^{j,N^\phi} - \int\int h(s_t, s_{t-1}) p(s_t, s_{t-1}|Y_{1:t-1}) ds_t ds_{t-1}\right)\\
&= I + II.
\end{aligned}$$

We now show that terms I and II in (A.2) converge to zero. According to the above definition

$$I = \frac{1}{M}\sum_{j=1}^{M}\left(h(\tilde{s}_t^{j}, s_{t-1}^{j,N^\phi}) - \mathbb{E}_{p(\cdot|s_{t-1}^{j,N^\phi})}[h]\right) W_{t-1}^{j,N^\phi}.$$

Here we used the abbreviation

$$\mathbb{E}_{p(\cdot|s_{t-1})}[h] = \mathbb{E}_{p(s_t|s_{t-1})}[h(s_t, s_{t-1})].$$

Conditional on the particles $\{s_{t-1}^{j,N^\phi}, W_{t-1}^{j,N^\phi}\}$ the summands in term I form a triangular array of mean-zero random variables that within each row are independently distributed. In Algorithm 4 the particles were resampled during the $t-1$ tempering iteration N^ϕ, such that $W_{t-1}^{N^\phi} = 1$. Using the bound

$$\mathbb{E}_{p(s_t|s_{t-1})}\left[\left|h(s_t, s_{t-1}) - \mathbb{E}_{p(\cdot|s_{t-1})}[h]\right|^{1+\delta}\right] < C < \infty$$

implied by the definition of $\mathcal{H}_t^1$, we can apply the SLLN to deduce that term $I \xrightarrow{a.s.} 0$.

The second term in (A.2) takes the form

$$II = \frac{1}{M}\sum_{j=1}^{M}\left(\mathbb{E}_{p(\cdot|s_{t-1}^{j})}[h] - \int\int h(s_t, s_{t-1}) p(s_t, s_{t-1}|Y_{1:t-1}) ds_t ds_{t-1}\right).$$

The definition of $\mathcal{H}_t^1$ implies that $\mathbb{E}_{p(\cdot|s_{t-1})}[h] \in \mathcal{H}_{t-1}^{N^\phi}$. The almost-sure convergence to zero of term II can now be deduced from the recursive Assumption 1. By combining the convergence

results for terms I and II we have established (34).

Part (ii). The convergences in (35) and (37) follow immediately from the fact that $p_1(y_t|s_t) \in \mathcal{H}_t^1$. Moreover, if $h(s_t, s_{t-1}) \in \mathcal{H}_t^1$, then $h(s_t, s_{t-1})p_1(y_t|s_t) \in \mathcal{H}_t^1$. Finally, $p_1(y_t|s_t) > 0$, which implies that the almost-sure limit of the denominator in (35) is strictly positive.

Part (iii). To verify (36), let $\tilde{F}_{t,1,M}$ denote the σ-algebra generated by the particles $\{\tilde{s}_t^{j,1}, s_{t-1}^{j,N^\phi}, W_t^{j,1}\}$. Moreover, define

$$\mathbb{E}[h|\tilde{F}_{t,1,M}] = \frac{1}{M}\sum_{j=1}^{M} h(\tilde{s}_t^{j,1}, s_{t-1}^{j,N^\phi})\tilde{W}_t^{j,1},$$

and write

$$\begin{aligned}
&\bar{h}_t^1 - \int h(s_t, s_{t-1})p_1(s_t, s_{t-1}|Y_{1:t})ds_t \qquad \text{(A.3)}\\
&= \frac{1}{M}\sum_{j=1}^{M}\left(h(s_t^{j,1}, s_{t-1}^{j,N^\phi}) - \mathbb{E}[h|\tilde{F}_{t,1,M}]\right)\\
&\quad + \left(\frac{1}{M}\sum_{j=1}^{M} h(\tilde{s}_t^{j,1}, s_{t-1}^{N^\phi})\tilde{W}_t^{j,1} - \int\int h(s_t, s_{t-1})p_1(s_t, s_{t-1}|Y_{1:t})ds_t ds_{t-1}\right)\\
&= \frac{1}{M}\sum_{j=1}^{M}\left(h(s_t^{j,1}, s_{t-1}^{j,N^\phi}) - \mathbb{E}[h|\tilde{F}_{t,1,M}]\right)\\
&\quad + \left(\tilde{h}_t^1 - \int\int h(s_t, s_{t-1})p_1(s_t, s_{t-1}|Y_{1:t})ds_t ds_{t-1}\right)\\
&= I + II.
\end{aligned}$$

From (35), we can immediately deduce that term II converges to zero almost surely. Recall that we are resampling the pairs $(\tilde{s}_t^{j,n}, s_{t-1}^{j,N^\phi})$. Thus, under multinomial resampling the $h(s_t^{j,1}, s_t^{j,N^\phi})$'s form a triangular array of *i.i.d.* random variables conditional on $\tilde{F}_{t,1,M}$. Using Kolmogorov's SLLN for *i.i.d.* sequences, it suffices to verify for that

$$\mathbb{E}\left[\left|h(s_t^{j,1}, s_t^{j,N^\phi})\right| \;\middle|\; \tilde{F}_{t,1,M}\right] < \infty.$$

We can manipulate the moment as follows

$$\begin{aligned}\mathbb{E}\left[\left|h(s_t^{j,1}, s_{t-1}^{j,N^\phi})\right| \,\middle|\, \tilde{F}_{t,1,M}\right] &= \frac{1}{M}\sum_{j=1}^{M}\left|h(\tilde{s}_t^{j,1}, s_{t-1}^{j,N^\phi})\right|\tilde{W}_t^{j,1} \\ &\xrightarrow{a.s} \int\left|h(s_t, s_{t-1})\right|p_1(s_t, s_{t-1}|Y_{1:t})ds_t ds_{t-1} < \infty.\end{aligned}$$

Because $h \in \mathcal{H}_t^1$ implies $|h| \in \mathcal{H}_t^1$, we obtain the almost-sure convergence from (35). ■

Proof of Lemma 2.

Part (i). We begin by establishing the convergence of the approximations in (39) and (41). Because for Gaussian measurement errors the incremental weights are bounded, for any $h(s_t, s_{t-1}) \in \mathcal{H}_t^{n-1}$:

$$\tilde{w}_t^{j,n} = \frac{p_n(y_t|s_t)}{p_{n-1}(y_t|s_t)} \in \mathcal{H}_t^{n-1} \quad \text{and} \quad h(s_t, s_{t-1})\frac{p_n(y_t|s_t)}{p_{n-1}(y_t|s_t)} \in \mathcal{H}_t^{n-1}.$$

Moreover,

$$\begin{aligned}&\frac{\int\int h(s_t, s_{t-1})\frac{p_n(y_t|s_t)}{p_{n-1}(y_t|s_t)}p_{n-1}(s_t, s_{t-1}|Y_{1:t})ds_t ds_{t-1}}{\int \frac{p_n(y_t|s_t)}{p_{n-1}(y_t|s_t)}p_{n-1}(s_t|Y_{1:t})ds_t} \\ &= \frac{\int\int h(s_t, s_{t-1})\frac{p_n(y_t|s_t)}{p_{n-1}(y_t|s_t)}\frac{p_{n-1}(y_t|s_t)p(s_t, s_{t-1}|Y_{1:t-1})}{p_{n-1}(y_t|Y_{1:t-1})}ds_t ds_{t-1}}{\int \frac{p_n(y_t|s_t)}{p_{n-1}(y_t|s_t)}\frac{p_{n-1}(y_t|s_t)p(s_t|Y_{1:t-1})}{p_{n-1}(y_t|Y_{1:t-1})}ds_t} \\ &= \frac{\int\int h(s_t, s_{t-1})p_n(y_t|s_t)p(s_t, s_{t-1}|Y_{1:t-1})ds_t ds_{t-1}}{\int p_n(y_t|s_t)p(s_t|Y_{1:t-1})ds_t} \\ &= \int\int h(s_t, s_{t-1})p_n(s_t, s_{t-1}|Y_{1:t})ds_t ds_{t-1}.\end{aligned} \tag{A.4}$$

The first equality is obtained by reversing Bayes Theorem and expressing the "posterior" $p_{n-1}(s_t, s_{t-1}|Y_{1:t})$ as the product of "likelihood" $p_{n-1}(y_t|s_t)$ and "prior" $p(s_t, s_{t-1}|Y_{1:t-1})$ divided by the "marginal likelihood" $p_{n-1}(y_t|Y_{1:t-1})$. We then cancel the $p_{n-1}(y_t|s_t)$ and the marginal likelihood terms to obtain the second equality. Finally, an application of Bayes Theorem leads to the third equality.

The recursive Assumption 2 in combination with (A.4) yields the almost-sure convergence in (39) and (41). Recall that $p_{N^\phi}(y_t|Y_{1:t-1}) = p(y_t|Y_{1:t-1})$ by construction and that an

approximation of $p_1(y_t|Y_{1:t-1})$ is generated in Step 2(a)iii of Algorithm 1. Together, this leads to the approximation of the likelihood increment $p(y_t|Y_{1:t-1})$ in (23).

Part (ii). Resampling preserves the SLLN obtained for the correction step. Formally, the convergence in (40) can be established with an argument similar to the one used in Step (iii) of the proof of Lemma 1.

Part (iii). We begin with an outline of how to prove the convergence in (42) and will subsequently provide some initially-omitted details. Abbreviate

$$\mathbb{E}_{K_n(\cdot|\hat{s}_t;s_{t-1})}[h] = \mathbb{E}_{K_n(s_t|\hat{s}_t;s_{t-1})}[h(s_t,s_{t-1})] = \int h(s_t,s_{t-1})K_n(s_t|\hat{s}_t;s_{t-1})ds_t,$$

which is a function of $(\hat{s}_t, s_{t-1})$. We can decompose the Monte Carlo approximation from the mutation step as follows:

$$\begin{aligned}
&\frac{1}{M}\sum_{j=1}^{M} h(s_t^{j,n}, s_{t-1}^{j,N^\phi})W_t^{j,n} - \int\int h(s_t,s_{t-1})p_n(s_t,s_{t-1}|Y_{1:t})ds_t ds_{t-1} \qquad \text{(A.5)}\\
= \;& \frac{1}{M}\sum_{j=1}^{M}\left(h(s_t^{j,n}, s_{t-1}^{j,N^\phi}) - \mathbb{E}_{K_n(\cdot|\hat{s}_t^{j,n};s_{t-1}^{j,N^\phi})}[h]\right)W_t^{j,n}\\
&+\frac{1}{M}\sum_{j=1}^{M}\left(\mathbb{E}_{K_n(\cdot|\hat{s}_t^{j,n};s_{t-1}^{j,N^\phi})}[h] - \int\int h(s_t,s_{t-1})p_n(s_t,s_{t-1}|Y_{1:t})ds_t ds_{t-1}\right)W_t^{j,n}\\
= \;& I + II, \quad \text{say.}
\end{aligned}$$

By construction, conditional on the particles $\{\hat{s}_t^{j,n}, s_{t-1}^{j,N^\phi}, W_t^{j,n}\}$, term I is an average of independent mean-zero random variables, which converges to zero.

The analysis of term II is more involved for two reasons. First, as previously highlighted, $\mathbb{E}_{K_n(\cdot|\hat{s}_t^{j,n};s_{t-1}^{j,N^\phi})}[h]$ is a function not only of $\hat{s}_t$ but also of s_{t-1}. Second, while the invariance

property (21) implies that

$$\begin{aligned}
&\int \mathbb{E}_{K_n(\cdot|\hat{s}_t;s_{t-1})}[h] p_n(\hat{s}_t|y_t, s_{t-1}) d\hat{s}_t \qquad (A.6)\\
&= \int \left(\int h(s_t, s_{t-1}) K_n(s_t|\hat{s}_t; s_{t-1}) ds_t \right) p_n(\hat{s}_t|y_t, s_{t-1}) d\hat{s}_t \\
&= \int h(s_t, s_{t-1}) \left(\int K_n(s_t|\hat{s}_t; s_{t-1}) p_n(\hat{s}_t|y_t, s_{t-1}) d\hat{s}_t \right) ds_t \\
&= \int h(s_t, s_{t-1}) p_n(s_t|y_t, s_{t-1}) ds_t,
\end{aligned}$$

the summation over $(\hat{s}_t^{j,n}, s_{t-1}^{j,N^\phi}, W_t^{j,n})$ generates an integral with respect to $p_n(s_t, s_{t-1}|Y_{1:t})$ instead of $p_n(s_t|y_t, s_{t-1})$; see (40).

To obtain the expected value of $\mathbb{E}_{K_n(\cdot|\hat{s}_t;s_{t-1})}[h]$ under the distribution $p_n(\hat{s}_t, s_{t-1}|Y_{1:t})$, notice that

$$\begin{aligned}
p_n(s_t, s_{t-1}|Y_{1:t}) &= p_n(s_t, s_{t-1}|y_t, Y_{1:t-1}) \qquad (A.7)\\
&= p_n(s_t|s_{t-1}, y_t, Y_{1:t-1}) p(s_{t-1}|y_t, Y_{1:t-1}) \\
&= p_n(s_t|s_{t-1}, y_t) p(s_{t-1}|y_t, Y_{1:t-1}).
\end{aligned}$$

The last equality holds because, using the first-order Markov structure of the state-space model, we can write

$$\begin{aligned}
p_n(s_t|y_t, s_{t-1}, Y_{1:t-1}) &= \frac{p_n(y_t|s_t, s_{t-1}, Y_{1:t-1}) p(s_t|s_{t-1}, Y_{1:t-1})}{\int p_n(y_t|s_t, s_{t-1}, Y_{1:t-1}) p(s_t|s_{t-1}, Y_{1:t-1}) ds_t} \\
&= \frac{p_n(y_t|s_t) p(s_t|s_{t-1})}{\int p_n(y_t|s_t) p(s_t|s_{t-1}) ds_t} \\
&= p_n(s_t|y_t, s_{t-1}).
\end{aligned}$$

Therefore, we obtain

$$\begin{aligned}
&\int\int \mathbb{E}_{K_n(\cdot|\hat{s}_t;s_{t-1})}[h]p_n(\hat{s}_t, s_{t-1}|Y_{1:t})d\hat{s}_t ds_{t-1} \qquad (A.8)\\
&= \int\left(\int \mathbb{E}_{K_n(\cdot|\hat{s}_t;s_{t-1})}[h]p_n(\hat{s}_t|y_t, s_{t-1})d\hat{s}_t\right)p_n(s_{t-1}|y_t, Y_{1:t-1})ds_{t-1}\\
&= \int\left(\int h(s_t, s_{t-1})p_n(s_t|y_t, s_{t-1})ds_t\right)p_n(s_{t-1}|y_t, Y_{1:t-1})ds_{t-1}\\
&= \int\int h(s_t, s_{t-1})p_n(s_t, s_{t-1}|Y_{1:t})ds_t ds_{t-1}.
\end{aligned}$$

The first equality uses (A.7). The second equality follows from the invariance property (A.6). For the third equality, we used (A.7) again. Thus, under suitable regularity conditions, term II also converges to zero almost surely, which leads to the convergence in (42).

To complete the proof, we need to construct moment bounds for the terms I and II that appear in (A.5). Under the assumption that the resampling step is executed at every iteration n, term I takes the form:

$$I = \frac{1}{M}\sum_{j=1}^{M}\left(h(s_t^{j,n}, s_{t-1}^{j,N^\phi}) - \mathbb{E}_{K_n(\cdot|\hat{s}_t^{j,n};s_{t-1}^{j,N^\phi})}[h]\right).$$

Conditional on the σ-algebra generated by the particles of the selection step, term I is an average of independently distributed mean-zero random variables. By virtue of $h \in \mathcal{H}_t^n$, we can deduce that, omitting the j and n superscripts,

$$\mathbb{E}_{K_n(\cdot|\hat{s}_t;s_{t-1})}\left[\left|h(s_t, s_{t-1}) - \mathbb{E}_{K_n(\cdot|\hat{s}_t;s_{t-1})}[h]\right|^{1+\delta}\right] < C < \infty.$$

Therefore, the SLLN implies that $I \xrightarrow{a.s.} 0$. For term II, we have

$$II = \frac{1}{M}\sum_{j=1}^{M}\left(\mathbb{E}_{K_n(\cdot|\hat{s}_t^{j,n};s_{t-1}^{j,N^\phi})}[h] - \int\int h(s_t, s_{t-1})p_n(s_t, s_{t-1}|Y_{1:t})ds_t ds_{t-1}\right).$$

Now define

$$\psi(\hat{s}_t, s_{t-1}) = \mathbb{E}_{K_n(\cdot|\hat{s}_t;s_{t-1})}[h].$$

The definition of $\mathcal{H}_t^n$ implies that $\psi(\hat{s}_t, s_{t-1}) \in \mathcal{H}_t^{n-1}$. Thus, we can deduce from (40) that $II \xrightarrow{a.s.} 0$. ■

A.3 Proofs for Section 3.2

The subsequent proof of the unbiasedness of the particle filter approximation uses Lemmas 3 and 5 below. Throughout this section, we use the convention that $W_t^{j,0} = W_{t-1}^{j,N^\phi}$. Moreover, we often use the j subscript to denote a fixed particle as well as a running index in a summation. That is, we write $a^j / \sum_{j=1}^M a^j$ instead of $a^j / \sum_{l=1}^M a^l$. We also define the information set

$$\begin{aligned} \mathcal{F}_{t-1,n,M} &= \big\{(s_0^{j,N^\phi}, W_0^{j,N^\phi}), (s_1^{j,1}, W_1^{j,1}), \ldots, (s_1^{j,N^\phi}, W_1^{j,N^\phi}), \ldots, \\ &\quad (s_{t-1}^{j,1}, W_{t-1}^{j,1}), \ldots, (s_{t-1}^{j,n}, W_{t-1}^{j,n})\big\}_{j=1}^M. \end{aligned} \tag{A.9}$$

A.3.1 Additional Lemmas

Lemma 3 *Suppose that the incremental weights $\tilde{w}_t^{j,n}$ are defined as in (9) and (16) and that there is no resampling. Then*

$$\prod_{n=1}^{N^\phi} \left(\frac{1}{M} \sum_{j=1}^M \tilde{w}_T^{j,n} W_T^{j,n-1} \right) = \frac{1}{M} \sum_{j=1}^M \left(\prod_{n=1}^{N^\phi} \tilde{w}_T^{j,n} \right) W_{T-1}^{j,N^\phi} \tag{A.10}$$

and

$$W_{T-h-1}^{j,N^\phi} \prod_{n=1}^{N^\phi} \left(\frac{1}{M} \sum_{j=1}^M \tilde{w}_{T-h-1}^{j,n} W_{T-h-1}^{j,n-1} \right) = \left(\prod_{n=1}^{N^\phi} \tilde{w}_{T-h-1}^{j,n} \right) W_{T-h-2}^{j,N^\phi}. \tag{A.11}$$

Proof of Lemma 3. The lemma can be proved by induction. If there is no resampling, then $W_t^{j,n} = \tilde{W}_t^{j,n}$.

Part 1. The inductive hypothesis to show (A.10) takes the form

$$\prod_{n=n_*}^{N^\phi} \left(\frac{1}{M} \sum_{j=1}^M \tilde{w}_T^{j,n} W_T^{j,n-1} \right) = \frac{1}{M} \sum_{j=1}^M \left(\prod_{n=n_*}^{N^\phi} \tilde{w}_T^{j,n} \right) W_T^{j,n_*-1}. \tag{A.12}$$

If the hypothesis is correct, then

$$\begin{aligned}
&\prod_{n=n_*-1}^{N^\phi}\left(\frac{1}{M}\sum_{j=1}^{M}\tilde{w}_T^{j,n}W_T^{j,n-1}\right) \qquad (A.13)\\
&= \left(\frac{1}{M}\sum_{j=1}^{M}\left(\prod_{n=n_*}^{N^\phi}\tilde{w}_T^{j,n}\right)W_T^{j,n_*-1}\right)\left(\frac{1}{M}\sum_{j=1}^{M}\tilde{w}_T^{j,n_*-1}W_T^{j,n_*-2}\right)\\
&= \left(\frac{1}{M}\sum_{j=1}^{M}\left(\prod_{n=n_*}^{N^\phi}\tilde{w}_T^{j,n}\right)\frac{\tilde{w}_T^{j,n_*-1}W_T^{j,n_*-2}}{\frac{1}{M}\sum_{j=1}^{M}\tilde{w}_T^{j,n_*-1}W_T^{j,n_*-2}}\right)\left(\frac{1}{M}\sum_{j=1}^{M}\tilde{w}_T^{j,n_*-1}W_T^{j,n_*-2}\right)\\
&= \frac{1}{M}\sum_{j=1}^{M}\left(\prod_{n=n_*-1}^{N^\phi}\tilde{w}_T^{j,n}\right)W_T^{j,n_*-2}.
\end{aligned}$$

The first equality follows from (A.12), and the second equality is obtained by using the definition of W_T^{j,n_*-1}.

It is straightforward to verify that the inductive hypothesis (A.12) is satisfied for $n_* = N^\phi$. Setting $n_* = 1$ in (A.12) and noticing that $W_T^{j,0} = W_{T-1}^{j,N^\phi}$ leads the desired result.

Part 2. To show (A.11), we can use the inductive hypothesis

$$W_{T-h-1}^{j,N^\phi}\prod_{n=n_*}^{N^\phi}\left(\frac{1}{M}\sum_{j=1}^{M}\tilde{w}_{T-h-1}^{j,n}W_{T-h-1}^{j,n-1}\right) = \left(\prod_{n=n_*}^{N^\phi}\tilde{w}_{T-h-1}^{j,n}\right)W_{T-h-1}^{j,n_*-1}. \qquad (A.14)$$

If the inductive hypothesis is satisfied, then

$$\begin{aligned}
&W_{T-h-1}^{j,N^\phi}\prod_{n=n_*-1}^{N^\phi}\left(\frac{1}{M}\sum_{j=1}^{M}\tilde{w}_{T-h-1}^{j,n}W_{T-h-1}^{j,n-1}\right) \qquad (A.15)\\
&= W_{T-h-1}^{j,N^\phi}\prod_{n=n_*}^{N^\phi}\left(\frac{1}{M}\sum_{j=1}^{M}\tilde{w}_{T-h-1}^{j,n}W_{T-h-1}^{j,n-1}\right)\left(\frac{1}{M}\sum_{j=1}^{M}\tilde{w}_{T-h-1}^{j,n_*-1}W_{T-h-1}^{j,n_*-2}\right)\\
&= \left(\prod_{n=n_*}^{N^\phi}\tilde{w}_{T-h-1}^{j,n}\right)\frac{\tilde{w}_{T-h-1}^{j,n_*-1}W_{T-h-1}^{j,n_*-2}}{\frac{1}{M}\sum_{j=1}^{M}\tilde{w}_{T-h-1}^{j,n_*-1}W_{T-h-1}^{j,n_*-2}}\left(\frac{1}{M}\sum_{j=1}^{M}\tilde{w}_{T-h-1}^{j,n_*-1}W_{T-h-1}^{j,n_*-2}\right)\\
&= \left(\prod_{n=n_*-1}^{N^\phi}\tilde{w}_{T-h-1}^{j,n}\right)W_{T-h-1}^{j,n_*-2}.
\end{aligned}$$

For $n_* = N^\phi$ the validity of the inductive hypothesis can be verified as follows:

$$\begin{aligned} & W_{T-h-1}^{j,N^\phi}\left(\frac{1}{M}\sum_{j=1}^{M}\tilde{w}_{T-h-1}^{j,N^\phi}W_{T-h-1}^{j,N^\phi-1}\right) \\ = & \frac{\tilde{w}_{T-h-1}^{j,N^\phi}W_{T-h-1}^{j,N^\phi-1}}{\frac{1}{M}\sum_{j=1}^{M}\tilde{w}_{T-h-1}^{j,N^\phi}W_{T-h-1}^{j,N^\phi-1}}\left(\frac{1}{M}\sum_{j=1}^{M}\tilde{w}_{T-h-1}^{j,N^\phi}W_{T-h-1}^{j,N^\phi-1}\right) \\ = & \tilde{w}_{T-h-1}^{j,N^\phi}W_{T-h-1}^{j,N^\phi-1}. \end{aligned} \tag{A.16}$$

Setting $n_* = 1$ in (A.14) leads to the desired result. ■

The following lemma simply states that the expected value of a sum is the sum of the expected values, but it does so using a notation that we will encounter below.

Lemma 4 *Suppose s^j, $j = 1, \ldots, M$, is a sequence of random variables with density $\prod_{j=1}^{M} p(s^j)$, then*

$$\int\cdots\int\left(\frac{1}{M}\sum_{j=1}^{M}f(s^j)\right)\left(\prod_{j=1}^{M}p(s^j)\right)ds^1\cdots ds^M = \frac{1}{M}\sum_{j=1}^{M}\int f(s^j)p(s^j)ds^j.$$

Proof of Lemma 4. The statement is trivially satisfied for $M = 1$. Suppose that it is true for $M - 1$, then

$$\int\cdots\int\left(\frac{1}{M}\sum_{j=1}^{M}f(s^j)\right)\left(\prod_{j=1}^{M}p(s^j)\right)ds^1\cdots ds^M \tag{A.17}$$

$$\begin{aligned} = & \int\cdots\int\left(\frac{1}{M}f(s^M)+\frac{M-1}{M}\frac{1}{M-1}\sum_{j=1}^{M-1}f(s^j)\right)\left(p(s^M)\prod_{j=1}^{M-1}p(s^j)\right)ds^1\cdots ds^M \\ = & \left(\frac{1}{M}\int f(s^M)p(s^M)ds^M\right)\prod_{j=1}^{M-1}\int p(s^j)ds^j \\ & +\left(\frac{M-1}{M}\frac{1}{M-1}\sum_{j=1}^{M-1}\int f(s^j)p(s^j)ds^j\right)\int p(s^M)ds^M \\ = & \frac{1}{M}\sum_{j=1}^{M}\int f(s^j)p(s^j)ds^j, \end{aligned} \tag{A.18}$$

which verifies the claim for all M by induction. ■

Lemma 5 *Suppose that the incremental weights $\tilde{w}_t^{j,n}$ are defined as in (9) and (16) and that the selection step is implemented by multinomial resampling for a predetermined set of iterations $n \in \mathcal{N}$. Then,*

$$\mathbb{E}\left[\prod_{n=1}^{N^\phi}\left(\frac{1}{M}\sum_{j=1}^{M}\tilde{w}_T^{j,n}W_T^{j,n-1}\right)\middle|\mathcal{F}_{T-1,N^\phi,M}\right] = \frac{1}{M}\sum_{j=1}^{M}p(y_T|s_{T-1}^{j,N^\phi})W_{T-1}^{j,N^\phi} \tag{A.19}$$

and

$$\begin{aligned}\frac{1}{M}\sum_{j=1}^{M}\mathbb{E}\left[p(Y_{T-h:T}|s_{T-h-1}^{j,N^\phi})W_{T-h-1}^{j,N^\phi}\prod_{n=1}^{N^\phi}\left(\frac{1}{M}\sum_{j=1}^{M}\tilde{w}_{T-h-1}^{j,n}W_{T-h-1}^{j,n-1}\right)\middle|\mathcal{F}_{T-h-2,N^\phi,M}\right] \\ = \frac{1}{M}\sum_{j=1}^{M}p(Y_{T-h-1:T}|s_{T-h-2}^{j,N^\phi})W_{T-h-2}^{j,N^\phi}.\end{aligned} \tag{A.20}$$

Proof of Lemma 5. We first prove the lemma under the assumption of no resampling, i.e., $\mathcal{N} = \emptyset$. We then discuss how the proof can be modified to allow for resampling.

Part 1 (No Resampling). We deduce from Lemma 3 that

$$\mathbb{E}\Big[\prod_{n=1}^{N^\phi}\left(\frac{1}{M}\sum_{j=1}^{M}\tilde{w}_T^{j,n}W_T^{j,n-1}\right)\Big|\mathcal{F}_{T-1,N^\phi,M}\Big] = \frac{1}{M}\sum_{j=1}^{M}\mathbb{E}\Big[\left(\prod_{n=1}^{N^\phi}\tilde{w}_T^{j,n}\right)W_{T-1}^{j,N^\phi}\Big|\mathcal{F}_{T-1,N^\phi,M}\Big]. \tag{A.21}$$

The subsequent derivations focus on the evaluation of the expectation on the right-hand side of this equation. We will subsequently integrate over the particles $s_T^{1:M,1},\ldots,s_T^{1:M,N^\phi-1}$, which enter the incremental weights $\tilde{w}_T^{j,n}$. We use $s_T^{1:M,n}$ to denote the set of particle values $\{s_T^{1,n},\ldots,s_T^{M,n}\}$. Because $W_{T-1}^{j,N^\phi} \in \mathcal{F}_{T-1,N^\phi,M}$ it suffices to show that

$$\mathbb{E}\Big[\left(\prod_{n=1}^{N^\phi}\tilde{w}_T^{j,n}\right)\Big|\mathcal{F}_{T-1,N^\phi,M}\Big] = p(y_T|s_{T-1}^{j,N^\phi}). \tag{A.22}$$

Recall that the initial state particle $s_T^{j,1}$ is generated from the state-transition equation $p(s_T|s_{T-1}^{j,N^\phi})$. The first incremental weight is defined as

$$\tilde{w}_T^{j,1} = p_1(y_T|s_T^{j,1}).$$

The incremental weight in tempering iteration n is given by

$$\tilde{w}_T^{j,n} = \frac{p_n(y_T|s_T^{j,n-1})}{p_{n-1}(y_T|s_T^{j,n-1})}.$$

Because we are omitting the selection step, the new particle value is generated in the mutation step by sampling from the Markov transition kernel

$$s_T^{j,n} \sim K_n(s_T^n|s_T^{j,n-1}, s_{T-1}^{j,N^\phi}), \tag{A.23}$$

which has the invariance property

$$p_n(s_T|y_T, s_{T-1}) = \int K_n(s_T|\hat{s}_T; s_{T-1}) p_n(\hat{s}_T|y_T, s_{T-1}) d\hat{s}_T. \tag{A.24}$$

Using the previous notation, we can write

$$\begin{aligned} &\mathbb{E}\left[\left(\prod_{n=1}^{N^\phi} \tilde{w}_T^{j,n}\right) \middle| \mathcal{F}_{T-1,N^\phi,M}\right] \\ &= \int \cdots \int \left(\prod_{n=3}^{N^\phi} \frac{p_n(y_T|s_T^{j,n-1})}{p_{n-1}(y_T|s_T^{j,n-1})} K_{n-1}(s_T^{j,n-1}|s_T^{j,n-2}, s_{T-1}^{j,N^\phi})\right) \\ &\quad \times \frac{p_2(y_T|s_T^{j,1})}{p_1(y_T|s_T^{j,1})} p_1(y_T|s_T^{j,1}) p(s_T^{j,1}|s_{T-1}^{j,N^\phi}) ds_T^{j,1} \cdots ds_T^{j,N^\phi-1}. \end{aligned} \tag{A.25}$$

The bridge posterior densities were defined as

$$p_n(s_t|y_t, s_{t-1}) = \frac{p_n(y_t|s_t)p(s_t|s_{t-1})}{p_n(y_t|s_{t-1})}, \quad p_n(y_t|s_{t-1}) = \int p_n(y_t|s_t)p(s_t|s_{t-1})ds_t. \tag{A.26}$$

Using the invariance property of the transition kernel in (A.24) and the definition of the bridge posterior densities, we deduce that

$$\begin{aligned}
&\int K_{n-1}(s_T^{j,n-1}|s_T^{j,n-2}, s_{T-1}^{j,N^\phi}) p_{n-1}(y_T|s_T^{j,n-2}) p(s_T^{j,n-2}|s_{T-1}^{j,N^\phi}) ds_T^{j,n-2} \qquad \text{(A.27)}\\
&= \int K_{n-1}(s_T^{j,n-1}|s_T^{j,n-2}, s_{T-1}^{j,N^\phi}) p_{n-1}(s_T^{j,n-2}|y_T, s_{T-1}^{j,N^\phi}) p_{n-1}(y_T|s_{T-1}^{j,N^\phi}) ds_T^{j,n-2}\\
&= p_{n-1}(s_T^{j,n-1}|y_T, s_{T-1}^{j,N^\phi}) p_{n-1}(y_T|s_{T-1}^{j,N^\phi})\\
&= p_{n-1}(y_T|s_T^{j,n-1}) p(s_T^{j,n-1}|s_{T-1}^{j,N^\phi}).
\end{aligned}$$

The first equality follows from Bayes Theorem in (A.26). The second equality follows from the invariance property of the transition kernel. The third equality uses Bayes Theorem again.

We can now evaluate the integrals in (A.25). Consider the terms involving $s_T^{j,1}$:

$$\begin{aligned}
&\int K_2(s_T^{j,2}|s_T^{j,1}, s_{T-1}^{j,N^\phi}) \frac{p_2(y_T|s_T^{j,1})}{p_1(y_T|s_T^{j,1})} p_1(y_T|s_T^{j,1}) p(s_T^{j,1}|s_{T-1}^{j,N^\phi}) ds_T^{j,1} \qquad \text{(A.28)}\\
&= \int K_2(s_T^{j,2}|s_T^{j,1}, s_{T-1}^{j,N^\phi}) p_2(y_T|s_T^{j,1}) p(s_T^{j,1}|s_{T-1}^{j,N^\phi}) ds_T^{j,1}\\
&= p_2(y_T|s_T^{j,2}) p(s_T^{j,2}|s_{T-1}^{j,N^\phi}).
\end{aligned}$$

Thus,

$$\begin{aligned}
&\mathbb{E}\left[\left(\prod_{n=1}^{N^\phi} \tilde{w}_T^{j,n}\right) \middle| \mathcal{F}_{T-1,N^\phi,M}\right] \qquad \text{(A.29)}\\
&= \int \cdots \int \left(\prod_{n=4}^{N^\phi} \frac{p_n(y_T|s_T^{j,n-1})}{p_{n-1}(y_T|s_T^{j,n-1})} K_{n-1}(s_T^{j,n-1}|s_T^{j,n-2}, s_{T-1}^{j,N^\phi})\right)\\
&\quad \times \frac{p_3(y_T|s_T^{j,2})}{p_2(y_T|s_T^{j,2})} p_2(y_T|s_T^{j,2}) p(s_T^{j,2}|s_{T-1}^{j,N^\phi}) ds_T^{j,2} \cdots ds_T^{j,N^\phi-1}\\
&= \int \frac{p_{N^\phi}(y_T|s_T^{j,N^\phi-1})}{p_{N^\phi-1}(y_T|s_T^{j,N^\phi-1})} p_{N^\phi-1}(y_T|s_T^{j,N^\phi-1}) p(s_T^{j,N^\phi-1}|s_{T-1}^{j,N^\phi}) ds_T^{j,N^\phi-1}\\
&= p(y_T|s_{T-1}^{j,N^\phi}).
\end{aligned}$$

The first equality follows from (A.28). The second equality is obtained by sequentially integrating out $s_T^{j,2}, \ldots, s_T^{j,N_{\phi-2}}$, using a similar argument as for $s_T^{j,1}$. This proves the first part of the lemma.

Part 2 (No Resampling). Using Lemma 3, we write

$$\begin{aligned}
&\mathbb{E}\left[p(Y_{T-h:T}|s_{T-h-1}^{j,N^\phi},\theta)W_{T-h-1}^{j,N^\phi}\prod_{n=1}^{N^\phi}\left(\frac{1}{M}\sum_{j=1}^{M}\tilde{w}_{T-h-1}^{j,n}W_{T-h-1}^{j,n-1}\right)\middle|\mathcal{F}_{T-h-2,N^\phi,M}\right] \\
&= \mathbb{E}\left[p(Y_{T-h:T}|s_{T-h-1}^{j,N^\phi},\theta)\left(\prod_{n=1}^{N^\phi}\tilde{w}_{T-h-1}^{j,n}\right)W_{T-h-2}^{j,N^\phi}\middle|\mathcal{F}_{T-h-2,N^\phi,M}\right] \qquad \text{(A.30)}
\end{aligned}$$

To prove the second part of the lemma, we slightly modify the last step of the integration in (A.29):

$$\begin{aligned}
&\mathbb{E}\left[p(Y_{T-h:T}|s_{T-h-1}^{j,N^\phi})\left(\prod_{n=1}^{N^\phi}\tilde{w}_{T-h-1}^{j,n}\right)\middle|\mathcal{F}_{T-2,N^\phi,M}\right] \qquad \text{(A.31)} \\
&= \int p(Y_{T-h:T}|s_{T-h-1}^{j,N^\phi})p_{N^\phi}(y_{T-h-1}|s_{T-h-1}^{j,N^\phi-1})p(s_{T-h-1}^{j,N^\phi-1}|s_{T-h-2}^{j,N^\phi})ds_{T-h-1}^{j,N^\phi-1} \\
&= p(Y_{T-h-1:T}|s_{T-h-2}^{j,N^\phi}),
\end{aligned}$$

as required.

Part 1 (Resampling in tempering iteration $\bar{n}$). We now assume that the selection step is executed once, in iteration $\bar{n}$, i.e., $\mathcal{N} = \{\bar{n}\}$. For reasons that will become apparent subsequently, we will use i subscripts for particles in stages $n = 1, \ldots, \bar{n}-1$. Using Lemma 3, we deduce that it suffices to show:

$$\begin{aligned}
&\mathbb{E}\left[\left(\prod_{n=1}^{\bar{n}-1}\left(\frac{1}{M}\sum_{i=1}^{M}\tilde{w}_T^{i,n}W_T^{i,n-1}\right)\right)\left(\frac{1}{M}\sum_{j=1}^{M}\tilde{w}_T^{j,\bar{n}}W_T^{j,\bar{n}-1}\right)\right. \qquad \text{(A.32)} \\
&\qquad \left.\times\left(\frac{1}{M}\sum_{j=1}^{M}\left(\prod_{n=\bar{n}+1}^{N^\phi}\tilde{w}_T^{j,n}\right)W_T^{j,\bar{n}}\right)\middle|\mathcal{F}_{T-1,N^\phi,M}\right] \\
&\qquad = \frac{1}{M}\sum_{j=1}^{M}p(y_T|s_{T-1}^{j,N^\phi})W_{T-1}^{j,N^\phi}.
\end{aligned}$$

To evaluate the expectation, we need to integrate over the particles $s_T^{1:M,1}, \dots, s_T^{1:M,N^\phi}$ as well as the particles $\hat{s}_T^{1:M,\bar{n}}$ generated during the selection step. We have to distinguish two cases:

$$\begin{aligned}
\text{Case 1, } n \neq \bar{n} \quad &: \quad s_T^{j,n} \sim K_n(s_T^{j,n} | s_T^{j,n-1}, s_T^{j,N^\phi}), \quad j = 1, \dots, M \\
\text{Case 2, } n = \bar{n} \quad &: \quad s_T^{j,n} \sim K_n(s_T^{j,n} | \hat{s}_T^{j,n}, s_T^{j,N^\phi}), \quad j = 1, \dots, M; \\
&\quad\;\; \hat{s}_T^{j,n} \sim MN\big(s_T^{1:M,n-1}, \tilde{W}_T^{1:M,n}\big), \quad j = 1, \dots, M
\end{aligned}$$

where $MN(\cdot)$ here denotes the multinomial distribution.

In a preliminary step, we are integrating out the particles $\hat{s}_T^{1:M,\bar{n}}$. These particles enter the Markov transition kernel $K_{\bar{n}}(s_T^{j,\bar{n}} | \hat{s}_T^{j,\bar{n}}, s_{T-1}^{j,N^\phi})$ as well as the conditional density $p(\hat{s}_T^{j,\bar{n}} | s_T^{1:M,\bar{n}-1})$. Under the assumption that the resampling step is executed using multinomial resampling,

$$p(\hat{s}_T^{j,\bar{n}} | s_T^{1:M,\bar{n}-1}) = \frac{1}{M} \sum_{i=1}^{M} \tilde{W}_T^{j,\bar{n}} \delta(\hat{s}_T^{j,\bar{n}} - s_T^{i,\bar{n}-1}),$$

where $\delta(x)$ is the Dirac function with the property that $\delta(x) = 0$ for $x \neq 0$ and $\int \delta(x) dx = 1$. Integrating out the resampled particles yields

$$\begin{aligned}
&p(s_T^{1:M,\bar{n}} | s_T^{1:M,\bar{n}-1}) \qquad\qquad (A.33) \\
&= \int \prod_{j=1}^{M} K_{\bar{n}}(s_T^{j,\bar{n}} | \hat{s}_T^{j,\bar{n}}, s_{T-1}^{j,N^\phi}) \left[\frac{1}{M} \sum_{i=1}^{M} \tilde{W}_T^{i,\bar{n}} \delta(\hat{s}_T^{j,\bar{n}} - s_T^{i,\bar{n}-1}) \right] d\hat{s}_T^{1:M,\bar{n}} \\
&= \prod_{j=1}^{M} \int K_{\bar{n}}(s_T^{j,\bar{n}} | \hat{s}_T^{j,\bar{n}}, s_{T-1}^{j,N^\phi}) \left[\frac{1}{M} \sum_{i=1}^{M} \tilde{W}_T^{i,\bar{n}} \delta(\hat{s}_T^{j,\bar{n}} - s_T^{i,\bar{n}-1}) \right] d\hat{s}_T^{j,\bar{n}} \\
&= \prod_{j=1}^{M} \left[\frac{1}{M} \sum_{i=1}^{M} \tilde{W}_T^{i,\bar{n}} K_{\bar{n}}(s_T^{j,\bar{n}} | s_T^{i,\bar{n}-1}, s_{T-1}^{i,N^\phi}) \right].
\end{aligned}$$

In the last equation, the superscript for s_{T-1} changes from j to i because during the resampling, we keep track of the history of the particle. Thus, if for particle $j = 1$ the value $\hat{s}_T^{1,\bar{n}}$ is set to $s_T^{3,\bar{n}-1}$, we also use s_{T-1}^{3,N^ϕ} for this particle.

We can now express the expected value, which we abbreviate as $\mathcal{E}$, as the following integral:

$$\begin{aligned}
\mathcal{E} &= \mathbb{E}\Bigg[\Bigg(\prod_{n=1}^{\bar{n}-1}\Bigg(\frac{1}{M}\sum_{i=1}^{M}\tilde{w}_T^{i,n}W_{T-1}^{i,n-1}\Bigg)\Bigg)\Bigg(\frac{1}{M}\sum_{j=1}^{M}\tilde{w}_T^{j,\bar{n}}W_T^{j,\bar{n}-1}\Bigg) \\
&\quad\times\Bigg(\frac{1}{M}\sum_{j=1}^{M}\Bigg(\prod_{n=\bar{n}+1}^{N^\phi}\tilde{w}_T^{j,n}\Bigg)W_T^{j,\bar{n}}\Bigg)\Bigg|\mathcal{F}_{T-1,N^\phi,M}\Bigg] \\
&= \int\cdots\int\Bigg(\prod_{n=1}^{\bar{n}-1}\Bigg(\frac{1}{M}\sum_{i=1}^{M}\tilde{w}_T^{i,n}W_{T-1}^{i,n-1}\Bigg)\Bigg)\Bigg(\frac{1}{M}\sum_{j=1}^{M}\tilde{w}_T^{j,\bar{n}}W_T^{j,\bar{n}-1}\Bigg)\Bigg(\frac{1}{M}\sum_{j=1}^{M}\Bigg(\prod_{n=\bar{n}+1}^{N^\phi}\tilde{w}_T^{j,n}\Bigg)\Bigg) \\
&\quad\times\Bigg(\prod_{n=1}^{\bar{n}-1}\prod_{j=1}^{M}K_n(s_T^{i,n}|s_T^{i,n-1},s_{T-1}^{i,N^\phi})\Bigg)\Bigg(\prod_{j=1}^{M}\Bigg[\frac{1}{M}\sum_{i=1}^{M}\tilde{W}_T^{i,\bar{n}}K_{\bar{n}}(s_T^{j,\bar{n}}|s_T^{i,\bar{n}-1},s_{T-1}^{i,N^\phi})\Bigg]\Bigg) \\
&\quad\times\Bigg(\prod_{n=\bar{n}+1}^{N^\phi-1}\prod_{j=1}^{M}K_n(s_T^{j,n}|s_T^{j,n-1},s_{T-1}^{j,N^\phi})\Bigg)ds_T^{1:M,1}\cdots ds_T^{1:M,N^\phi-1}.
\end{aligned} \tag{A.34}$$

For the second equality, we used the fact that $W_T^{j,\bar{n}}=1$.

Using Lemma 4, we can write

$$\begin{aligned}
&\int\cdots\int\Bigg(\frac{1}{M}\sum_{j=1}^{M}\Bigg(\prod_{n=\bar{n}+1}^{N^\phi}\tilde{w}_T^{j,n}\Bigg)\Bigg(\prod_{n=\bar{n}+1}^{N^\phi-1}\prod_{j=1}^{M}K_n(s_T^{j,n}|s_T^{j,n-1},s_{T-1}^{j,N^\phi})\Bigg)ds_T^{1:M,\bar{n}+1}\cdots ds_T^{1:M,N^\phi-1} \\
&= \frac{1}{M}\sum_{j=1}^{M}\int\cdots\int\Bigg(\prod_{n=\bar{n}+1}^{N^\phi}\tilde{w}_T^{j,n}\Bigg)\Bigg(\prod_{n=\bar{n}+1}^{N^\phi-1}K_n(s_T^{j,n}|s_T^{j,n-1},s_{T-1}^{j,N^\phi})\Bigg)ds_T^{j,\bar{n}+1}\cdots ds_T^{j,N^\phi-1} \\
&= \frac{1}{M}\sum_{j=1}^{M}F(s_T^{j,\bar{n}},s_{T-1}^{j,N^\phi}).
\end{aligned} \tag{A.35}$$

Now consider the following integral involving terms that depend on $s_T^{1:M,\bar{n}}$:

$$\begin{aligned} I_1 &= \int \left(\frac{1}{M}\sum_{j=1}^{M} F\big(s_T^{j,\bar{n}}, s_{T-1}^{j,N^\phi}\big)\right)\left(\frac{1}{M}\sum_{j=1}^{M} \tilde{w}_T^{j,\bar{n}} W_T^{j,\bar{n}-1}\right) \\ &\quad \times \prod_{j=1}^{M}\left[\frac{1}{M}\sum_{i=1}^{M} \tilde{W}_T^{i,\bar{n}} K_{\bar{n}}(s_T^{j,\bar{n}}|s_T^{i,\bar{n}-1}, s_{T-1}^{i,N^\phi})\right] ds_T^{1:M,\bar{n}} \\ &= \left(\frac{1}{M}\sum_{j=1}^{M}\int F\big(s_T^{j,\bar{n}}, s_{T-1}^{j,N^\phi}\big)\left[\frac{1}{M}\sum_{i=1}^{M} \tilde{W}_T^{i,\bar{n}} K_{\bar{n}}(s_T^{j,\bar{n}}|s_T^{i,\bar{n}-1}, s_{T-1}^{i,N^\phi})\right] ds_T^{j,\bar{n}}\right) \\ &\quad \times\left(\frac{1}{M}\sum_{j=1}^{M} \tilde{w}_T^{j,\bar{n}} W_T^{j,\bar{n}-1}\right) \\ &= \frac{1}{M}\sum_{j=1}^{M}\int F\big(s_T^{j,\bar{n}}, s_{T-1}^{j,N^\phi}\big)\left[\frac{1}{M}\sum_{i=1}^{M} \tilde{w}_T^{i,\bar{n}} W_T^{i,\bar{n}-1} K_{\bar{n}}(s_T^{j,\bar{n}}|s_T^{i,\bar{n}-1}, s_{T-1}^{i,N^\phi})\right] ds_T^{j,\bar{n}}. \end{aligned} \tag{A.36}$$

The first equality is the definition of I_1. The second equality is a consequence of Lemma 4. The last equality is obtained by recalling that

$$\tilde{W}_T^{i,\bar{n}} = \frac{\tilde{w}_T^{i,\bar{n}} W_T^{i,\bar{n}-1}}{\frac{1}{M}\sum_{i=1}^{M} \tilde{w}_T^{i,\bar{n}} W_T^{i,\bar{n}-1}}.$$

We proceed in the evaluation of the expected value $\mathcal{E}$ by integrating over the particle values $s_T^{1:M,1}, \ldots, s_T^{1:M,\bar{n}-1}$:

$$\begin{aligned} \mathcal{E} &= \int \cdots \int I_1 \cdot \left(\prod_{n=1}^{\bar{n}-1}\left(\frac{1}{M}\sum_{i=1}^{M} \tilde{w}_T^{i,n} W_T^{i,n-1}\right)\right) \\ &\quad \times\left(\prod_{n=1}^{\bar{n}-1}\prod_{j=1}^{M} K_n(s_T^{i,n}|s_T^{i,n-1}, s_{T-1}^{i,N^\phi})\right) ds_T^{1:M,1}\cdots ds_T^{1:M,\bar{n}-1}, \end{aligned} \tag{A.37}$$

where

$$
\begin{aligned}
& I_1 \cdot \Big(\prod_{n=1}^{\bar{n}-1} \Big(\frac{1}{M} \sum_{i=1}^{M} \tilde{w}_T^{i,n} W_T^{i,n-1} \Big) \Big) \\
&= \Big(\frac{1}{M} \sum_{j=1}^{M} \int F\big(s_T^{j,\bar{n}}, s_{T-1}^{j,N^\phi}\big) \Big[\frac{1}{M} \sum_{i=1}^{M} \tilde{w}_T^{i,\bar{n}} W_T^{i,\bar{n}-1} K_{\bar{n}}(s_T^{j,\bar{n}} | s_T^{i,\bar{n}-1}, s_{T-1}^{i,N^\phi}) \Big] ds_T^{j,\bar{n}} \Big) \\
&\quad \times \Big(\prod_{n=1}^{\bar{n}-1} \Big(\frac{1}{M} \sum_{i=1}^{M} \tilde{w}_T^{i,n} W_T^{i,n-1} \Big) \Big) \\
&= \frac{1}{M} \sum_{j=1}^{M} \int F\big(s_T^{j,\bar{n}}, s_{T-1}^{j,N^\phi}\big) \Big[\frac{1}{M} \sum_{i=1}^{M} \tilde{w}_T^{i,\bar{n}} W_T^{i,\bar{n}-1} \Big(\prod_{n=1}^{\bar{n}-1} \Big(\frac{1}{M} \sum_{i=1}^{M} \tilde{w}_T^{i,n} W_T^{i,n-1} \Big) \Big) \\
&\quad \times K_{\bar{n}}(s_T^{j,\bar{n}} | s_T^{i,\bar{n}-1}, s_{T-1}^{i,N^\phi}) \Big] ds_T^{j,\bar{n}} \\
&= \frac{1}{M} \sum_{j=1}^{M} \int F\big(s_T^{j,\bar{n}}, s_{T-1}^{j,N^\phi}\big) \Big[\frac{1}{M} \sum_{i=1}^{M} \tilde{w}_T^{i,\bar{n}} \Big(\prod_{n=1}^{\bar{n}-1} \tilde{w}_T^{i,n} \Big) W_{T-1}^{i,N^\phi} \\
&\quad \times K_{\bar{n}}(s_T^{j,\bar{n}} | s_T^{i,\bar{n}-1}, s_{T-1}^{i,N^\phi}) \Big] ds_T^{j,\bar{n}}.
\end{aligned}
$$

The last equality follows from the second part of Lemma 3. Notice the switch from j to i superscript for functions of particles in stages $n < \bar{n}$. Thus,

$$
\begin{aligned}
\mathcal{E} &= \frac{1}{M} \sum_{j=1}^{M} \int F\big(s_T^{j,\bar{n}}, s_{T-1}^{j,N^\phi}\big) \int \cdots \int \Big[\frac{1}{M} \sum_{i=1}^{M} \tilde{w}_T^{i,\bar{n}} \Big(\prod_{n=1}^{\bar{n}-1} \tilde{w}_T^{i,n} \Big) W_{T-1}^{i,N^\phi} \qquad \text{(A.38)} \\
&\quad \times K_{\bar{n}}(s_T^{j,\bar{n}} | s_T^{i,\bar{n}-1}, s_{T-1}^{i,N^\phi}) \Big] \Big(\prod_{n=1}^{\bar{n}-1} \prod_{i=1}^{M} K_n(s_T^{i,n} | s_T^{i,n-1}, s_{T-1}^{i,N^\phi}) \Big) ds_T^{1:M,1} \cdots ds_T^{1:M,\bar{n}-1} ds_T^{j,\bar{n}} \\
&= \frac{1}{M} \sum_{j=1}^{M} \int F\big(s_T^{j,\bar{n}}, s_{T-1}^{j,N^\phi}\big) \Big[\frac{1}{M} \sum_{i=1}^{M} \int \cdots \int \Big(\prod_{n=1}^{\bar{n}} \tilde{w}_T^{i,n} \Big) W_{T-1}^{i,N^\phi} \\
&\quad \times K_{\bar{n}}(s_T^{j,\bar{n}} | s_T^{i,\bar{n}-1}, s_{T-1}^{i,N^\phi}) \prod_{n=1}^{\bar{n}-1} K_n(s_T^{i,n} | s_T^{i,n-1}, s_{T-1}^{i,N^\phi}) ds_T^{i,1} \cdots ds_T^{i,\bar{n}-1} \Big] ds_T^{j,\bar{n}}.
\end{aligned}
$$

The second equality follows from Lemma 4. The calculations in (A.29) imply that

$$
\begin{aligned}
& \int \cdots \int \Big(\prod_{n=1}^{\bar{n}} \tilde{w}_T^{i,n} \Big) W_{T-1}^{i,N^\phi} \prod_{n=1}^{\bar{n}-1} K_n(s_T^{i,n} | s_T^{i,n-1}, s_{T-1}^{i,N^\phi}) ds_T^{i,1} \cdots ds_T^{i,\bar{n}-2} \qquad \text{(A.39)} \\
&\qquad\qquad = p_{\bar{n}-1}(y_T | s_T^{i,\bar{n}-1}) p(s_T^{i,\bar{n}-1} | s_{T-1}^{i,N^\phi}) W_{T-1}^{i,N^\phi}.
\end{aligned}
$$

In turn,

$$
\begin{aligned}
\mathcal{E} &= \frac{1}{M}\sum_{j=1}^{M}\int F\big(s_T^{j,\bar{n}}, s_{T-1}^{j,N^\phi}\big)\Bigg[\frac{1}{M}\sum_{i=1}^{M}\int K_{\bar{n}}(s_T^{j,\bar{n}}|s_T^{i,\bar{n}-1}, s_{T-1}^{i,N^\phi}) \\
&\quad \times p_{\bar{n}}(y_T|s_T^{i,\bar{n}-1})p(s_T^{i,\bar{n}-1}|s_{T-1}^{i,N^\phi})W_{T-1}^{i,N^\phi}ds_T^{i,\bar{n}-1}\Bigg]ds_T^{j,\bar{n}} \\
&= \frac{1}{M}\sum_{i=1}^{M}\Bigg[\frac{1}{M}\sum_{j=1}^{M}\int F\big(s_T^{j,\bar{n}}, s_{T-1}^{j,N^\phi}\big)K_{\bar{n}}(s_T^{j,\bar{n}}|s_T^{i,\bar{n}-1}, s_{T-1}^{i,N^\phi})ds_T^{j,\bar{n}} \\
&\quad \times p_{\bar{n}}(y_T|s_T^{i,\bar{n}-1})p(s_T^{i,\bar{n}-1}|s_{T-1}^{i,N^\phi})W_{T-1}^{i,N^\phi}ds_T^{i,\bar{n}-1}\Bigg] \\
&= \frac{1}{M}\sum_{i=1}^{M}\int F\big(s_T^{i,\bar{n}}, s_{T-1}^{i,N^\phi}\big)p_{\bar{n}}(y_T|s_T^{i,\bar{n}})p(s_T^{i,\bar{n}}|s_{T-1}^{i,N^\phi})W_{T-1}^{i,N^\phi}ds_T^{i,\bar{n}} \\
&= \frac{1}{M}\sum_{j=1}^{M}\int\cdots\int\Bigg(\prod_{n=\bar{n}+1}^{N^\phi}\tilde{w}_T^{j,n}\Bigg)\Bigg(\prod_{n=\bar{n}+1}^{N^\phi-1}K_n(s_T^{j,n}|s_T^{j,n-1}, s_{T-1}^{j,N^\phi})\Bigg) \\
&\quad \times p_{\bar{n}}(y_T|s_T^{j,\bar{n}})p(s_T^{j,\bar{n}}|s_{T-1}^{j,N^\phi})W_{T-1}^{j,N^\phi}ds_T^{j,\bar{n}+1}\cdots ds_T^{j,N^\phi-1}p_{\bar{n}}(y_T|s_T^{j,\bar{n}})p(s_T^{j,\bar{n}}|s_{T-1}^{j,N^\phi})ds_T^{j,\bar{n}} \\
&= \frac{1}{M}\sum_{j=1}^{M}p(y_T|s_{T-1}^{j,N^\phi})W_{T-1}^{j,N^\phi}.
\end{aligned}
\tag{A.40}
$$

The second equality is obtained by changing the order of two summations. To obtain the third equality, we integrate out the $s_T^{i,\bar{n}-1}$ terms along the lines of (A.27). Notice that the value of the integral is identical for all values of the j superscript. Thus, we simply set $j = i$ and drop the average. For the fourth equality, we plug in the definition of $F\big(s_T^{i,\bar{n}}, s_{T-1}^{i,N^\phi}\big)$ and replace the i index with a j index. The last equality follows from calculations similar to those in (A.29). This completes the analysis of Part 1.

Part 2 (Resampling in tempering iteration $\bar{n}$). A similar argument as for Part 1 can be used to extend the result for Part 2.

Resampling in multiple tempering iterations. The previous analysis can be extended to the case in which the selection step is executed in multiple tempering iterations $n \in \mathcal{N}$, assuming that the set $\mathcal{N}$ does not itself depend on the particle system. ■

A.3.2 Proof of Main Theorem

Proof of Theorem 2. Suppose that for any h such that $0 \leq h \leq T-1$

$$\mathbb{E}\left[\hat{p}(Y_{T-h:T}|Y_{1:T-h-1},\theta)|\mathcal{F}_{T-h-1,N^{\phi},M}\right] = \frac{1}{M}\sum_{j=1}^{M} p(Y_{T-h:T}|s_{T-h-1}^{j,N^{\phi}},\theta)W_{T-h-1}^{j,N^{\phi}}, \tag{A.41}$$

where

$$\hat{p}(Y_{T-h:T}|Y_{1:T-h-1},\theta) = \prod_{t=T-h}^{T}\left(\prod_{n=1}^{N^{\phi}}\left(\frac{1}{M}\sum_{j=1}^{M}\tilde{w}_t^{j,n}W_t^{j,n-1}\right)\right).$$

Then, by setting $h = T-1$, we can deduce that

$$\mathbb{E}\left[\hat{p}(Y_{1:T}|\theta)|\mathcal{F}_{0,N^{\phi},M}\right] = \frac{1}{M}\sum_{j=1}^{M} p(Y_{1:T}|s_0^{j,N^{\phi}},\theta)W_0^{j,N^{\phi}}. \tag{A.42}$$

Recall that for period $t=0$, we adopted the convention that $N^{\phi}=1$ and assumed that the states were initialized by direct sampling: $s_0^{j,N^{\phi}} \sim p(s_0)$ and $W_0^{j,N^{\phi}} = 1$. Thus,

$$\begin{aligned}
\mathbb{E}\big[\hat{p}(Y_{1:T}|\theta)\big] &= \mathbb{E}\Big[\mathbb{E}\big[\hat{p}(Y_{1:T}|\theta)|\mathcal{F}_{0,N^{\phi},M}\big]\Big] \\
&= \mathbb{E}\left[\frac{1}{M}\sum_{j=1}^{M} p(Y_{1:T}|s_0^{j,N^{\phi}},\theta)W_0^{j,N^{\phi}}\right] \\
&= \int p(Y_{1:T}|s_0,\theta)p(s_0)ds_0 \\
&= p(Y_{1:T}|\theta),
\end{aligned} \tag{A.43}$$

as desired.

In the remainder of the proof, we use an inductive argument to establish (A.41). If (A.41)

holds for h, it also has to hold for $h+1$:

$$\begin{aligned}
&\mathbb{E}\left[\hat{p}(Y_{T-h-1:T}|Y_{1:T-h-2},\theta)|\mathcal{F}_{T-h-2,N^\phi,M}\right] \\
&= \mathbb{E}\Bigg[\mathbb{E}\big[\hat{p}(Y_{T-h:T}|Y_{1:T-h-1},\theta)\big|\mathcal{F}_{T-h-1,N^\phi,M}\big]\hat{p}(y_{T-h-1}|Y_{1:T-h-2},\theta)\Bigg|\mathcal{F}_{T-h-2,N^\phi,M}\Bigg] \\
&= \frac{1}{M}\sum_{j=1}^{M}\mathbb{E}\big[p(Y_{T-h:T}|s_{T-h-1}^{j,N^\phi},\theta)W_{T-h-1}^{j,N^\phi}\hat{p}(y_{T-h-1}|Y_{1:T-h-2},\theta)\big|\mathcal{F}_{T-h-2,N^\phi,M}\big] \\
&= \frac{1}{M}\sum_{j=1}^{M}\mathbb{E}\left[p(Y_{T-h:T}|s_{T-h-1}^{j,N^\phi},\theta)W_{T-h-1}^{j,N^\phi}\left(\prod_{n=1}^{N^\phi}\left(\frac{1}{M}\sum_{j=1}^{M}\tilde{w}_{T-h-1}^{j,n}W_{T-h-1}^{j,n-1}\right)\right)\Bigg|\mathcal{F}_{T-h-2,N^\phi,M}\right] \\
&= \frac{1}{M}\sum_{j=1}^{M}p(Y_{T-h-1:T}|s_{T-h-2}^{j,N^\phi},\theta)W_{T-h-2}^{j,N^\phi}.
\end{aligned}$$

Note that $\mathcal{F}_{T-h-2,N^\phi,M} \subset \mathcal{F}_{T-h-1,N^\phi,M}$. Thus, the first equality follows from the law of iterated expectations. The second equality follows from the inductive hypothesis (A.41). The third equality uses the definition of the period-likelihood approximation in (23) of Algorithm 2. The last equality follows from the second part of Lemma 5.

We now verify that the inductive hypothesis (A.41) holds for $h=0$. Using the definition of $\hat{p}(y_T|Y_{1:T-1},\theta)$, we can write

$$\begin{aligned}
\mathbb{E}\left[\hat{p}(y_T|Y_{1:T-1},\theta)|\mathcal{F}_{T-1,N^\phi,M}\right] &= \mathbb{E}\left[\prod_{n=1}^{N^\phi}\left(\frac{1}{M}\sum_{j=1}^{M}\tilde{w}_T^{j,n}W_T^{j,n-1}\right)\Bigg|\mathcal{F}_{T-1,N^\phi,M}\right] \quad \text{(A.44)} \\
&= \frac{1}{M}\sum_{j=1}^{M}p(y_T|s_{T-1}^{j,N^\phi})W_{T-1}^{j,N^\phi}.
\end{aligned}$$

The second equality follows from the first part of Lemma 5. Thus, we can deduce that (A.41) holds for $h=T-1$ as required. This completes the proof. ■

B DSGE Models and Data Sources

B.1 Small-Scale DSGE Model

B.1.1 Equilibrium Conditions

We write the equilibrium conditions by expressing each variable in terms of percentage deviations from its steady state value. Let $\hat{x}_t = \ln(x_t/x)$ and write

$$
\begin{aligned}
1 &= \beta \mathbb{E}_t \left[e^{-\tau \hat{c}_{t+1} + \tau \hat{c}_t + \hat{R}_t - \hat{z}_{t+1} - \hat{\pi}_{t+1}} \right] && \text{(A.45)} \\
0 &= \left(e^{\hat{\pi}_t} - 1 \right) \left[\left(1 - \frac{1}{2\nu} \right) e^{\hat{\pi}_t} + \frac{1}{2\nu} \right] && \text{(A.46)} \\
&\quad - \beta \mathbb{E}_t \left[\left(e^{\hat{\pi}_{t+1}} - 1 \right) e^{-\tau \hat{c}_{t+1} + \tau \hat{c}_t + \hat{y}_{t+1} - \hat{y}_t + \hat{\pi}_{t+1}} \right] \\
&\quad + \frac{1-\nu}{\nu \phi \pi^2} \left(1 - e^{\tau \hat{c}_t} \right) \\
e^{\hat{c}_t - \hat{y}_t} &= e^{-\hat{g}_t} - \frac{\phi \pi^2 g}{2} \left(e^{\hat{\pi}_t} - 1 \right)^2 && \text{(A.47)} \\
\hat{R}_t &= \rho_R \hat{R}_{t-1} + (1-\rho_R) \psi_1 \hat{\pi}_t && \text{(A.48)} \\
&\quad + (1-\rho_R) \psi_2 \left(\hat{y}_t - \hat{g}_t \right) + \epsilon_{R,t} \\
\hat{g}_t &= \rho_g \hat{g}_{t-1} + \epsilon_{g,t} && \text{(A.49)} \\
\hat{z}_t &= \rho_z \hat{z}_{t-1} + \epsilon_{z,t}. && \text{(A.50)}
\end{aligned}
$$

Log-linearization and straightforward manipulation of Equations (A.45) to (A.47) yield the following representation for the consumption Euler equation, the New Keynesian Phillips curve, and the monetary policy rule:

$$
\begin{aligned}
\hat{y}_t &= \mathbb{E}_t[\hat{y}_{t+1}] - \frac{1}{\tau} \left(\hat{R}_t - \mathbb{E}_t[\hat{\pi}_{t+1}] - \mathbb{E}_t[\hat{z}_{t+1}] \right) && \text{(A.51)} \\
&\quad + \hat{g}_t - \mathbb{E}_t[\hat{g}_{t+1}] \\
\hat{\pi}_t &= \beta \mathbb{E}_t[\hat{\pi}_{t+1}] + \kappa (\hat{y}_t - \hat{g}_t) \\
\hat{R}_t &= \rho_R \hat{R}_{t-1} + (1-\rho_R) \psi_1 \hat{\pi}_t + (1-\rho_R) \psi_2 \left(\hat{y}_t - \hat{g}_t \right) + \epsilon_{R,t}
\end{aligned}
$$

where

$$\kappa = \tau \frac{1-\nu}{\nu \pi^2 \phi}. \tag{A.52}$$

To construct a likelihood function, we have to relate the model variables to a set of observables y_t. We use the following three observables for estimation: quarter-to-quarter per capita GDP growth rates (YGR), annualized quarter-to-quarter inflation rates (INFL), and annualized nominal interest rates (INT). The three series are measured in percentages, and their relationship to the model variables is given by the following set of equations:

$$\begin{aligned} YGR_t &= \gamma^{(Q)} + 100(\hat{y}_t - \hat{y}_{t-1} + \hat{z}_t) \\ INFL_t &= \pi^{(A)} + 400\hat{\pi}_t \\ INT_t &= \pi^{(A)} + r^{(A)} + 4\gamma^{(Q)} + 400\hat{R}_t. \end{aligned} \tag{A.53}$$

The parameters $\gamma^{(Q)}$, $\pi^{(A)}$, and $r^{(A)}$ are related to the steady states of the model economy as follows:

$$\gamma = 1 + \frac{\gamma^{(Q)}}{100}, \quad \beta = \frac{1}{1 + r^{(A)}/400}, \quad \pi = 1 + \frac{\pi^{(A)}}{400}.$$

The structural parameters are collected in the vector θ. Since in the first-order approximation the parameters ν and ϕ are not separately identifiable, we express the model in terms of κ, defined in (A.52). Let

$$\theta = [\tau, \kappa, \psi_1, \psi_2, \rho_R, \rho_g, \rho_z, r^{(A)}, \pi^{(A)}, \gamma^{(Q)}, \sigma_R, \sigma_g, \sigma_z]'.$$

B.1.2 Data Sources

1. **Per Capita Real Output Growth** Take the level of real gross domestic product, (`FRED` mnemonic "GDPC1"), call it GDP_t. Take the quarterly average of the Civilian Non-institutional Population (`FRED` mnemonic "CNP16OV" / BLS series "LNS10000000"),

call it POP_t. Then,

$$\begin{aligned}&\text{Per Capita Real Output Growth}\\ &= \quad 100\left[\ln\left(\frac{GDP_t}{POP_t}\right) - \ln\left(\frac{GDP_{t-1}}{POP_{t-1}}\right)\right].\end{aligned}$$

2. **Annualized Inflation.** Take the CPI price level, (`FRED` mnemonic "CPIAUCSL"), call it CPI_t. Then,

$$\text{Annualized Inflation} = 400\ln\left(\frac{CPI_t}{CPI_{t-1}}\right).$$

3. **Federal Funds Rate.** Take the effective federal funds rate (`FRED` mnemonic "FEDFUNDS"), call it FFR_t. Then,

$$\text{Federal Funds Rate} = FFR_t.$$

B.2 The Smets-Wouters Model

B.2.1 Equilibrium Conditions

The log-linearized equilibrium conditions of the Smets and Wouters (2007) model take the following form:

$$\begin{aligned}
\hat{y}_t &= c_y\hat{c}_t + i_y\hat{i}_t + z_y\hat{z}_t + \varepsilon_t^g && \text{(A.54)}\\
\hat{c}_t &= \frac{h/\gamma}{1+h/\gamma}\hat{c}_{t-1} + \frac{1}{1+h/\gamma}\mathbb{E}_t\hat{c}_{t+1} && \text{(A.55)}\\
&\quad + \frac{wl_c(\sigma_c-1)}{\sigma_c(1+h/\gamma)}(\hat{l}_t - \mathbb{E}_t\hat{l}_{t+1})\\
&\quad - \frac{1-h/\gamma}{(1+h/\gamma)\sigma_c}(\hat{r}_t - \mathbb{E}_t\hat{\pi}_{t+1}) - \frac{1-h/\gamma}{(1+h/\gamma)\sigma_c}\varepsilon_t^b\\
\hat{i}_t &= \frac{1}{1+\beta\gamma^{(1-\sigma_c)}}\hat{i}_{t-1} + \frac{\beta\gamma^{(1-\sigma_c)}}{1+\beta\gamma^{(1-\sigma_c)}}\mathbb{E}_t\hat{i}_{t+1} && \text{(A.56)}\\
&\quad + \frac{1}{\varphi\gamma^2(1+\beta\gamma^{(1-\sigma_c)})}\hat{q}_t + \varepsilon_t^i\\
\hat{q}_t &= \beta(1-\delta)\gamma^{-\sigma_c}\mathbb{E}_t\hat{q}_{t+1} - \hat{r}_t + \mathbb{E}_t\hat{\pi}_{t+1} && \text{(A.57)}\\
&\quad + (1-\beta(1-\delta)\gamma^{-\sigma_c})\mathbb{E}_t\hat{r}_{t+1}^k - \varepsilon_t^b\\
\hat{y}_t &= \Phi(\alpha\hat{k}_t^s + (1-\alpha)\hat{l}_t + \varepsilon_t^a) && \text{(A.58)}\\
\hat{k}_t^s &= \hat{k}_{t-1} + \hat{z}_t && \text{(A.59)}\\
\hat{z}_t &= \frac{1-\psi}{\psi}\hat{r}_t^k && \text{(A.60)}\\
\hat{k}_t &= \frac{(1-\delta)}{\gamma}\hat{k}_{t-1} + (1-(1-\delta)/\gamma)\hat{i}_t && \text{(A.61)}\\
&\quad + (1-(1-\delta)/\gamma)\varphi\gamma^2(1+\beta\gamma^{(1-\sigma_c)})\varepsilon_t^i\\
\hat{\mu}_t^p &= \alpha(\hat{k}_t^s - \hat{l}_t) - \hat{w}_t + \varepsilon_t^a && \text{(A.62)}\\
\hat{\pi}_t &= \frac{\beta\gamma^{(1-\sigma_c)}}{1+\iota_p\beta\gamma^{(1-\sigma_c)}}\mathbb{E}_t\hat{\pi}_{t+1} + \frac{\iota_p}{1+\beta\gamma^{(1-\sigma_c)}}\hat{\pi}_{t-1} && \text{(A.63)}\\
&\quad - \frac{(1-\beta\gamma^{(1-\sigma_c)}\xi_p)(1-\xi_p)}{(1+\iota_p\beta\gamma^{(1-\sigma_c)})(1+(\Phi-1)\varepsilon_p)\xi_p}\hat{\mu}_t^p + \varepsilon_t^p
\end{aligned}$$

$$\hat{r}_t^k = \hat{l}_t + \hat{w}_t - \hat{k}_t^s \tag{A.64}$$

$$\hat{\mu}_t^w = \hat{w}_t - \sigma_l \hat{l}_t - \frac{1}{1-h/\gamma}(\hat{c}_t - h/\gamma \hat{c}_{t-1}) \tag{A.65}$$

$$\begin{aligned}\hat{w}_t = {} & \frac{\beta\gamma^{(1-\sigma_c)}}{1+\beta\gamma^{(1-\sigma_c)}}(\mathbb{E}_t\hat{w}_{t+1} \\ & +\mathbb{E}_t\hat{\pi}_{t+1}) + \frac{1}{1+\beta\gamma^{(1-\sigma_c)}}(\hat{w}_{t-1} - \iota_w\hat{\pi}_{t-1}) \\ & -\frac{1+\beta\gamma^{(1-\sigma_c)}\iota_w}{1+\beta\gamma^{(1-\sigma_c)}}\hat{\pi}_t \\ & -\frac{(1-\beta\gamma^{(1-\sigma_c)}\xi_w)(1-\xi_w)}{(1+\beta\gamma^{(1-\sigma_c)})(1+(\lambda_w-1)\epsilon_w)\xi_w}\hat{\mu}_t^w + \varepsilon_t^w\end{aligned} \tag{A.66}$$

$$\begin{aligned}\hat{r}_t = {} & \rho\hat{r}_{t-1} + (1-\rho)(r_\pi\hat{\pi}_t + r_y(\hat{y}_t - \hat{y}_t^*)) \\ & +r_{\Delta y}((\hat{y}_t - \hat{y}_t^*) - (\hat{y}_{t-1} - \hat{y}_{t-1}^*)) + \varepsilon_t^r.\end{aligned} \tag{A.67}$$

The exogenous shocks evolve according to

$$\varepsilon_t^a = \rho_a\varepsilon_{t-1}^a + \eta_t^a \tag{A.68}$$

$$\varepsilon_t^b = \rho_b\varepsilon_{t-1}^b + \eta_t^b \tag{A.69}$$

$$\varepsilon_t^g = \rho_g\varepsilon_{t-1}^g + \rho_{ga}\eta_t^a + \eta_t^g \tag{A.70}$$

$$\varepsilon_t^i = \rho_i\varepsilon_{t-1}^i + \eta_t^i \tag{A.71}$$

$$\varepsilon_t^r = \rho_r\varepsilon_{t-1}^r + \eta_t^r \tag{A.72}$$

$$\varepsilon_t^p = \rho_r\varepsilon_{t-1}^p + \eta_t^p - \mu_p\eta_{t-1}^p \tag{A.73}$$

$$\varepsilon_t^w = \rho_w\varepsilon_{t-1}^w + \eta_t^w - \mu_w\eta_{t-1}^w. \tag{A.74}$$

The counterfactual no-rigidity prices and quantities evolve according to

$$\begin{aligned}
\hat{y}_t^* &= c_y\hat{c}_t^* + i_y\hat{i}_t^* + z_y\hat{z}_t^* + \varepsilon_t^g && \text{(A.75)}\\
\hat{c}_t^* &= \frac{h/\gamma}{1+h/\gamma}\hat{c}_{t-1}^* + \frac{1}{1+h/\gamma}\mathbb{E}_t\hat{c}_{t+1}^* && \text{(A.76)}\\
&\quad + \frac{wl_c(\sigma_c-1)}{\sigma_c(1+h/\gamma)}(\hat{l}_t^* - \mathbb{E}_t\hat{l}_{t+1}^*)\\
&\quad - \frac{1-h/\gamma}{(1+h/\gamma)\sigma_c}r_t^* - \frac{1-h/\gamma}{(1+h/\gamma)\sigma_c}\varepsilon_t^b\\
\hat{i}_t^* &= \frac{1}{1+\beta\gamma^{(1-\sigma_c)}}\hat{i}_{t-1}^* + \frac{\beta\gamma^{(1-\sigma_c)}}{1+\beta\gamma^{(1-\sigma_c)}}\mathbb{E}_t\hat{i}_{t+1}^*\\
&\quad + \frac{1}{\varphi\gamma^2(1+\beta\gamma^{(1-\sigma_c)})}\hat{q}_t^* + \varepsilon_t^i && \text{(A.77)}\\
\hat{q}_t^* &= \beta(1-\delta)\gamma^{-\sigma_c}\mathbb{E}_t\hat{q}_{t+1}^* - r_t^* && \text{(A.78)}\\
&\quad + (1-\beta(1-\delta)\gamma^{-\sigma_c})\mathbb{E}_t r_{t+1}^{k*} - \varepsilon_t^b\\
\hat{y}_t^* &= \Phi(\alpha k_t^{s*} + (1-\alpha)\hat{l}_t^* + \varepsilon_t^a) && \text{(A.79)}\\
\hat{k}_t^{s*} &= k_{t-1}^* + z_t^* && \text{(A.80)}\\
\hat{z}_t^* &= \frac{1-\psi}{\psi}\hat{r}_t^{k*} && \text{(A.81)}\\
\hat{k}_t^* &= \frac{(1-\delta)}{\gamma}\hat{k}_{t-1}^* + (1-(1-\delta)/\gamma)\hat{i}_t && \text{(A.82)}\\
&\quad + (1-(1-\delta)/\gamma)\varphi\gamma^2(1+\beta\gamma^{(1-\sigma_c)})\varepsilon_t^i\\
\hat{w}_t^* &= \alpha(\hat{k}_t^{s*} - \hat{l}_t^*) + \varepsilon_t^a && \text{(A.83)}\\
\hat{r}_t^{k*} &= \hat{l}_t^* + \hat{w}_t^* - \hat{k}_t^* && \text{(A.84)}\\
\hat{w}_t^* &= \sigma_l\hat{l}_t^* + \frac{1}{1-h/\gamma}(\hat{c}_t^* + h/\gamma\hat{c}_{t-1}^*). && \text{(A.85)}
\end{aligned}$$

The steady state (ratios) that appear in the measurement equation or the log-linearized equilibrium conditions are given by

$$\begin{aligned}
\gamma &= \bar{\gamma}/100 + 1 && \text{(A.86)}\\
\pi^* &= \bar{\pi}/100 + 1 && \text{(A.87)}\\
\bar{r} &= 100(\beta^{-1}\gamma^{\sigma_c}\pi^* - 1) && \text{(A.88)}\\
r^k_{ss} &= \gamma^{\sigma_c}/\beta - (1-\delta) && \text{(A.89)}\\
w_{ss} &= \left(\frac{\alpha^\alpha(1-\alpha)^{(1-\alpha)}}{\Phi r^{k\ \alpha}_{ss}}\right)^{\frac{1}{1-\alpha}} && \text{(A.90)}\\
i_k &= (1-(1-\delta)/\gamma)\gamma && \text{(A.91)}\\
l_k &= \frac{1-\alpha}{\alpha}\frac{r^k_{ss}}{w_{ss}} && \text{(A.92)}\\
k_y &= \Phi l_k^{(\alpha-1)} && \text{(A.93)}\\
i_y &= (\gamma - 1 + \delta)k_y && \text{(A.94)}\\
c_y &= 1 - g_y - i_y && \text{(A.95)}\\
z_y &= r^k_{ss}k_y && \text{(A.96)}\\
wl_c &= \frac{1}{\lambda_w}\frac{1-\alpha}{\alpha}\frac{r^k_{ss}k_y}{c_y}. && \text{(A.97)}
\end{aligned}$$

The measurement equations take the form:

$$\begin{aligned}
YGR_t &= \bar{\gamma} + \hat{y}_t - \hat{y}_{t-1} && \text{(A.98)}\\
INF_t &= \bar{\pi} + \hat{\pi}_t\\
FFR_t &= \bar{r} + \hat{R}_t\\
CGR_t &= \bar{\gamma} + \hat{c}_t - \hat{c}_{t-1}\\
IGR_t &= \bar{\gamma} + \hat{i}_t - \hat{i}_{t-1}\\
WGR_t &= \bar{\gamma} + \hat{w}_t - \hat{w}_{t-1}\\
HOURS_t &= \bar{l} + \hat{l}_t.
\end{aligned}$$

B.2.2 Data

The data cover 1966Q1 to 2004Q4. The construction follows that of Smets and Wouters (2007). Output data come from the NIPA; other sources are noted in the exposition.

1. **Per Capita Real Output Growth.** Take the level of real gross domestic product (`FRED` mnemonic "GDPC1"), call it GDP_t. Take the quarterly average of the Civilian Non-institutional Population (`FRED` mnemonic "CNP16OV" and BLS series "LNS10000000") normalized so that its 1992Q3 value is 1 and call it POP_t. Then,

$$\begin{aligned}&\text{Per Capita Real Output Growth}\\ &= 100\left[\ln\left(\frac{GDP_t}{POP_t}\right) - \ln\left(\frac{GDP_{t-1}}{POP_{t-1}}\right)\right].\end{aligned}$$

2. **Per Capita Real Consumption Growth.** Take the level of personal consumption expenditures (`FRED` mnemonic "PCEC"), call it $CONS_t$. Take the level of the GDP price deflator (`FRED` mnemonic "GDPDEF") and call it $GDPP_t$. Then,

$$\begin{aligned}&\text{Per Capita Real Consumption Growth}\\ &= 100\left[\ln\left(\frac{CONS_t}{GDPP_t POP_t}\right)\right.\\ &\quad\left. - \ln\left(\frac{CONS_{t-1}}{GDPP_{t-1} POP_{t-1}}\right)\right].\end{aligned}$$

3. **Per Capita Real Investment Growth.** Take the level of fixed private investment (`FRED` mnemonic "FPI") and call it INV_t. Then,

$$\begin{aligned}&\text{Per Capita Real Investment Growth}\\ &= 100\left[\ln\left(\frac{INV_t}{GDPP_t POP_t}\right)\right.\\ &\quad\left. - \ln\left(\frac{INV_{t-1}}{GDPP_{t-1} POP_{t-1}}\right)\right].\end{aligned}$$

4. **Per Capita Real Wage Growth.** Take the BLS measure of compensation per hour for the nonfarm business sector (`FRED` mnemonic "COMPNFB" / BLS series

"PRS85006103") and call it W_t. Then,

$$\begin{aligned}&\text{Per Capita Real Wage Growth}\\ &= \quad 100\left[\ln\left(\frac{W_t}{GDPP_t}\right) - \ln\left(\frac{W_{t-1}}{GDPP_{t-1}}\right)\right].\end{aligned}$$

5. **Per Capita Hours Index.** Take the index of average weekly nonfarm business hours (`FRED` mnemonic / BLS series "PRS85006023") and call it $HOURS_t$. Take the number of employed civilians (`FRED` mnemonic "CE16OV"), normalized so that its 1992Q3 value is 1 and call it EMP_t. Then,

$$\text{Per Capita Hours} = 100\ln\left(\frac{HOURS_t EMP_t}{POP_t}\right).$$

   The series is then demeaned.

6. **Inflation.** Take the GDP price deflator, then

$$\text{Inflation} = 100\ln\left(\frac{GDPP_t}{GDPP_{t-1}}\right).$$

7. **Federal Funds Rate.** Take the effective federal funds rate (`FRED` mnemonic "FEDFUNDS") and call it FFR_t. Then,

$$\text{Federal Funds Rate} = FFR_t/4.$$

C Computational Details

The code for this project is available at `http://github.com/eph/tempered_pf`. The applications in Section 4 were coded in Fortran and compiled using the Intel Fortran Compiler (version: 13.0.0), including the math kernel library. The calculations in Algorithm 1, part 2(a)ii, Algorithm 2, part 1(a)i, and Algorithm 2, part 2(c) were implemented using OpenMP (shared memory) multithreading.

D Additional Numerical Results

D.1 Filtered States for Small-Scale DSGE Model

To document the accuracy of the filtered state, we consider the latent government spending shock as a prototypical hidden state. Using the Kalman filter, we can compute $\mathbb{E}[\hat{g}_t|Y_{1:T}]$, which we compare to the particle filter approximation, denoted by $\hat{\mathbb{E}}[\hat{g}_t|Y_{1:T}]$. Figure A-1 plots root-mean-squared errors (RMSEs) for $\hat{\mathbb{E}}[\hat{g}_t|Y_{1:T}]$. The ranking of the filters is consistent with the ranking based on the accuracy of the likelihood approximations. The BSPF performs the worst. Using the TPF with $M = 40,000$ particles reduces the RMSE roughly by a factor of three.

Figure A-1: Small-Scale Model: Accuracy of Filtered State

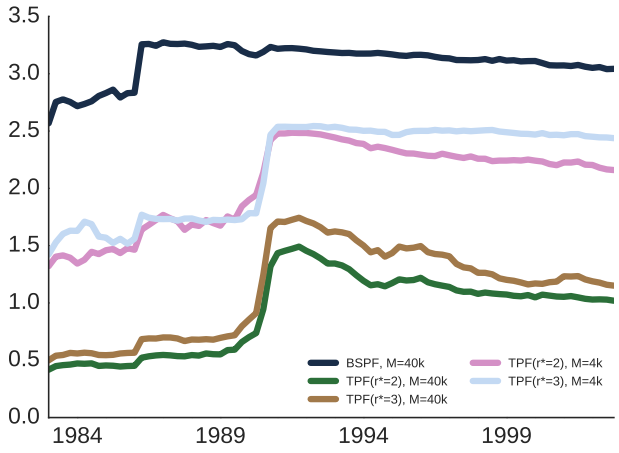

Notes: The figure depicts RMSEs associated with $\hat{E}[\hat{g}_t|Y_{1:t}]$. Results are based on $N_{run} = 100$ independent runs of the particle filters.

D.2 Smets-Wouters Model

The parameters used for the likelihood evaluation of the SW model are summarized in Table A-1.

In Table A-2 we report the accuracy statistics for the TPF with $N^{MH} = 1$. Holding the number of particles fixed at $M = 40,000$ and reducing the number of mutation steps from

Table A-1: SW Model: Parameter Values

	θ^m	θ^l		θ^m	θ^l
$\tilde{\beta}$	0.159	0.182	$\bar{\pi}$	0.774	0.571
$\bar{l}$	−1.078	0.019	α	0.181	0.230
σ	1.016	1.166	Φ	1.342	1.455
φ	6.625	4.065	h	0.597	0.511
ξ_w	0.752	0.647	σ_l	2.736	1.217
ξ_p	0.861	0.807	ι_w	0.259	0.452
ι_p	0.463	0.494	ψ	0.837	0.828
r_π	1.769	1.827	ρ	0.855	0.836
r_y	0.090	0.069	$r_{\Delta y}$	0.168	0.156
ρ_a	0.982	0.962	ρ_b	0.868	0.849
ρ_g	0.962	0.947	ρ_i	0.702	0.723
ρ_r	0.414	0.497	ρ_p	0.782	0.831
ρ_w	0.971	0.968	ρ_{ga}	0.450	0.565
μ_p	0.673	0.741	μ_w	0.892	0.871
σ_a	0.375	0.418	σ_b	0.073	0.075
σ_g	0.428	0.444	σ_i	0.350	0.358
σ_r	0.144	0.131	σ_p	0.101	0.117
σ_w	0.311	0.382	$\ln p(Y\|\theta)$	−943.0	−956.1

Notes: $\tilde{\beta} = 100(\beta^{-1} - 1)$.

$N^{MH} = 10$ to $N^{MH} = 1$ speeds up the run time by a factor of three. Note that this is less than you might expect, given the fact that the number of Metropolis-Hastings steps at each iteration has decreased by a factor of ten. This reflects two things. First, the mutation phase is easily parallelizable on a multi-core desktop computer. Second, a substantial fraction of computational time is spent during the resampling (selection) phase, which is not affected by increasing the number of Metropolis-Hastings steps.

To match the run times of the TPF($N^{MH} = 1$) with the run time of the BSPF($M = 40,000$) we reduce the number of particles to $M = 8,000$ for θ^m and to $M = 6,000$ for θ^l. Compared to the results reported in the main text for $N^{MH} = 10$ in Table 4, the number of particles for the TPF is about 3 times larger. However, even with the larger number of particles, the MSE of the log-likelihood approximation is a lot worse than what is obtained with $N^{MH} = 10$, highlighting the importance of the mutation.

Table A-2: SW Model: PF Summary Statistics

	BSPF	TPF			
Target Ineff. Ratio r^*		2	3	2	3
High Posterior Density: $\theta = \theta^m$					
Number of Particles M	40,000	8,000	8,000	40,000	40,000
MSE($\hat{\Delta}$)	63,881.68	11,349.01	18,676.99	3,858.63	5,911.39
Bias($\hat{\Delta}$)	-245.64	-100.65	-128.98	-57.71	-72.92
Variance($\hat{\Delta}$)	3,543.79	1,219.55	2,041.44	527.94	594.46
$T^{-1}\sum_{t=1}^{T} N_{\phi,t}$	1.00	6.17	4.75	6.13	4.72
Average Run Time (sec)	3.33	3.97	3.01	22.41	17.54
Low Posterior Density: $\theta = \theta^l$					
Number of Particles M	40,000	6,000	6,000	40,000	40,000
MSE($\hat{\Delta}$)	69,612.88	22,052.28	30,372.77	5,578.91	7,155.54
Bias($\hat{\Delta}$)	-255.06	-142.43	-167.17	-71.37	-80.58
Variance($\hat{\Delta}$)	4,559.09	1,766.12	2,426.31	485.38	661.68
$T^{-1}\sum_{t=1}^{T} N_{\phi,t}$	1.00	6.26	4.81	6.22	4.77
Average Run Time (sec)	3.28	3.35	2.35	22.69	18.19

Notes: Results are based on $N_{run} = 100$ independent runs of the particle filters and $N^{MH} = 1$. The log likelihood discrepancy is defined as $\hat{\Delta} = \ln \hat{p}(Y_{1:T}|\theta) - \ln p(Y_{1:T}|\theta)$.

Frank Schorfheide
Professor of Economics
University of Pennsylvania

July 21, 2017

Dr. Sylvia Kaufmann
Journal of Econometrics, Guest Editor
Study Center Gerzensee
VIA EMAIL

RE: Revision *Tempered Particle Filtering*

Dear Sylvia:

We are very grateful for the conditional acceptance of our paper *Tempered Particle Filtering* in the special issue of the *Journal of Econometrics*. Many thanks for your careful reading of the draft and your suggestions on how to improve the manuscript.

We reduced the length of the paper from 41 pages to 34 pages (keeping the formatting the same). Foremost, the reduction was achieved by moving some material from the theory section (Section 3) as well as some tables and figures from the empirical section (Section 4) into the Online Appendix. We also condensed the exposition throughout the manuscript. In response to your specific comments, here is what we did.

Notation:

1. We now make use of t subscripts, writing $\phi_{n,t}$ and $N_{\phi,t}$, except in parts where the notation gets too cumbersome or where it is assumed that the tempering schedule is fixed (Section 3).

2. We removed the M subscripts.

3. We re-wrote the description of Algorithm 2. In particular, we changed the termination condition to $\phi_{n,t} = 1$ as you suggested and re-wrote/re-formatted Step 1(a)iii, which describes when the *do*-loop is terminated.

Typos:

1. We corrected the typos flagged in line items 1. – 10.

11. We harmonized the use of the $h(\cdot)$ notation with and without arguments.

12. Lemma 1: we now refer to the first Monte Carlo average as $\tilde{h}^1_{t|t-1}$, emphasizing that this is an expectation given $t-1$ information. We also explicitly write in Lemma 2 that the convergence results hold for $n \geq 2$. The main issue is that the order of correction, selection, and mutation is slightly different for $n = 1$.

13. We removed the ratio on the left-hand-side (it was essentially a labeling of the Monte Carlo average). The notation did not look particularly nice and it was not used elsewhere in the paper.

14. Done.

15. We fixed the notation. We meant to use $A_2^{(1)}$ to denote the first derivative of A_2 with respect to ϕ_n.

Finally, we adjusted the number of particles in columns 3 and 4 of Tables 2, 3, and 4 to approximately equalize the run times of the TPFs and the BSPF($M = 40,000$). We feel that the suggested edits led to an improved exposition and hope that we addressed your comments in a satisfactory manner.

With best wishes,

Edward Herbst
Frank Schorfheide